OK

GEAP-5591
JANUARY 1968

EURAEC - 2001
JOINT U.S. - EURATOM RESEARCH
AND DEVELOPMENT PROGRAM

POWER REACTOR HIGH PERFORMANCE UO_2 PROGRAM

FUEL DESIGN SUMMARY AND PROGRAM STATUS

S.Y. OGAWA
E.A. LEES
M.F. LYONS

U.S. ATOMIC ENERGY COMMISSION
CONTRACT AT (04-3)-189
PROJECT AGREEMENT 50

NUCLEAR FUELS DEPARTMENT
GENERAL ELECTRIC
SAN JOSE, CALIFORNIA

DISCLAIMER

GEAP-5591
Joint US-Euratom Research
and Development Program
January 1968

Power Reactor High Performance UO_2 Program
Fuel Design Summary and Program Status

S. Y. Ogawa
E. A. Lees
M. F. Lyons

Approved by: _____
H. H. Klepfer, Manager
Fuels and Materials Development

Printed in U.S.A. Available from the
Clearing House for Federal Scientific and Technical Information
National Bureau of Standards, U.S. Department of Commerce
Springfield, Virginia
Price: $3.00 per copy

U. S. Atomic Energy Commission
Contract AT (04-3) -189
Project Agreement 50

Nuclear Fuels Department
GENERAL ELECTRIC
SAN JOSE, CALIFORNIA

5500-NFD-87
175 sf 2/68

LEGAL NOTICE

THIS DOCUMENT WAS PREPARED UNDER THE SPONSORSHIP OF THE ATOMIC ENERGY COMMISSION PURSUANT TO THE JOINT RESEARCH AND DEVELOPMENT PROGRAM ESTABLISHED BY THE AGREEMENT FOR COOPERATION SIGNED NOVEMBER 8, 1958, BETWEEN THE GOVERNMENT OF THE UNITED STATES OF AMERICA AND THE EUROPEAN ATOMIC ENERGY COMMUNITY (EURATOM). NEITHER THE UNITED STATES, THE U.S. ATOMIC ENERGY COMMISSION, THE EUROPEAN ATOMIC ENERGY COMMUNITY, THE EURATOM COMMISSION, NOR ANY PERSON ACTING ON BEHALF OF EITHER COMMISSION:

A. MAKES ANY WARRANTY OR REPRESENTATION, EXPRESS OR IMPLIED, WITH RESPECT TO THE ACCURACY, COMPLETENESS, OR USEFULNESS OF THE INFORMATION CONTAINED IN THIS DOCUMENT, OR THAT THE USE OF ANY INFORMATION, APPARATUS, METHOD, OR PROCESS DISCLOSED IN THIS DOCUMENT MAY NOT INFRINGE PRIVATELY OWNED RIGHTS; OR

B. ASSUMES ANY LIABILITIES WITH RESPECT TO THE USE OF, OR FOR DAMAGES RESULTING FROM THE USE OF ANY INFORMATION, APPARATUS, METHOD OR PROCESS DISCLOSED IN THIS DOCUMENT.

AS USED IN THE ABOVE, "PERSON ACTING ON BEHALF OF EITHER COMMISSION" INCLUDES ANY EMPLOYEE OR CONTRACTOR OF EITHER COMMISSION OR EMPLOYEE OF SUCH CONTRACTOR TO THE EXTENT THAT SUCH EMPLOYEE OR CONTRACTOR OR EMPLOYEE OF SUCH CONTRACTOR PREPARES, HANDLES, DISSEMINATES, OR PROVIDES ACCESS TO, ANY INFORMATION PURSUANT TO HIS EMPLOYMENT OR CONTRACT WITH EITHER COMMISSION OR HIS EMPLOYMENT WITH SUCH CONTRACTOR.

FOREWORD

The United States and the European Atomic Energy Community (Euratom) signed, on May 29, and June 18, 1958, an agreement which provides a basis for cooperation in programs for the advancement of the peaceful applications of atomic energy. This agreement, in part, provides for establishment of a joint U.S.-Euratom research and development program which is intended to support design of reactors to be constructed in Europe under the joint program. The work from this joint program should through the spirit of cooperation and sharing of scientific and technical information, contribute to the common good and minimize duplication of effort by the limited pool of technical talent available in Western Europe and the United States.

TABLE OF CONTENTS

LIST OF ILLUSTRATIONS

LIST OF ILLUSTRATIONS (Continued)

ABSTRACT

A new AEC-Euratom research and development program has been undertaken at the Nuclear Energy Division of General Electric to provide a practical demonstration of centermelt operation with UO_2 fuel rods in a commercial power reactor core. This objective will be accomplished by irradiation of six fuel bundles containing 324 fuel rods in the Consumers Power Company Big Rock Point (BRP) reactor. Two discrete levels of melting will be evaluated. Two bundles contain 0.570-inch-o.d., Zircaloy-2-clad rods, half with vipak powder and half with pellet UO_2 fuel, and will operate with incipient centermelting. The other four bundles contain 0.700-inch-o.d., Zircaloy-2-clad rods, also half with vipak powder and half with pellet UO_2 fuel, and will operate with definite but moderate centermelting at rated power.

The initial phases of the program have been concerned with the detailed fuel design, fuel fabrication, safeguards analysis, and relicensing of the Big Rock Point reactor for the irradiations. This phase is now complete and an AEC-ACRS approval to proceed has been issued. The total program also provides for irradiation following, and detailed interim and final examinations on a significant number of rods, out to the target average rod burnup of 20,000 MWd/T_e. The irradiations are expected to commence in March 1968, with the first fuel pool examination in June and the first destructive rod examinations in early fall.

A unique fuel bundle design was conceived and evaluated to achieve the requisite high performance conditions in the BRP core. This report describes the detailed fuel design, bundle characteristics, briefly reviews the licensing effort, and indicates the current program status.

ACKNOWLEDGMENT

Other significant contributors to the work described in this report were:

W. H. Arlt	L. E. Miller
N. H. Barth	F. A. Schraub
J. T. Worthington	D. T. Weiss

SECTION I

INTRODUCTION

A new AEC-Euratom research and development project* was initiated at General Electric, Nuclear Energy Division on September 1, 1966, to exploit over 5 years of previous experience with UO_2 fuel operation with centermelting.[1] The objective of this follow-on program, designated the "Power Reactor High Performance UO_2 Program," is to irradiate a sufficient number of centermelt fuel rods in a power reactor core to constitute a demonstration-proof test of practical engineering significance. The specific implementation will be operation of Zircaloy-2-clad, UO_2 rods with unequivocal melting at rated reactor power to target average burnups of 20,000 MWd/T_e. The AEC-Euratom support provides for the detailed centermelt fuel design including safeguards analysis and reactor license changes necessary to its irradiation, indirect fuel fabrication supervision, irradiation following, and post-irradiation examination and reporting.

The centermelt fuel rods are incorporated in six fuel bundles to be irradiated in the Consumers Big Rock Point reactor. Two of the assemblies are designated "Intermediate Performance Fuel," and will operate with incipient melting in the central region of the UO_2 at rated power conditions. These two assemblies represent the next logical increment in fuel performance beyond current practice, moving toward an elimination of the centermelt restrictions applied to present designs. The remaining four assemblies are designated "Advanced Performance Fuel," and will operate with definite but moderate central melting at rated power conditions. These latter bundles constitute a further step in fuel performance and reactor experience, and will ultimately provide the practical engineering demonstration of the relative reliability and safety of centermelt fuel operation.

*Contract AT(04-3)-189, Project Agreement 50

SECTION II

CENTERMELT FUEL ROD DESIGN

2.1 GENERAL

A total of 324 fuel rods is incorporated into the six fuel assemblies. Of this total, 188 rods are enriched, high power producing rods, while the remaining 136 rods contain depleted UO_2. Two of the assemblies, the intermediate performance fuel, are composed of 64 rods each in an 8 × 8 array. One of these two assemblies contains sintered pellet fuel and the other vipak powder UO_2, with a total of 36 high power rods in each bundle. The other four assemblies, the advanced performance fuel, are composed of 49 rods each in a 7 × 7 array. Two assemblies contain sintered pellet UO_2 fuel and the other two contain vipak powder UO_2, with a total of 29 high power rods in each bundle. Table 2-1 summarizes the fuel and bundle details.

2.2 INTERMEDIATE PERFORMANCE FUEL

The rods in these assemblies are clad with 0.570-inch-o.d. × 0.035-inch-wall Zircaloy-2. A compression spring is included in the plenum region to minimize axial fuel movement during handling and shipping. A depleted UO_2 pellet is placed at each end of the enriched fuel column to minimize temperature effects at the lower end plug and the plenum spring. The pellets are dished to provide sufficient void volume to accommodate the potential UO_2 phase change volume expansion from melting at 122 percent overpower conditions. A nominal 12-mil pellet-cladding gap is used to minimize fuel-cladding interaction strains.

The UO_2 powder is vibratory compacted to a bulk density of 85 percent of theoretical. The inherent 15 percent fuel void volume is more than adequate to accommodate the phase change volume expansion which could occur on melting at 122 percent overpower in these rods. Dimensional details for the intermediate performance fuel rods are shown in Figure 2-1.

2.3 ADVANCED PERFORMANCE FUEL

All rods in the advanced performance bundles are clad with 0.700-inch-o.d. × 0.040-inch-wall Zircaloy-2 tubing. A compression spring is again included in the plenum region to minimize axial fuel movement during handling and shipping. A depleted UO_2 pellet is placed at each end of the enriched fuel column to minimize temperature effects on the lower end plug and the plenum spring. The pellet fuel is fabricated with a 0.100-inch-diameter center hole, sized to accommodate the potential UO_2 phase change volume expansion from melting at 122 percent overpower. A nominal 13-mil pellet-cladding gap is used in these rods.

The UO_2 powder rods are again compacted to 85% bulk density. The inherent 15 percent void space in the powder fuel exceeds that required to accommodate the phase change volume expansion on melting at overpower. The dimensional details for the advanced performance fuel rods are given in Figure 2-2.

TABLE 2-1

POWER REACTOR HIGH PERFORMANCE UO_2 PROGRAM FUEL DESIGN DETAILS AND OPERATING CONDITIONS

Fuel Assembly	UO_2 Fuel			Number of Rods	Cladding			
	Type	T.D.	U-235		Type	Outside Diameter (inches)	Wall Thickness (inches)	Condition
Group A								
D-50 (8 × 8 Lattice)	Pellet	95	4.3	12	Zircaloy-2 (Tube Reduction Process)	0.570	0.035	Cold Worked and Stress Relieved
	Pellet	95	5.0	16				
	Pellet	95	5.6	8				
	Powder	85	0.22	28				
D-51 (8 × 8 Lattice)	Powder	85	4.3	12		0.570	0.035	
	Powder	85	5.0	16				
	Powder	85	5.6	8				
	Powder	85	0.22	28				
Group B								
D-52 and D-53 (7 × 7 Lattice)	Pellet	95	4.3	12		0.700	0.040	
	Pellet	95	5.0	12				
	Pellet	95	5.6	5				
	Powder	85	0.22	20				
D-54 and D-55 (7 × 7 Lattice)	Powder	85	4.3	12		0.700	0.040	
	Powder	85	5.0	12				
	Powder	85	5.6	5				
	Powder	85	0.22	20				

TABLE 2-1 (Continued)

Fabrication Process		Design Burn-up (MWd/TU)	Design Heat Flux	
UO_2 Fuel	Fuel Rod		Normal Btu/h-ft^2	Overpower (Btu/h-ft^2)
Group A				
Cold Press and Sinter	Standard Dished	20,000	450,000	550,000
Dynapak	Vibratory Compaction			
Dynapak	Vibratory Compaction	20,000	450,000	550,000
Group B				
Cold Press and Sinter	Standard 2/0.100 inch Central Hole	20,000	450,000	550,000
Dynapak	Vibratory Compaction			
Dynapak	Vibratory Compaction	20,000	450,000	550,000

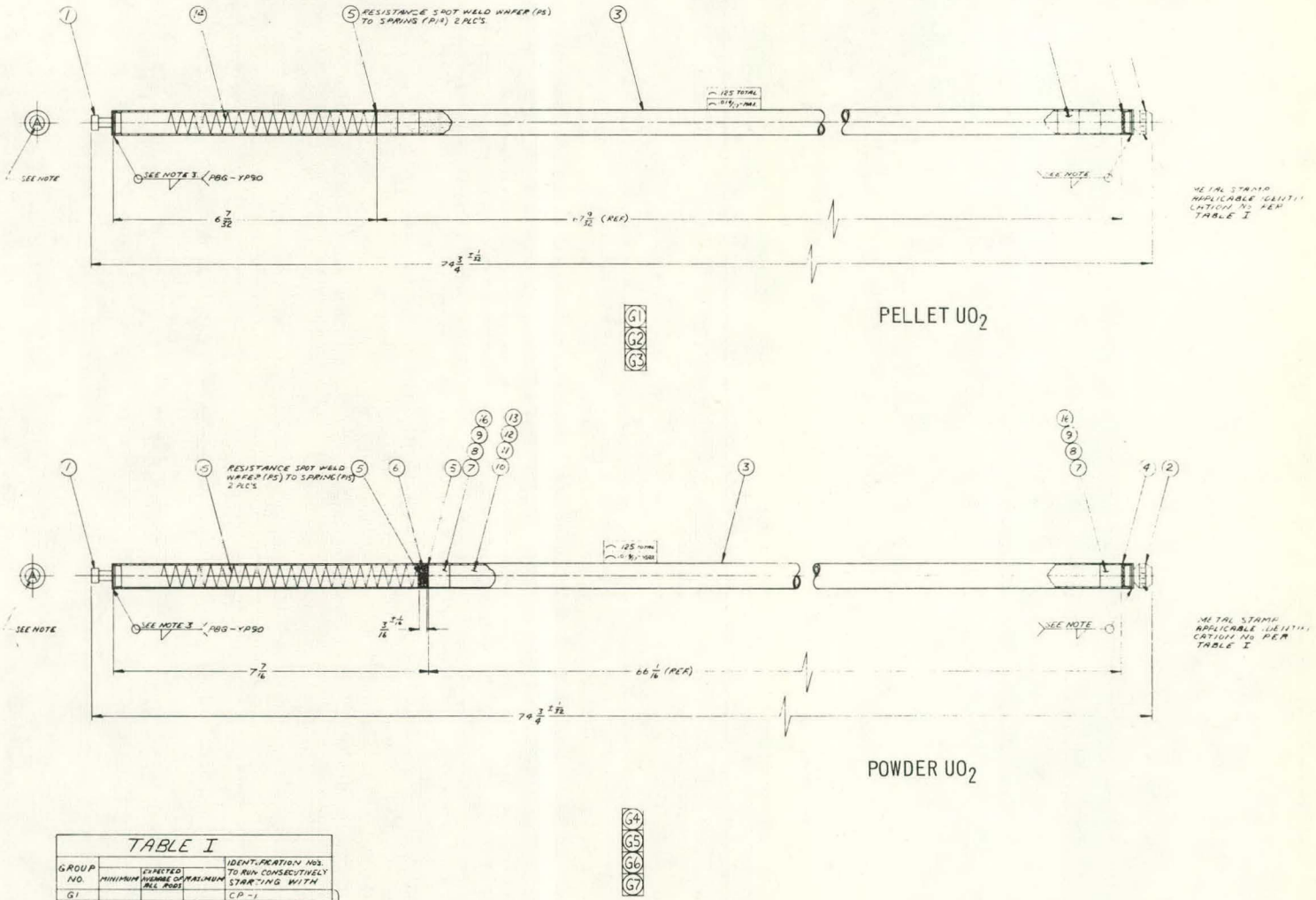

TABLE I

GROUP NO.	MINIMUM	EXPECTED NUMBER OF MAXIMUM ALL RODS		IDENTIFICATION NOS. TO RUN CONSECUTIVELY STARTING WITH
G1				CP-1
G2				CP-100
G3				CP-200
G4				CP-520
G5				CP-620
G6				CP-700
G7				CP-820

67-01537

FIGURE 2-1. DRAWING OF 0.570 OUTSIDE DIAMETER FUEL ROD

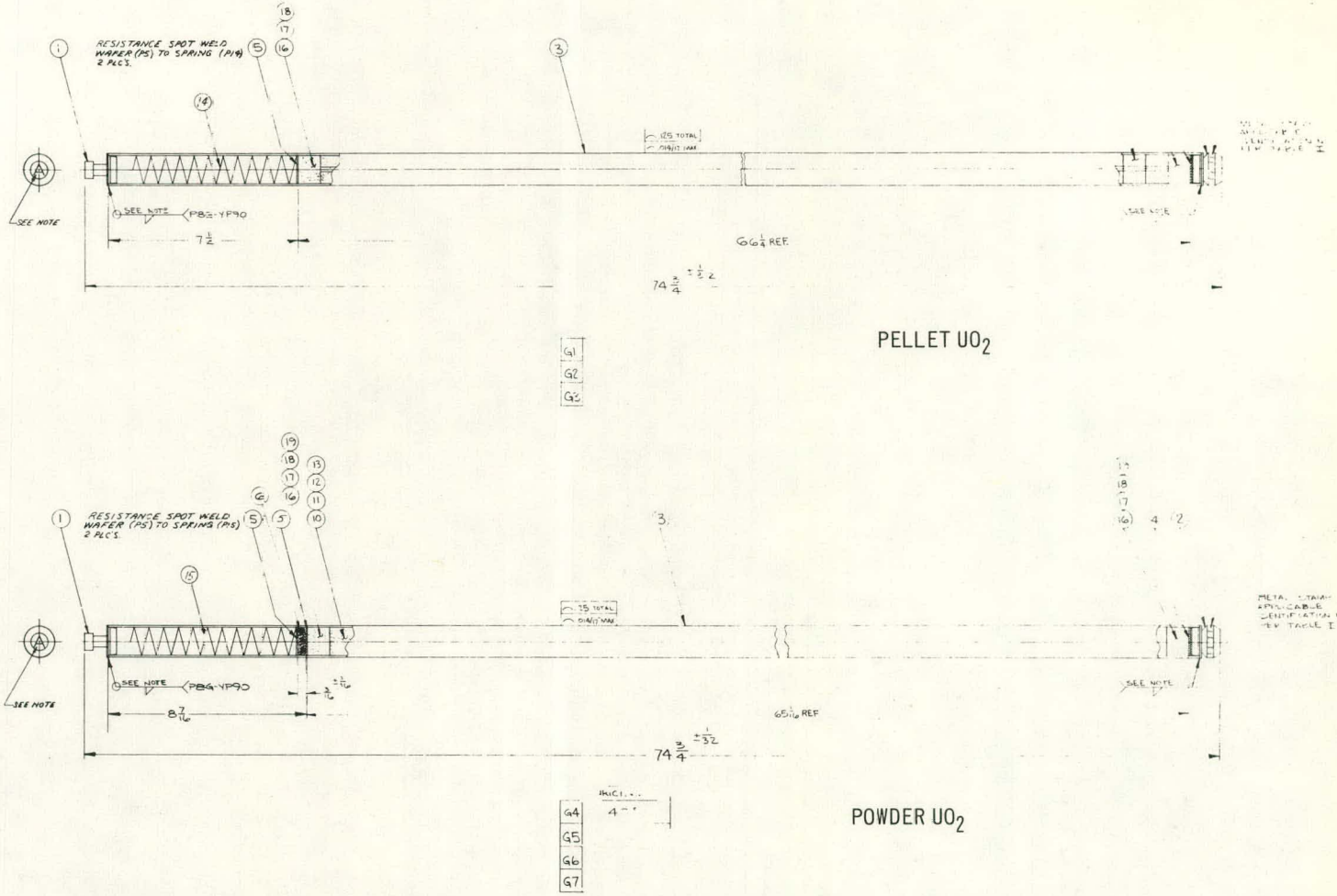

TABLE I

GROUP Nº	MINIMUM	EXPECTED AVERAGE OF ALL RODS	MAXIMUM	IDENTIFICATION Nº'S TO RUN CONSECUTIVELY STARTING WITH	
G1	3100	3162	3220	CM-1	
G2	3100	3162	3220	CM-120	SEE NOTE
G3	3100	3162	3220	CM-200	
G4	2904	2975	3045	CM-500	
G5	2904	2975	3045	CM-600	SEE NOTE
G6	2904	2975	3045	CM-700	
G7	2904	2975	3045	CM-800	

67-01538

FIGURE 2-2. DRAWING OF 0.700 OUTSIDE DIAMETER FUEL ROD

SECTION III

CENTERMELT FUEL DESIGN ANALYSIS

3.1 DESIGN CRITERIA

The single, most governing design factor is selection of the Big Rock Point reactor for these irradiations. The high power density characteristics of this core provide the flexibility to obtain the desired high fuel performance conditions. Further, the relatively short, 6-month reactor operating cycles are advantageous for frequent fuel inspections. Other general rules or criteria followed in the design of the assemblies are listed below.

The basic removable rod, fuel bundle design is similar to those used earlier in BRP for the High Power Density Fuel Development program.[2] This capability to remove and replace individual rods is invaluable during the conduct of a R and D program. Individual rods can be examined visually, dimensional measurements can be made and selected rods shipped to the Radioactive Materials Laboratory (RML) for destructive examination at various levels of exposure without destroying the integrity of the assembly.

The upper fuel performance limit is dictated by the reactor license requirement to maintain a minimum critical heat flux ratio (MCHFR) of 1.5 at 1.22 percent overpower conditions. The MCHFR is evaluated using a new critical heat flux correlation for the beginning-of-life and end-of-life conditions. The essential advantage in the new correlation over that previously used in the Big Rock reactor is to allow a higher exit quality for a given mass flow rate as indicated qualitatively in Figure 3-1.

Fuel rod diameters were selected so that when operated at a rated power surface heat flux of 450,000 ±50,000 Btu/h-ft^2, the intermediate performance fuel would experience incipient central melting while the advanced performance fuel would develop definite but moderate central melting.

Finally, the fuel bundle characteristics such as total power output, flow area, water-to-fuel ratio, and enrichment level were maintained as close as possible to a regular BRP fuel bundle in order to minimize adverse effects on over-all core performance.

3.2 CLADDING MATERIAL SELECTION

The cladding material selected for use in the program was Zircaloy-2. The material was fabricated by the tube reduction process and vacuum stress relieved. Stress relief time and temperature were determined so that the following minimum mechanical properties for the material were obtained.

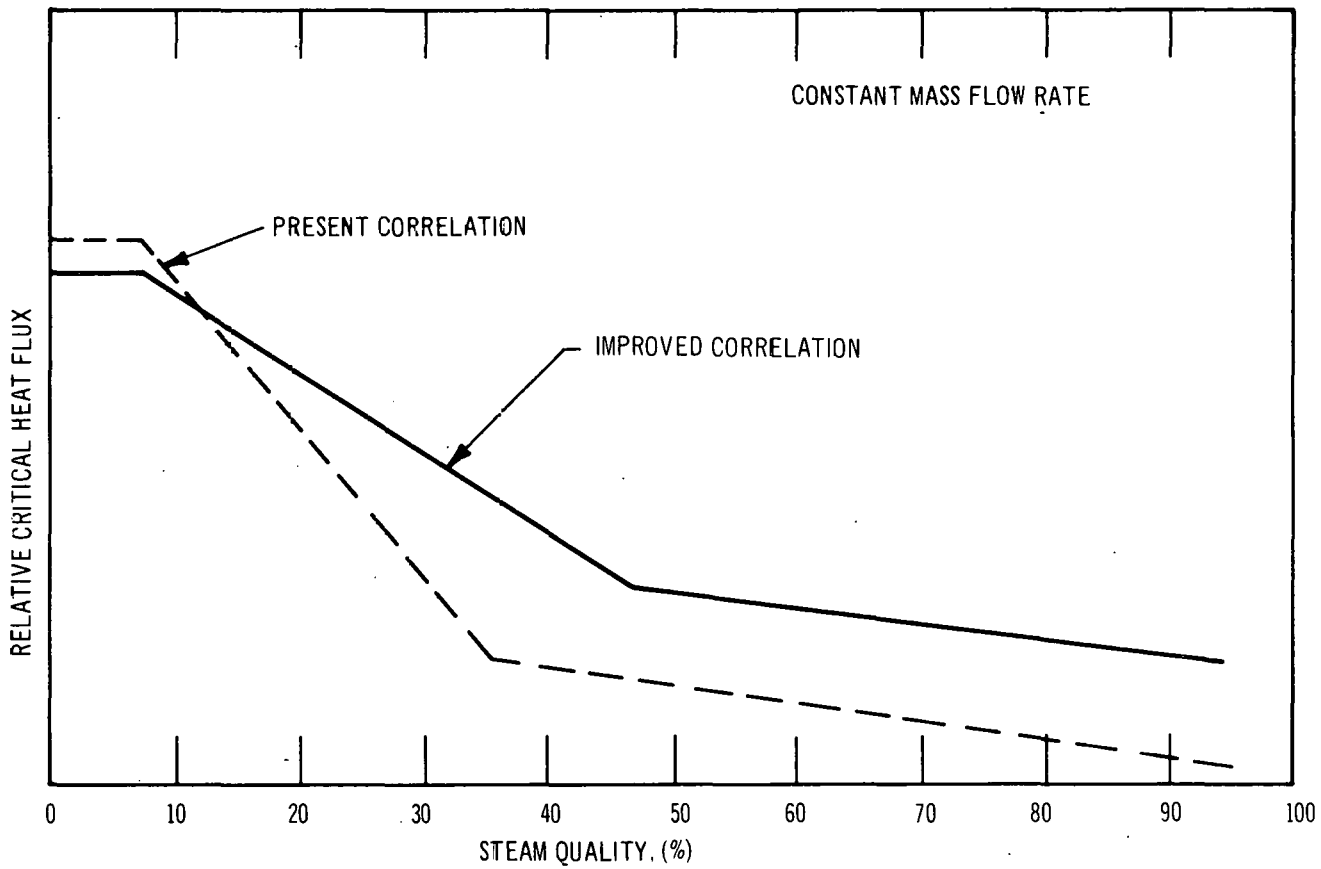

FIGURE 3-1. IMPROVED CRITICAL HEAT FLUX CORRELATION

Yield Strength (0.2 percent Offset) psi Minimum		Ultimate Tensile Strength psi Minimum		Elongation in 2 inches Minimum, percent
Room Temperature (°F)	650°F	Room Temperature (°F)	650°F	Room Temperature (°F)
60,000	32,000	70,000	41,000	16

The exact mechanical properties of the actual centermelt fuel tubing have been determined and will be documented.

3.3 CLADDING DIMENSIONS

The nominal tubing dimensions required to meet the program operating conditions are a function of the degree of melting at rated heat flux, critical collapse stresses at overpower and reactor overpressure (free-standing criteria), and material mechanical properties as a function of temperature and irradiation. The basic parameter for this fuel, the rated power peak heat flux, was specified as 450,000 ±50,000 Btu/h-ft^2, with a 1.22 overpower allowance. The analysis to establish the cladding dimensions was performed by trial and error until required strength and degree of melting criteria for both powder and pellet fuel were satisfied. Both the intermediate thermal performance fuel and advanced thermal performance fuel were sized in this manner; the results are as follows:

CLADDING DIMENSIONAL SPECIFICATIONS

Group	Description	Cladding	
		Inside Diameter (inch)	Wall Thickness (inch)
A	Intermediate thermal performance-pellet UO_2	0.500 ±0.002	0.035 ±0.0025
	Intermediate thermal performance-powder UO_2	0.500 ±0.002	0.035 ±0.0025
B	Advanced thermal performance-pellet UO_2	0.620 ±0.002	0.040 ±0.0025
	Advanced thermal performance-powder UO_2	0.620 ±0.002	0.040 ±0.0025

3.4 EXTERNAL PRESSURE COLLAPSE EVALUATION

A tube is considered to be "free-standing" if yielding of the material will not occur at the maximum, simultaneous external pressure and temperature condition. Referring to Timoshenko,[3] an ideal tube will collapse when the net external pressure reaches:

$$P_{cr} = \frac{E}{4\,(1 - \nu^2)} \left(\frac{h}{R}\right)^3 , \qquad (1)$$

where

P_{cr} = Critical collapse pressure, psi;

E = Modulus of elasticity = 10×10^6 psi;

ν = Poisson's ratio = 0.40;

h = Minimum tube wall thickness, inches; and

R = Tube mean radius:

For Group A = 0.0325 inch, and
For Group B = 0.0375 inch.

For a tube with less than ideal dimensions (e.g., commercial tubing), collapse may occur at less than P_{cr} due to the effects of ovality. The equation from Timoshenko for this condition accounts for both tube ovality and yield strength. In this case, the critical collapse pressure for yielding becomes

$$P_{cr_y} = 1/2 \left[A - \sqrt{A^2 - 4B} \right], \tag{2}$$

where

$$A = \sigma_y \frac{h}{R} + \left(1 + 6 \frac{U_o}{R} \frac{R}{h} \right) P_{cr},$$

σ_y = Yield strength = assumed to be 32,000 psi at 650°F,

h/R = As previously stated in Equation (1),

U_o = 1/4 (ID_{max} - ID_{min}),

P_{cr} = That value determined by Equation (1), and

$$B = \sigma y \frac{h}{R} P_{cr}.$$

The following collapse pressures were determined for Group A and Group B fuel:

Group	Yield Strength (psi)	P_{cr} (psia)	P_{cr_y} (psia)
0.570-inch o.d.	32,000	5340	2770
0.700-inch o.d.	32,000	4360	2100

The normal operating pressure in the Consumers reactor is 1350 psia, overpressure is 1550 psia, and the pressure vessel design and cold hydrostatic test pressure is 1750 psia. Thus, the margin of safety against collapse for both Group A tubing and Group B tubing appears to be more than adequate for the range of operating conditions expected.

3.5 CLADDING STRESS ANALYSIS

The tubing used as a cladding for a nuclear fuel rod is subjected to many forces both individually and in combination. Among these are forces due to external pressure, temperature gradients, internal pressure caused by fission gas release, and fuel-cladding interaction caused by differential thermal expansion and fission induced swelling of the fuel. In the centermelt rods an additional consideration is the phase change volume expansion of the UO_2 upon melting. The analysis of these stresses is presented in detail in the following pages. The analysis is based upon worst case conditions foreseen for operation of the fuel in the Consumers BRP reactor.

3.5.1 External Pressure Stress

The highest external pressure that could occur is the 1750-psia vessel design pressure. The likelihood of this condition occurring at any significant power level is extremely small, and would probably be associated with some sort of uncontrolled excursion. Hydrostatic tests are performed at pressures approaching 1750 psia; however, these tests are performed at zero power. Thus, fuel cladding temperatures are low and cladding strength more than sufficient to withstand high external pressures without collapse. The normal operating pressure for the Consumers reactor is 1350 psia. For design purposes, the most likely worst case condition was judged to be the minimum external pressure allowable by the reactor scram limit with the core at full power. The combination of stresses at this condition appears to produce the maximum allowable fiber tensile stresses in the cladding, and since external pressure creates primarily compressive stresses in the tube wall, a minimum pressure value is appropriate. The most extreme case of zero external pressure at full power, with maximum internal fission gas pressure, is not considered as a basic design limit. The likelihood of instantaneous loss of reactor pressure without a decrease in power is believed infinitesimal, and would normally be associated with a maximum credible accident.

The equations used to calculate external pressure stresses assume that the cladding material behaves elastically. The level of stress for a particular level of external pressure is a function of how perfectly circular a tube is prior to being subjected to external pressure. Bi-axial external pressure stress (hoop stress) is determined from the equation:

$$\sigma_\theta = -\frac{P_o R}{h}\left[1 + 6\frac{U_o}{h}\left(\frac{1}{1-\frac{P_o}{P_{cr}}}\right)\right], \qquad (3)$$

where

P_{cr} = Critical collapse pressure, psi;

P_o = External pressure, psi;

U_o = 1.4 (ID_{max} - ID_{min}), inches;

h = Minimum wall thickness, inches;

R = Tube radius, inches; and

σ_θ = Bi-axial stress or hoop stress, psi.

Axial external pressure stress (longitudinal stress) is determined from:

$$\sigma_z = -\frac{P_o R}{h}\left[1/2 + 6\,\nu\,\frac{U_o}{h}\left(\frac{1}{1-\frac{P_o}{P_{cr}}}\right)\right], \tag{4}$$

where

P_o, P_{cr}, h, U_o, and R are as above,

ν = Poisson's ratio, and

σ_z = Longitudinal stress.

Both of these stresses act in compression to resist diametral expansion of the tube by other forces. Table 3-1 indicates the minimum values for the compressive hoop stress, i.e., at the maximum radius of bending for the ovality condition.

3.5.2 Thermal Stresses

Thermal stresses are directly proportional to the temperature gradient across the cladding wall. From Timoshenko,[3] the thermal stresses at the surface may be written as:

$$\sigma_\theta = \sigma_z = \pm\frac{E\alpha\Delta T}{2(1-\nu)}, \tag{5}$$

where

E = Modulus of elasticity,

α = Coefficient of thermal expansion,

ΔT = Temperature difference between inner and outer surfaces of cladding,

ν = Poisson's ratio,

σ_θ = Hoop stress, and

σ_z = Longitudinal stress.

For thin wall cylinders ΔT may be written as

$$\Delta T = \frac{q}{A}\,\frac{h}{K}, \tag{6}$$

TABLE 3-1

STRESS ANALYSIS AND FISSION GAS STRESS LIMITS FOR CENTERMELT FUEL OPERATING AT MAXIMUM OVERPOWER (550,000) Btu/h-ft^2 AND END-OF-LIFE

Fuel Type	Critical Collapse Pressure for Yielding at 900°F (psia)	Compressive Hoop Stress Due to External Pressure[1] (psi)	Thermal Gradient Stress in Cladding Wall (psi)	Allowable Equivalent Tensile Stress Due to Internal Pressure[2] (psi)	Total Tensile Stress in Cladding[3] (psi)
0.570-inch-o.d. 95% Dense Pellet	2120	5750	±4980	14,500	13,730
0.570-inch-o.d. 85% Dense Powder	2120	5750	±4980	14,500	13,730
0.700-inch-o.d. 95% Dense Pellet	2030	6320	±5850	14,250	13,780
0.700-inch-o.d. 85% Dense Powder	2030	6320	±5850	14,250	13,780

(1) Equivalent to 900 psia external pressure at overpower and end-of-life.

(2) The maximum allowable tensile stress in the cladding wall for design purposes is set at two-thirds ultimate at 900° F, or 14,350 psi. This assumes no increase in mechanical strength due to irradiation, but implies that the cladding will have very low ductility at end-of-life.

(3) Summation of external pressure stress, thermal stress, and internal pressure stress

where

$\left(\frac{q}{A}\right)$ = Heat flux through cladding,

K = Thermal conductivity coefficient, and

h = Cladding wall thickness.

One of the objectives of the program is to maintain heat flux at the nominal rated level of 450,000 Btu/h-ft^2 throughout life. The design limit, however, is based upon overpower conditions (550,000 Btu/h-ft^2). The thermal stress results are also indicated in Table 3-1.

3.5.3 Other Miscellaneous Stresses

The design must consider all forces which may cause significant stress levels during the life of the fuel rods. However, some of these forces are quite complex and are not presently amenable to quantitative evaluation. Two such factors are residual stresses and local fuel-to-cladding interactions.

Residual stresses have been handled by stipulation of the tube stress relief process during fabrication, and should be substantially eliminated. Uniform fuel-to-cladding interaction has been excluded in the centermelt fuel by deliberately including sufficient cold gap to compensate for differential thermal expansion and fission swelling. In addition, the UO_2 phase change volume expansion upon melting has been compensated by fabricating the pellet fuel with a hollow central core or with dishes, while the low density powder fuel inherently has sufficient free void space to accommodate the expansion. Only the localized pellet interface interaction and resulting stresses are expected during actual operation and, hopefully, the large initial gap will minimize them.

3.5.4 Combination of Stresses

The most important factor affecting the level of tensile stress in the cladding is the release of fission gases. This factor, in turn, can be directly controlled by the plenum volume provided to accommodate the gas. Thus, the end-of-life stress due to internal pressure is the dependent variable, and the allowable stress value can be determined by properly calculating the combined stress from external pressure, thermal gradients, residual stresses, and fuel cladding interaction. This algebraically and geometrically combined stress value is then subtracted from the the design strength of the material to solve for the allowable internal pressure stress.

Using this procedure, the allowable stress due to internal pressure for the intermediate thermal performance fuel was established as 14,500 psi, and 14,250 psi for the advanced thermal performance fuel (Table 3-1).

The design yield strength for Zircaloy-2 was applied, for the above calculation, with a rather large factor of safety. The design strength used for the cladding was two-thirds the ultimate strength at 900°F (the maximum conceivable average cladding temperature under adverse conditions at end-of-life). Irradiation hardening was not considered to affect the ultimate and yield strength for design purposes.

3.6 FISSION GAS ANALYSIS

The allowable upper limit above for cladding stress caused by release of fission gases and volatile gases in the UO_2 was determined independently of the gas release analysis. The fission gas analysis problem, therefore, was one of determining the fission gas release for end-of-life conditions and then sizing the fission gas plenum to accommodate this quantity without overstressing the cladding. The design method for calculating fission gas release assumes that the maximum surface heat flux at end-of-life is 550,000 Btu/h-ft^2 (overpower), 20,000 MWd/T average burnup has been achieved, crud and oxide deposition are a maximum, and the fuel cladding interface heat transfer coefficient is a minimum. With these assumptions, the factors that affect fission gas release and internal pressure buildup were maximized. This procedure should provide an adequate margin of safety for normal operation at 450,000 Btu/h-ft^2.

The model used to calculate the fission gas release is based upon the following assumptions:

a. Volatile impurities and moisture are released in the same manner as fission gas.

b. At UO_2 temperatures greater than 3000°F, 100 percent fission gas and volatiles are released; at UO_2 temperatures below 3000°F, 4 percent is released.

c. All released gas eventually accumulates in the plenum void space. The value assumed for residual gas and moisture in the UO_2 was 100 μl/gm.

The fission gas analysis of the worst case fuel rod was made on a two-dimensional basis. The rod was divided into 20 axial nodes. The peak node was assumed to operate at 550,000 Btu/h-ft^2 at end-of-life. The remaining nodes were assumed to vary with the nominal shape of the axial neutron flux profile at end-of-life (Figure 3-2). The axial exposure distribution is based on the curve shown in Figure 3-3. The radial temperature profile was calculated using the $\int$kdT method. The thermal conductivity integral to melting for pellet fuel was assumed to be 92.5 W/cm, and the pellet-to-cladding interface conductivity used was 1000 Btu/h-ft^2/°F. The integral thermal conductivity used for powder fuel was 63.5 W/cm and the interface conductivity was 1000 Btu/h-ft^2/°F. The data for each node were summed, and an average release fraction for the rod was established. The results of the analysis are presented in Table 3-2.

3.7 FUEL THERMAL ANALYSIS

A thorough analysis was made to predict the temperatures of the fuel and cladding as a function of time in reactor. The average temperature of fuel and cladding increases during the irradiation from the combined effects of scale and oxide deposition on the cladding heat transfer surface. The program performance requirement that fuel operate near peak heat flux conditions throughout life serves to exaggerate this effect. The primary concern caused by the high cladding temperature is reduced cladding strength. Therefore, the stress limits on the cladding dictate that thermal conditions be predicted as accurately as possible. Deposition of scale was assumed to be 0.4 mil/yr at full power operation. The corrosion rate of Zircaloy-2 was assumed to vary as a function of the cladding surface temperature.[4,5] These data were used to establish a surface heat transfer coefficient which varied as a function of elapsed, equivalent full power operation in reactor.

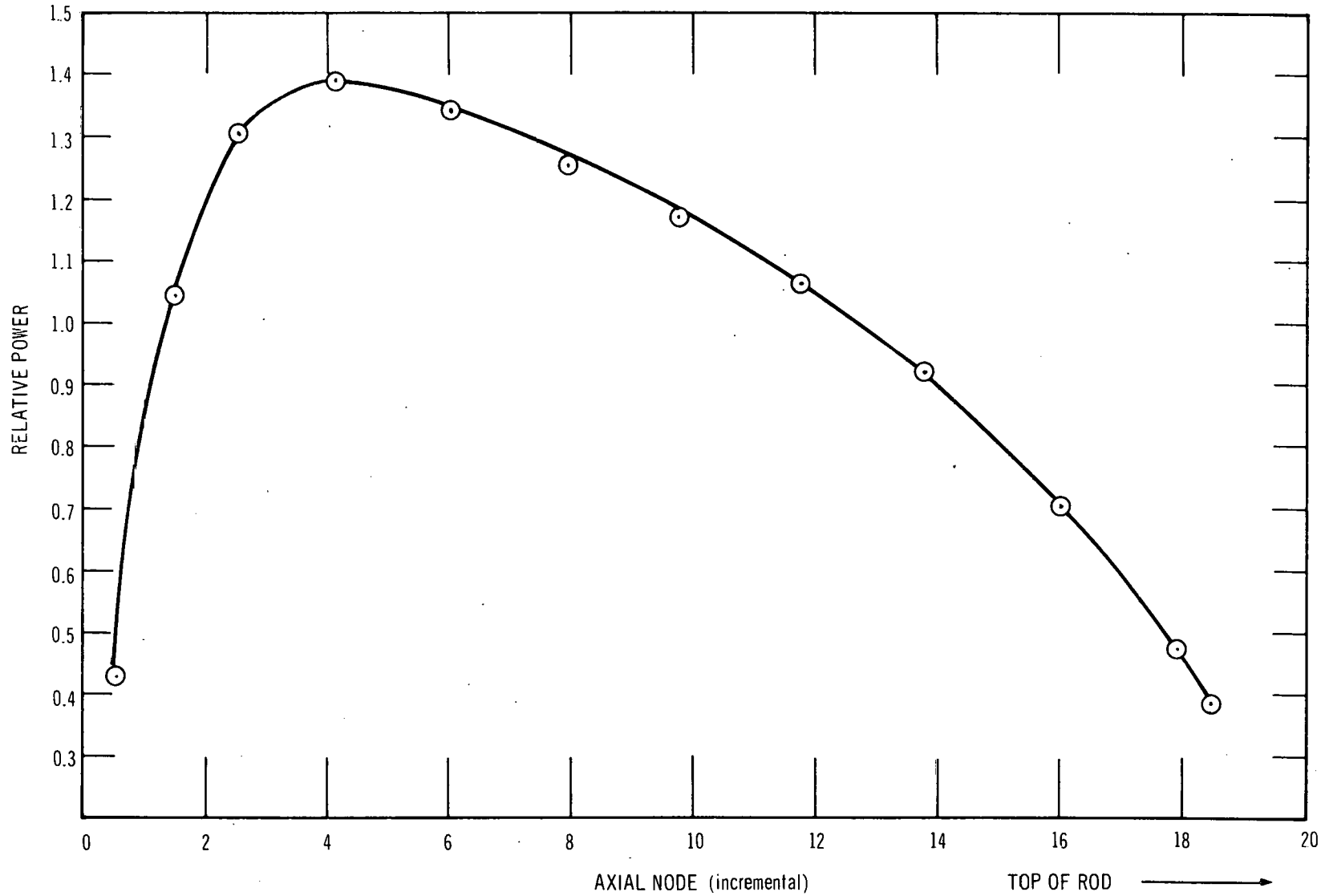

FIGURE 3-2. PREDICTED AXIAL RELATIVE POWER AT END OF CYCLE (BASIS FOR FISSION GAS RELEASE CALCULATIONS)

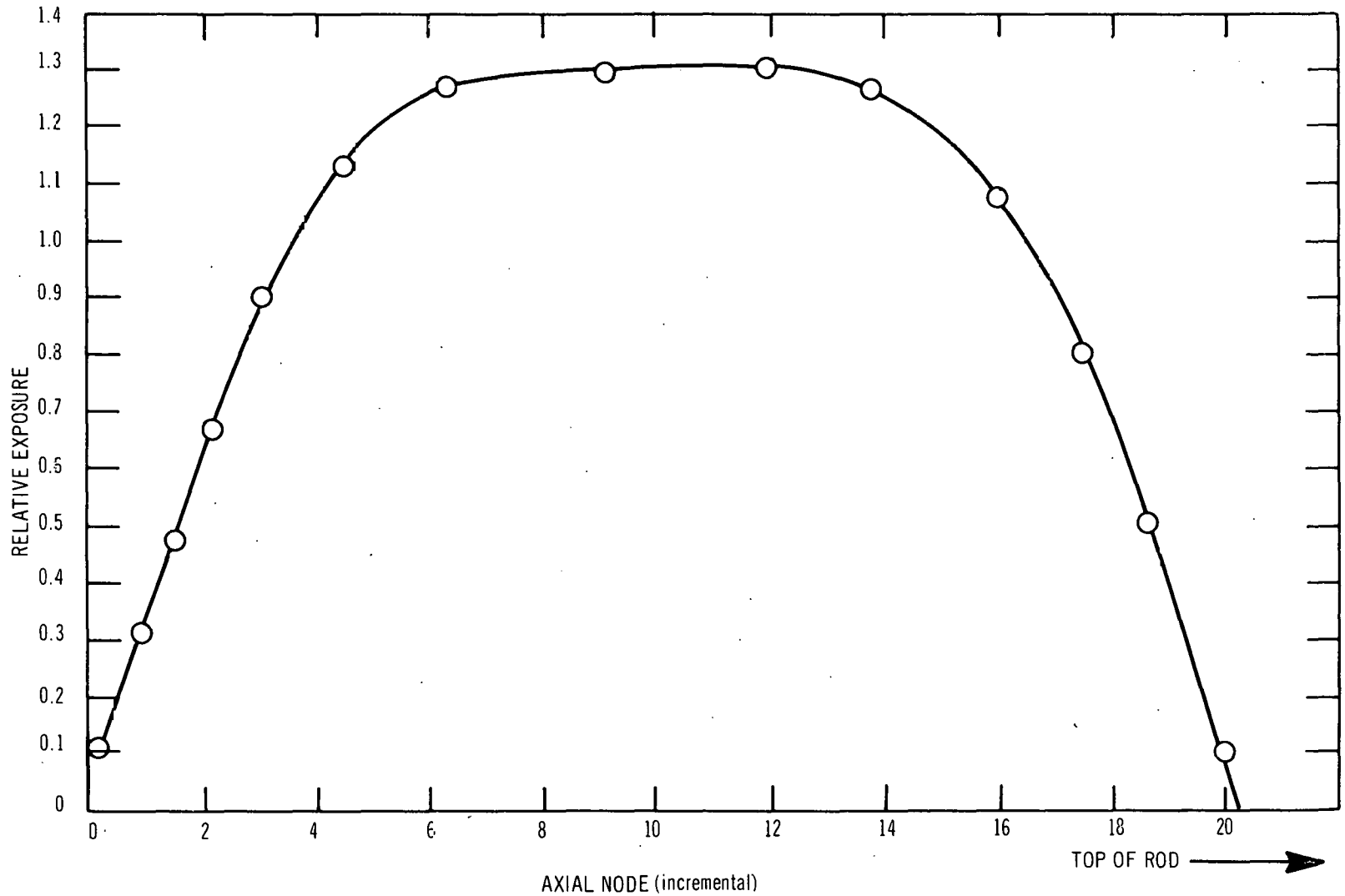

FIGURE 3-3. PREDICTED AXIAL BURNUP DISTRIBUTION

TABLE 3-2

RESULTS OF FISSION GAS RELEASE ANALYSIS PEAK Q/A=550,000 Btu/h-ft^2, 20,000 MWd/T AVERAGE EXPOSURE

Fuel Group	Rod o.d.	Fuel Type	lb-Moles of Fission Gas Produced	lb-Moles of Fission Gas Released	Total lb-Moles Gas Released*	Percent Release	Plenum Volume Required (in.^{3})	Plenum Length (inches)
A	0.570	Pellet	0.000129	0.0000545	0.0000585	43	1.164	6.0
	0.570	Powder	0.000121	0.0000674	0.0000722	56	1.40	7.0
B	0.700	Pellet	0.000199	0.000100	0.000107	51	2.19	7.25
	0.700	Powder	0.000186	0.000118	0.000126	64	2.54	8.0

*Includes volatile gases and water (100 μl/gm of UO_2) as well as fission gas.

The fuel-to-cladding gap heat transfer coefficient was assumed to decrease with exposure as a result of dilution of the helium internal atmosphere by fission gas. The gap coefficient assumed for pellet fuel decreases from 1500 Btu/h-ft^2°F at beginning-of-life to 1000 Btu/h-ft^2°F after one cycle of operation and remains constant at this value thereafter. The powder rod interface coefficient was assumed to be 2000 Btu/h-ft^2 at beginning-of-life and to decrease in steps to 1250 Btu/h-ft^2 at 10,000 MWd/T_e. It then further decreases to a constant value of 1000 Btu/h-ft^2 for 15,000 MWd/T and beyond.

3.7.1 UO_2 Thermal Conductivity

The UO_2 thermal conductivities used in this analysis were as follows:

Pellet Fuel:

$$K(T) = \frac{38.24}{402.4 + T} + 6.1256 \times 10^{-13} (T + 273)^3. \quad (7)$$

This equation results in an $\int_0^{2800°C} kdT = 93$ W/cm, and $\int_{500°C}^{2800°C} kdT = 62$ W/cm.

Powder Fuel:

$$K(T) = \frac{48.39}{1458.6 + T} + 5.2922 \times 10^{-13} (T + 273)^3. \quad (8)$$

This equation results in an $\int_0^{2800°C} kdT = 63$ W/cm and $\int_{500°C}^{2800°C} kdT = 49$ W/cm.

The $\int kdT$ curves for pellets and powder versus temperature are plotted in Figure 3-4. The pellet $\int kdT$ curves are from Lyons, et al.[6] The powder $\int kdT$ meets the constraints suggested by D. H. Coplin in Reference (7), and also agrees with post-irradiation measurement data points in Reference (7), Figure 7-3. The slope of the powder integral curve is essentially identical to that for sintered pellet UO_2 above 1500°C by virtue of the assumptions in the curve derivation.

3.7.2 General Results

The analysis results for the cladding and UO_2 temperature, and for the UO_2 thermal expansion are presented graphically for each fuel type, i.e., 0.570-inch-o.d. pellet, 0.570-inch-o.d. powder, etc. The cladding average temperature as a function of heat flux is shown in Figures 3-5, 3-8, 3-11, and 3-14; the fuel centerline temperature in Figures 3-6, 3-9, 3-12, and 3-15; and the UO_2 melt fraction variation with heat flux is shown in Figures 3-7, 3-10, 3-13, and 3-16.

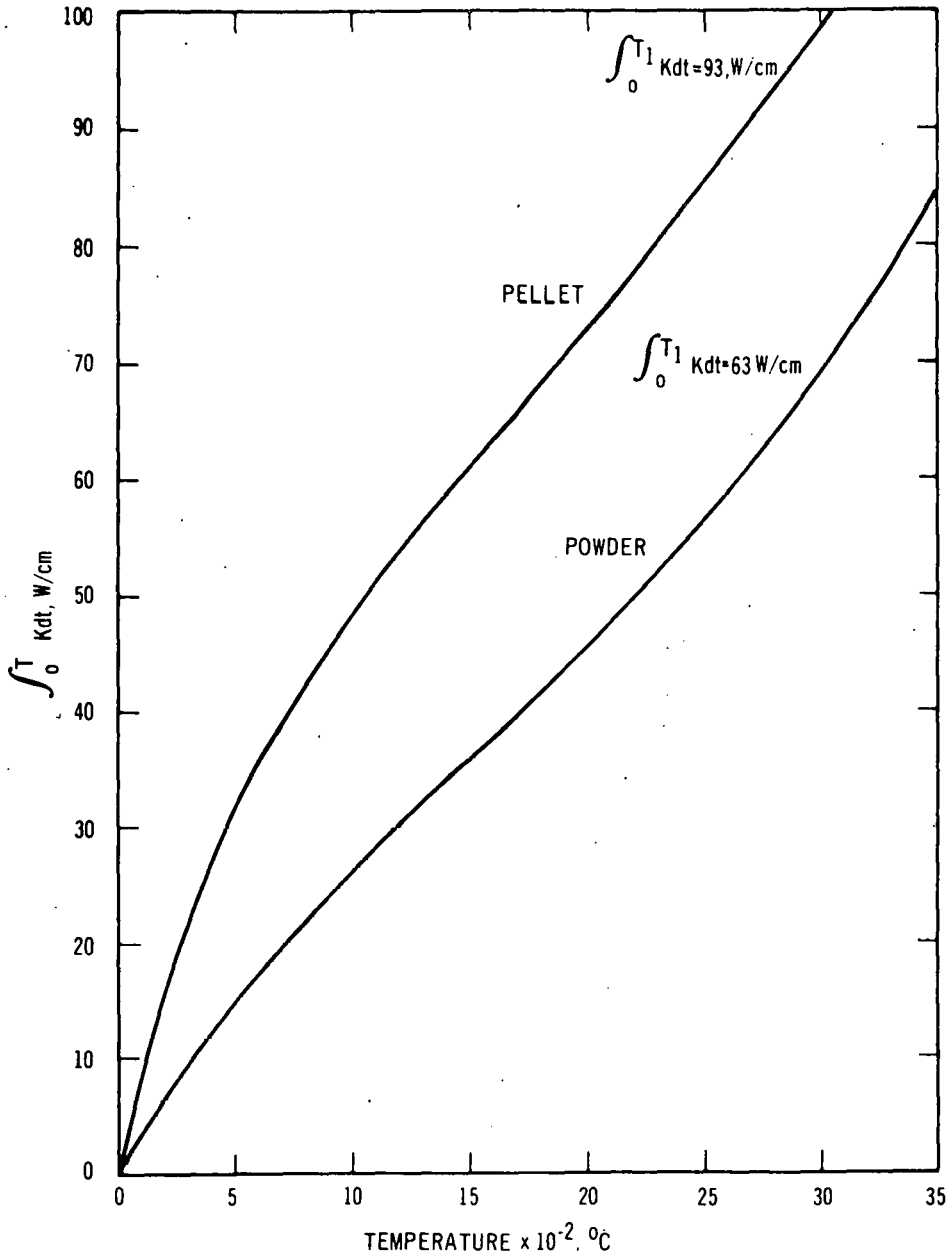

FIGURE 3-4. $\int$Kdt VERSUS TEMPERATURE

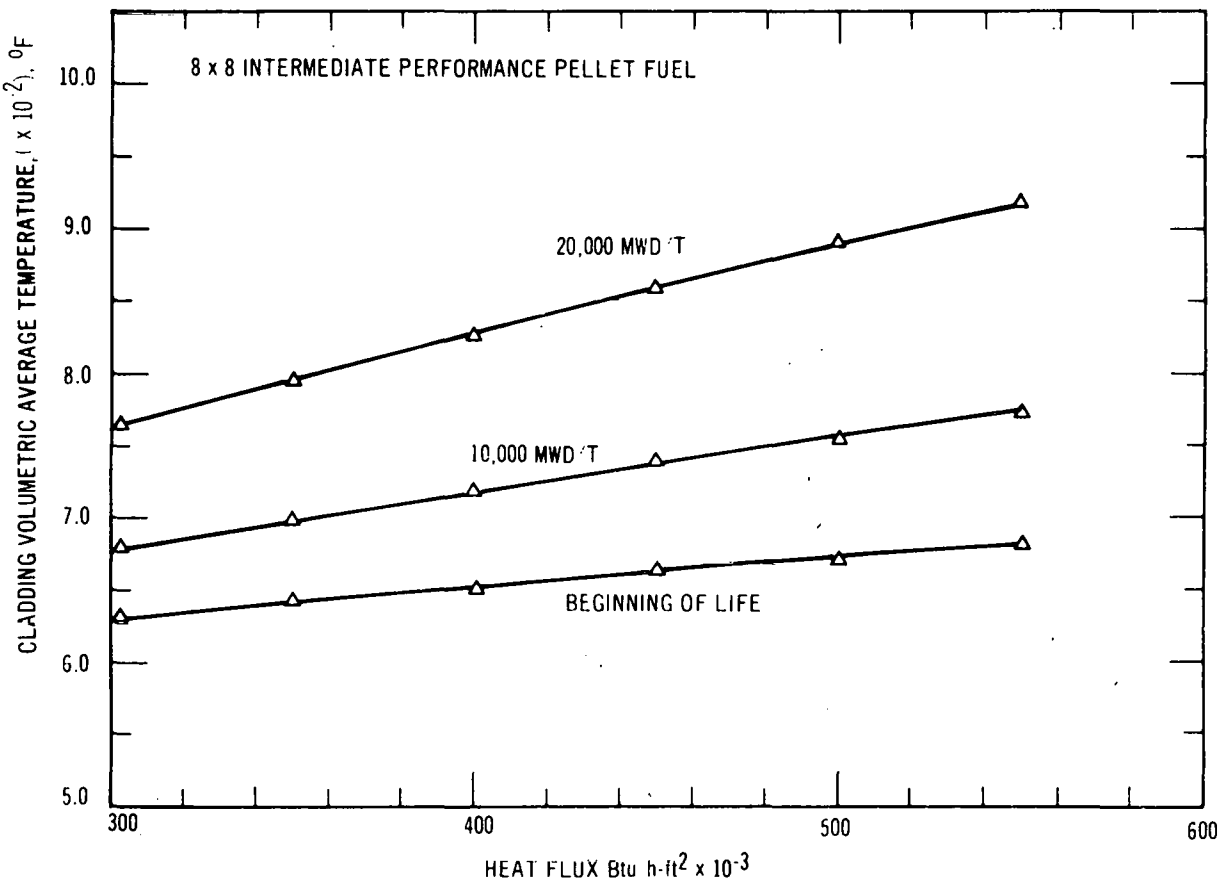

FIGURE 3-5. CLADDING VOLUMETRIC AVERAGE TEMPERATURE VERSUS HEAT FLUX

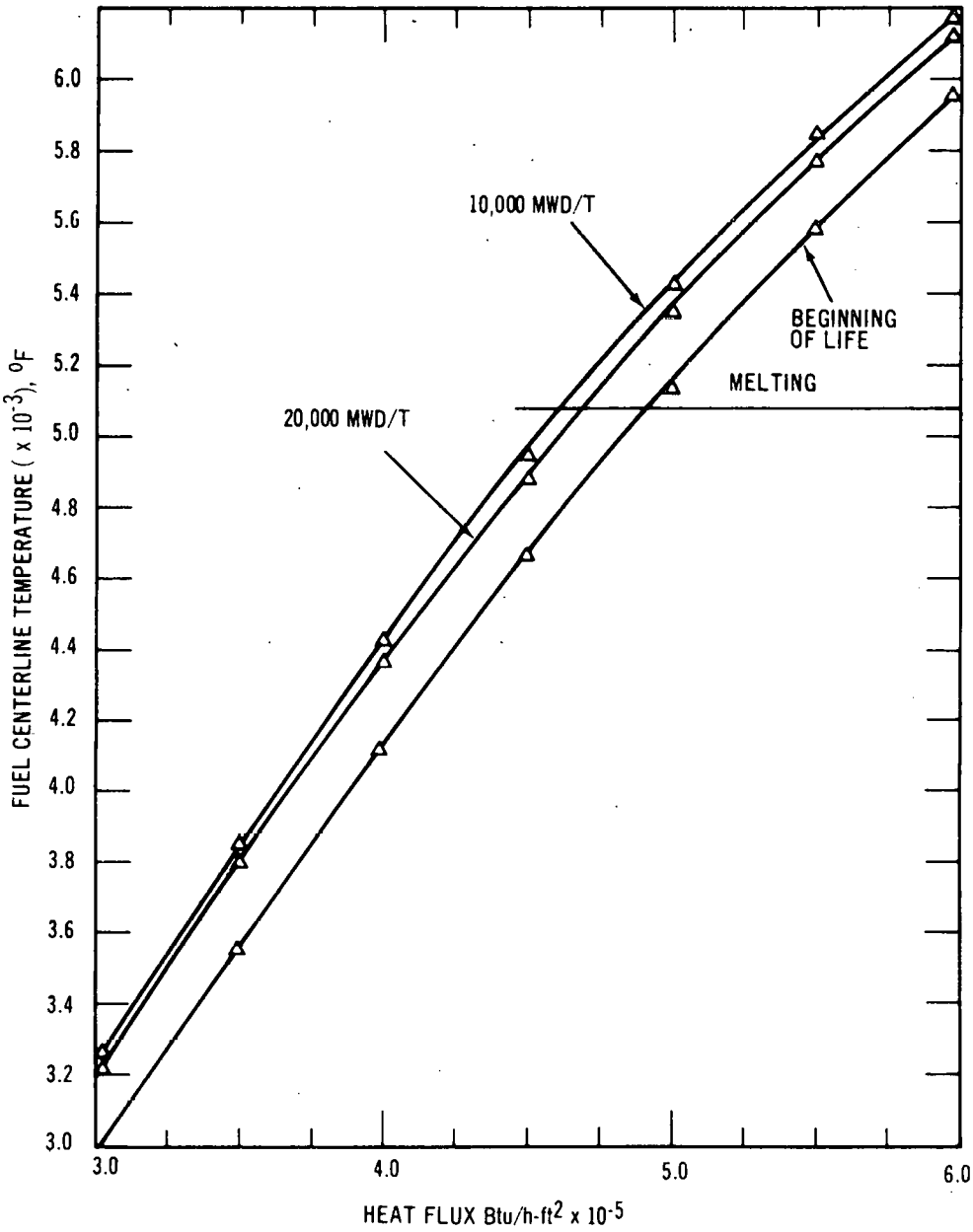

FIGURE 3–6. FUEL CENTERLINE TEMPERATURE VERSUS HEAT-FLUX, INTERMEDIATE PERFORMANCE PELLET FUEL

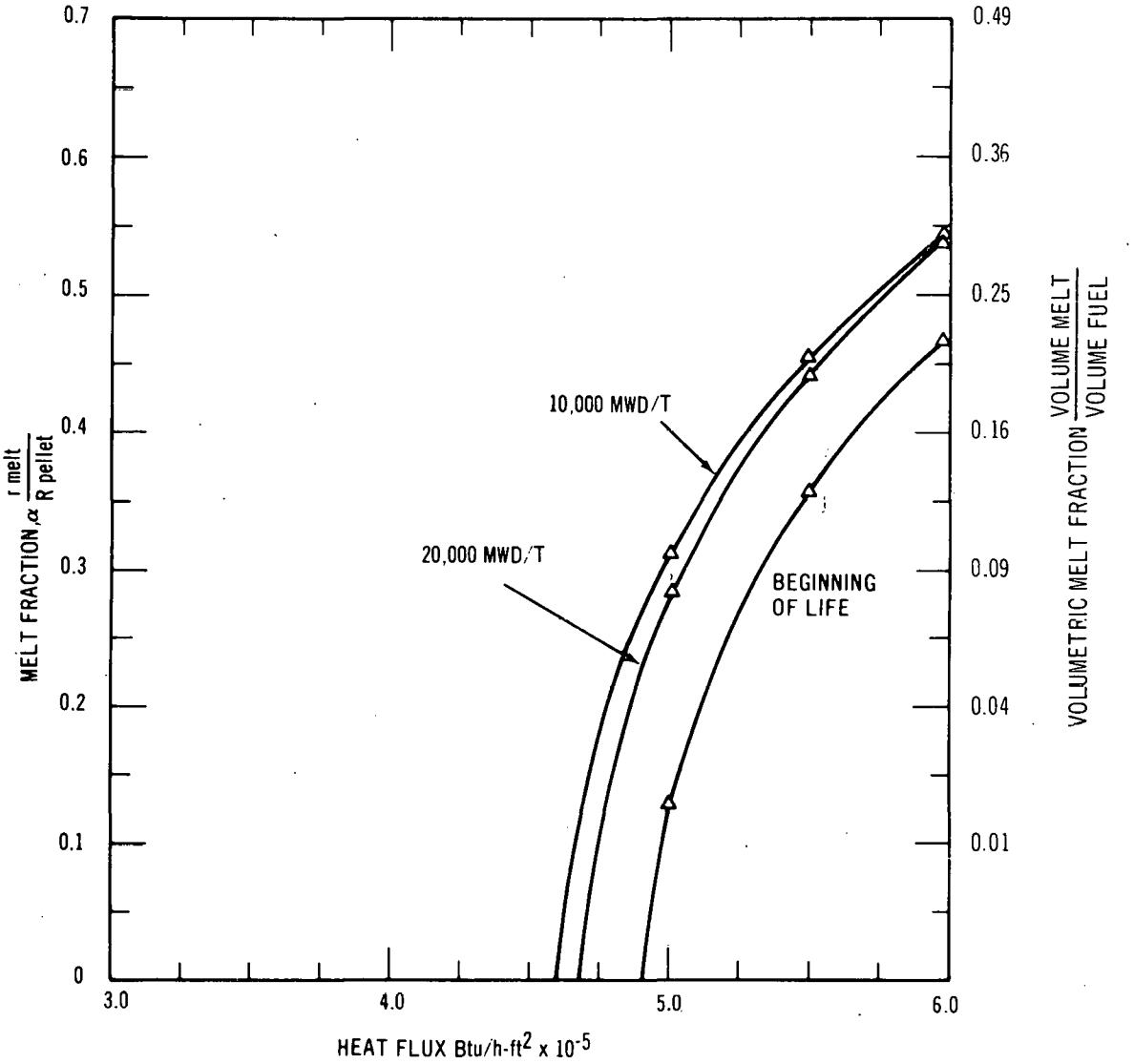

FIGURE 3-7. MELT FRACTION VERSUS HEAT FLUX - INTERMEDIATE PERFORMANCE PELLET FUEL

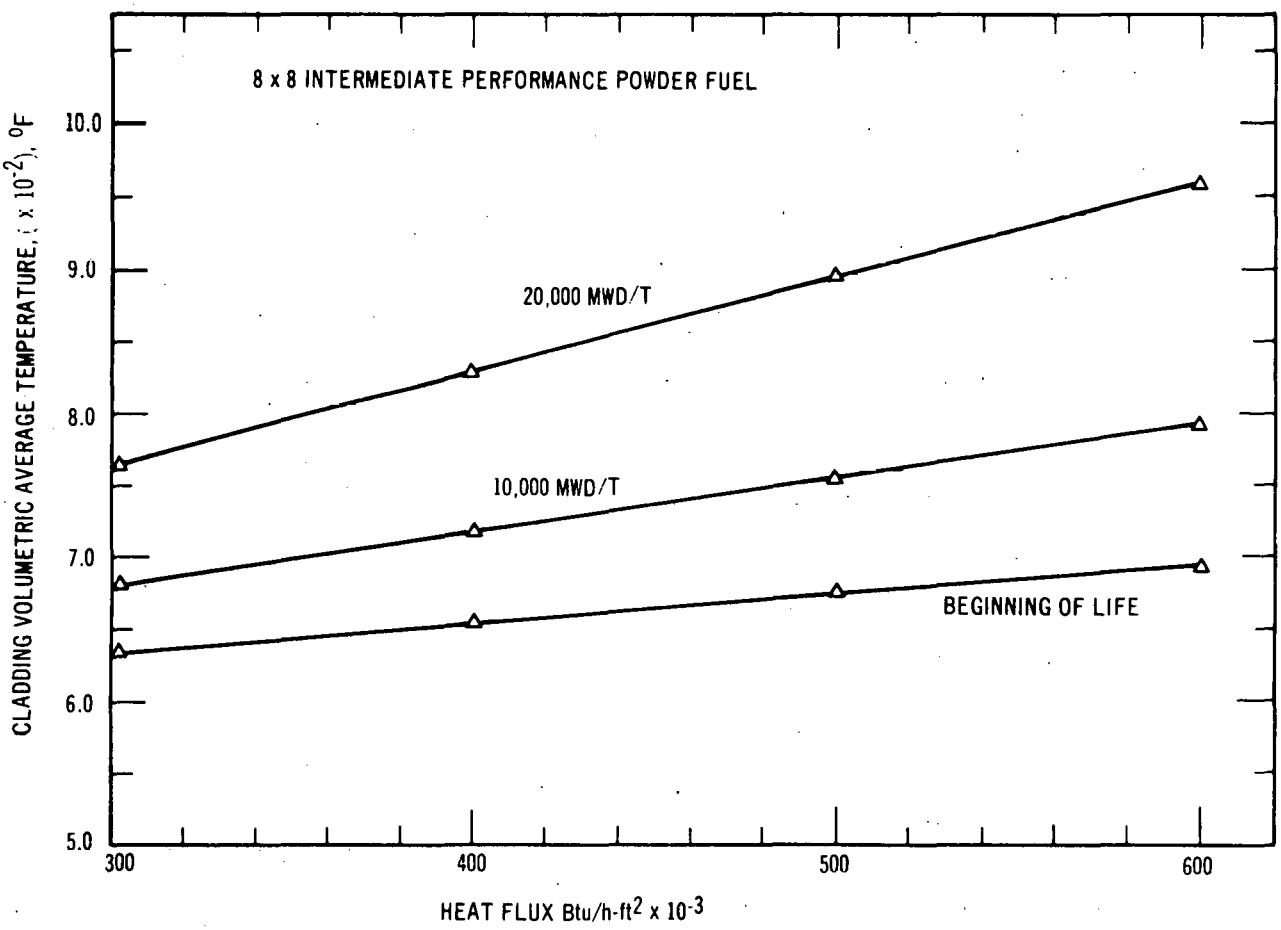

FIGURE 3-8. CLADDING VOLUMETRIC AVERAGE TEMPERATURE VERSUS HEAT FLUX

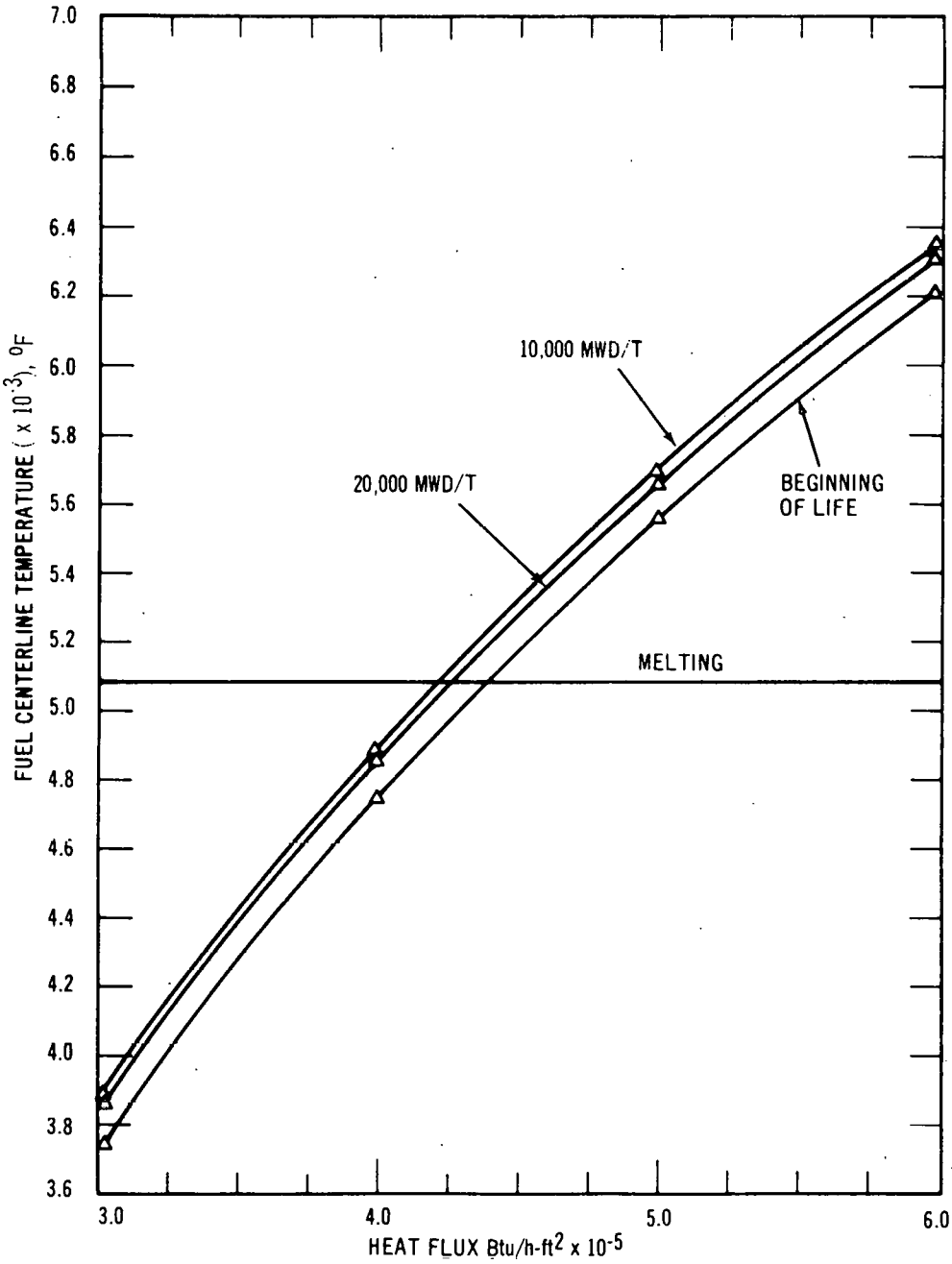

FIGURE 3-9. FUEL CENTERLINE TEMPERATURE VERSUS HEAT FLUX - INTERMEDIATE PERFORMANCE POWDER FUEL

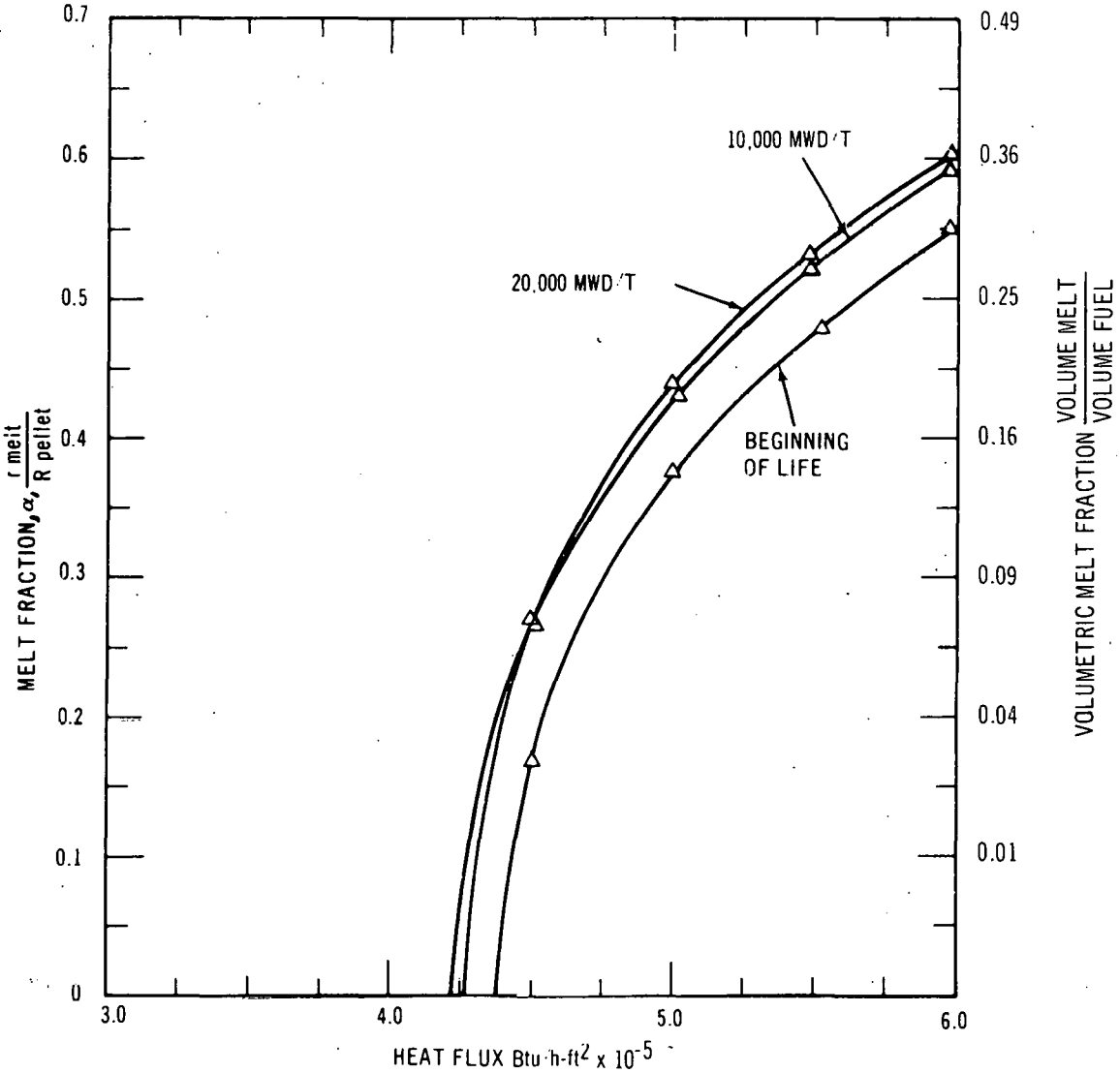

FIGURE 3-10. UO_2 MELT FRACTION VERSUS HEAT FLUX - INTERMEDIATE PERFORMANCE FUEL – POWDER

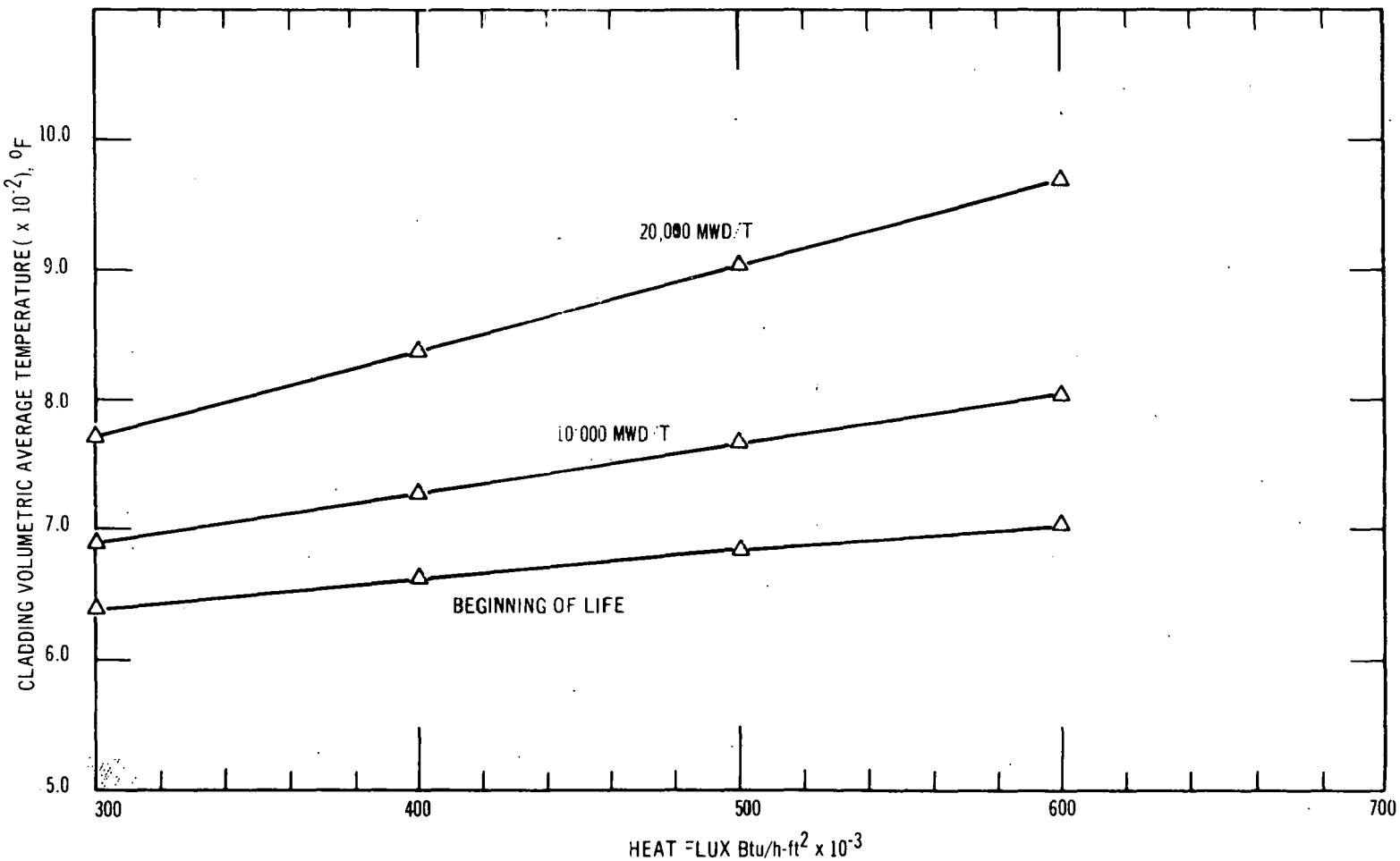

FIGURE 3-11. CLADDING VOLUMETRIC AVERAGE TEMPERATURE VERSUS HEAT FLUX 7x7 ADVANCED PERFORMANCE POWDER FUEL

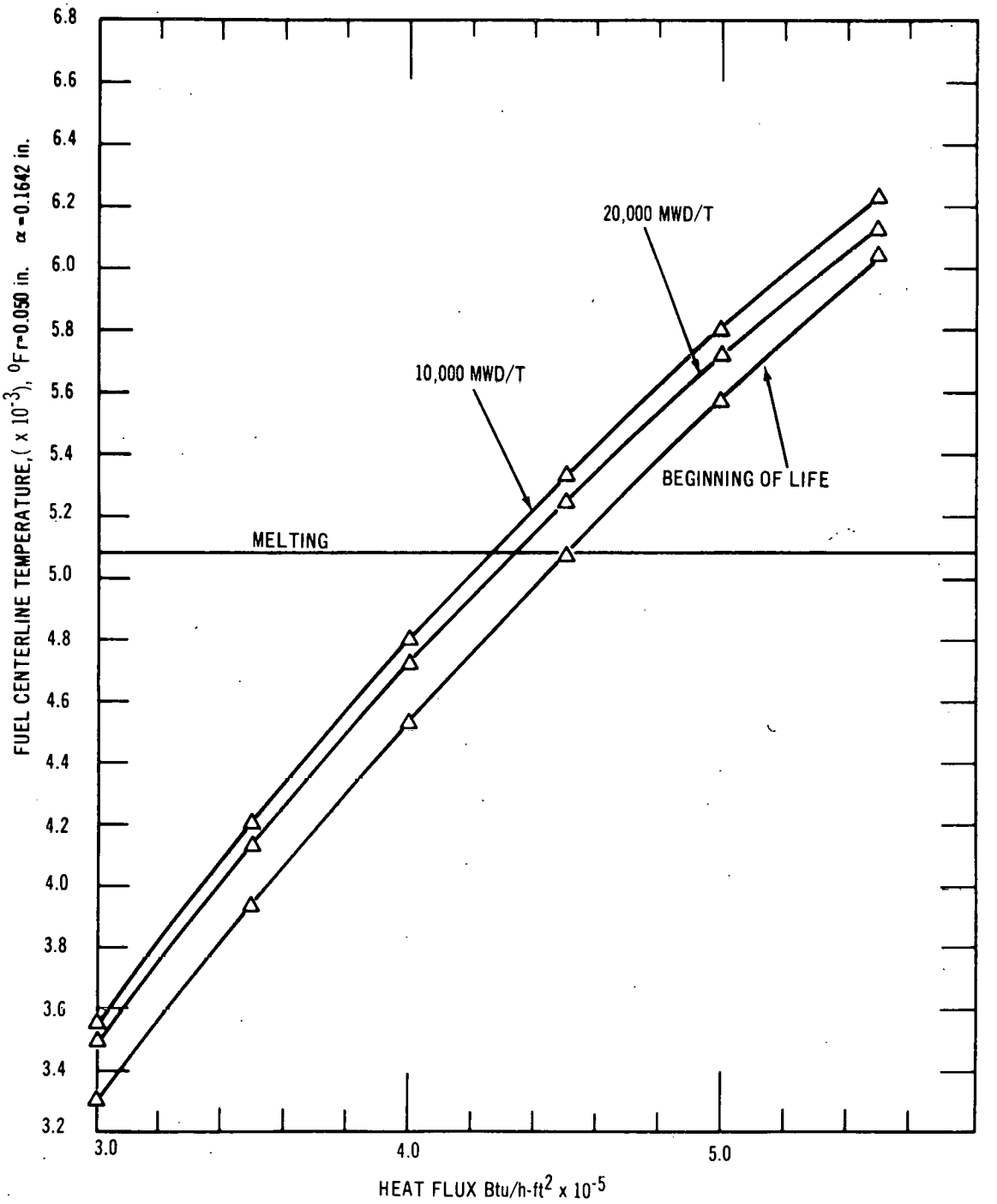

FIGURE 3–12. FUEL TEMPERATURE VERSUS Q/A, HIGH PERFORMANCE PELLET FUEL

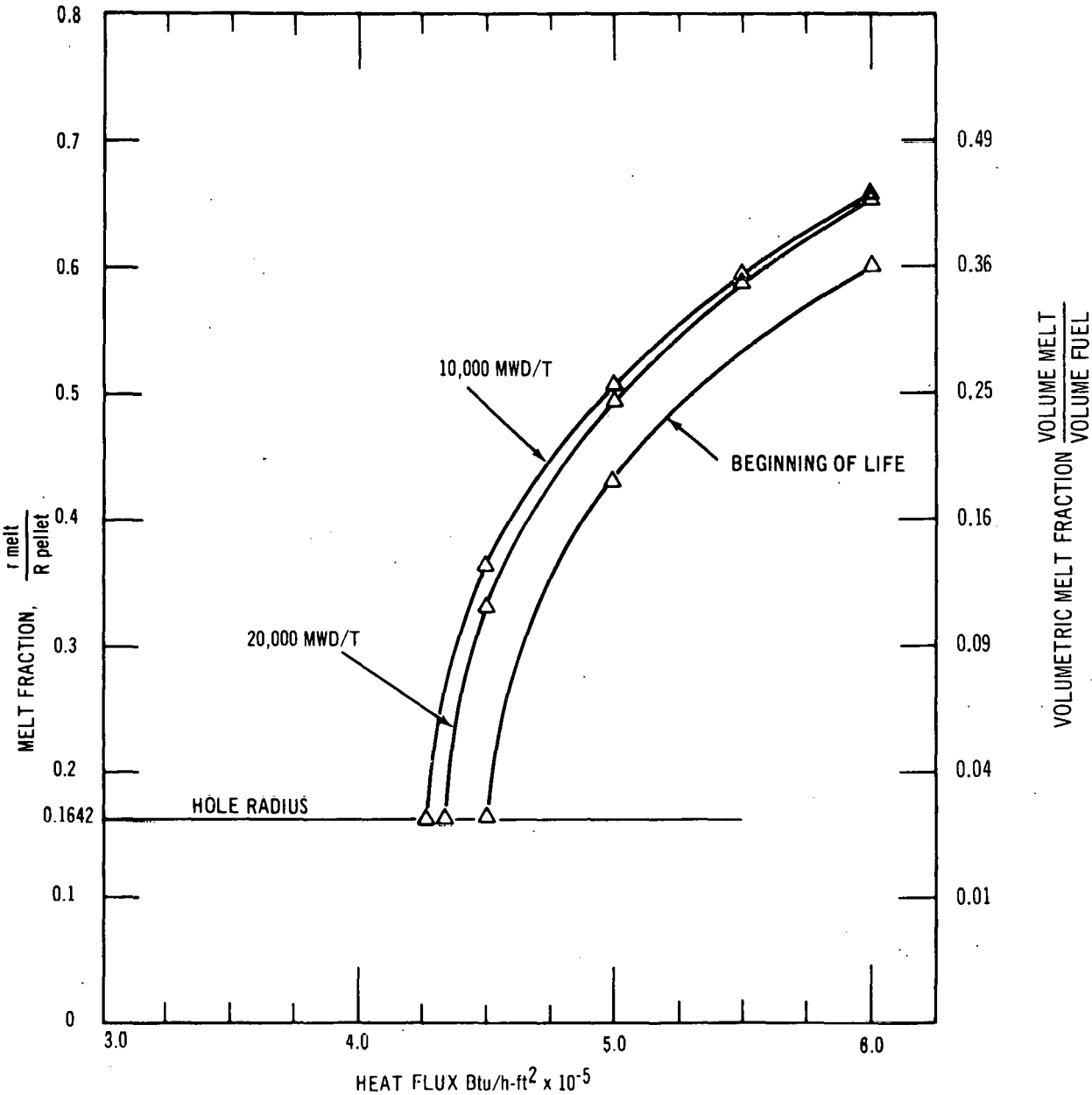

FIGURE 3-13. UO_2 MELT FRACTION VERSUS HEAT FLUX, HIGH PERFORMANCE PELLET FUEL, 0.100 in. CENTERLINE HOLE, $\alpha = 0.1642$

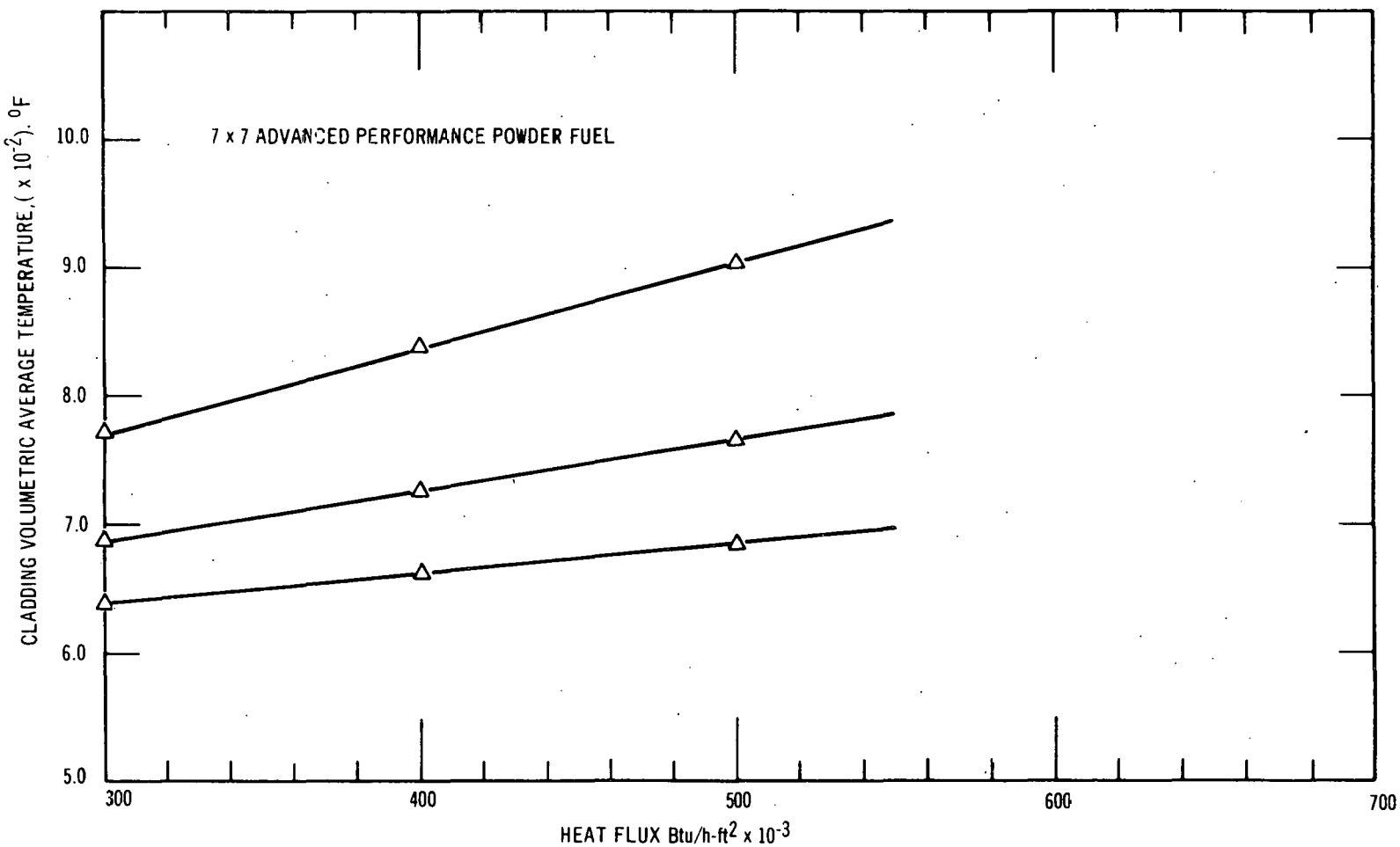

FIGURE 3-14. CLADDING VOLUMETRIC AVERAGE TEMPERATURE VERSUS HEAT FLUX

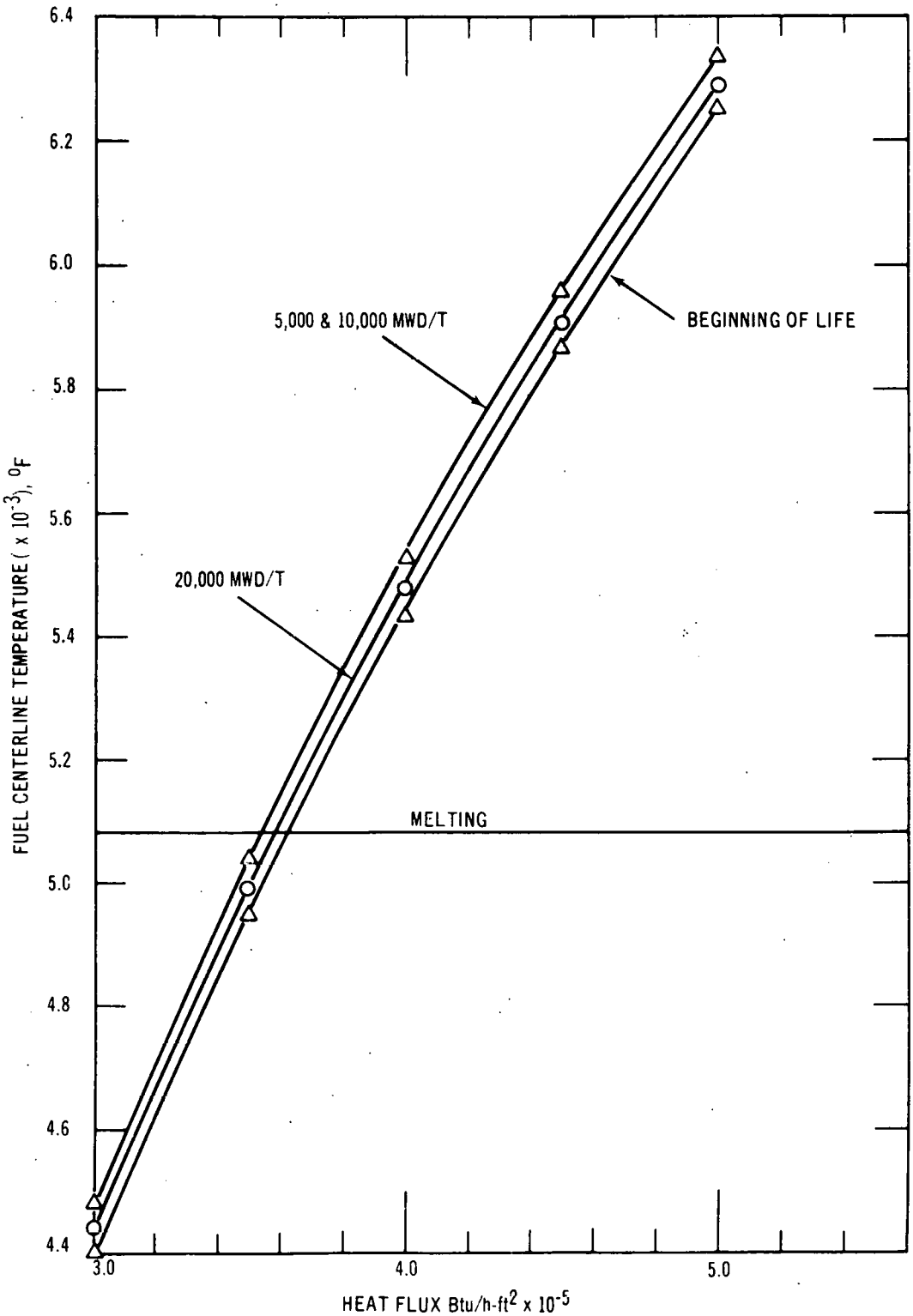

FIGURE 3-15. FUEL CENTERLINE TEMPERATURE VERSUS Q/A, HIGH PERFORMANCE POWDER FUEL

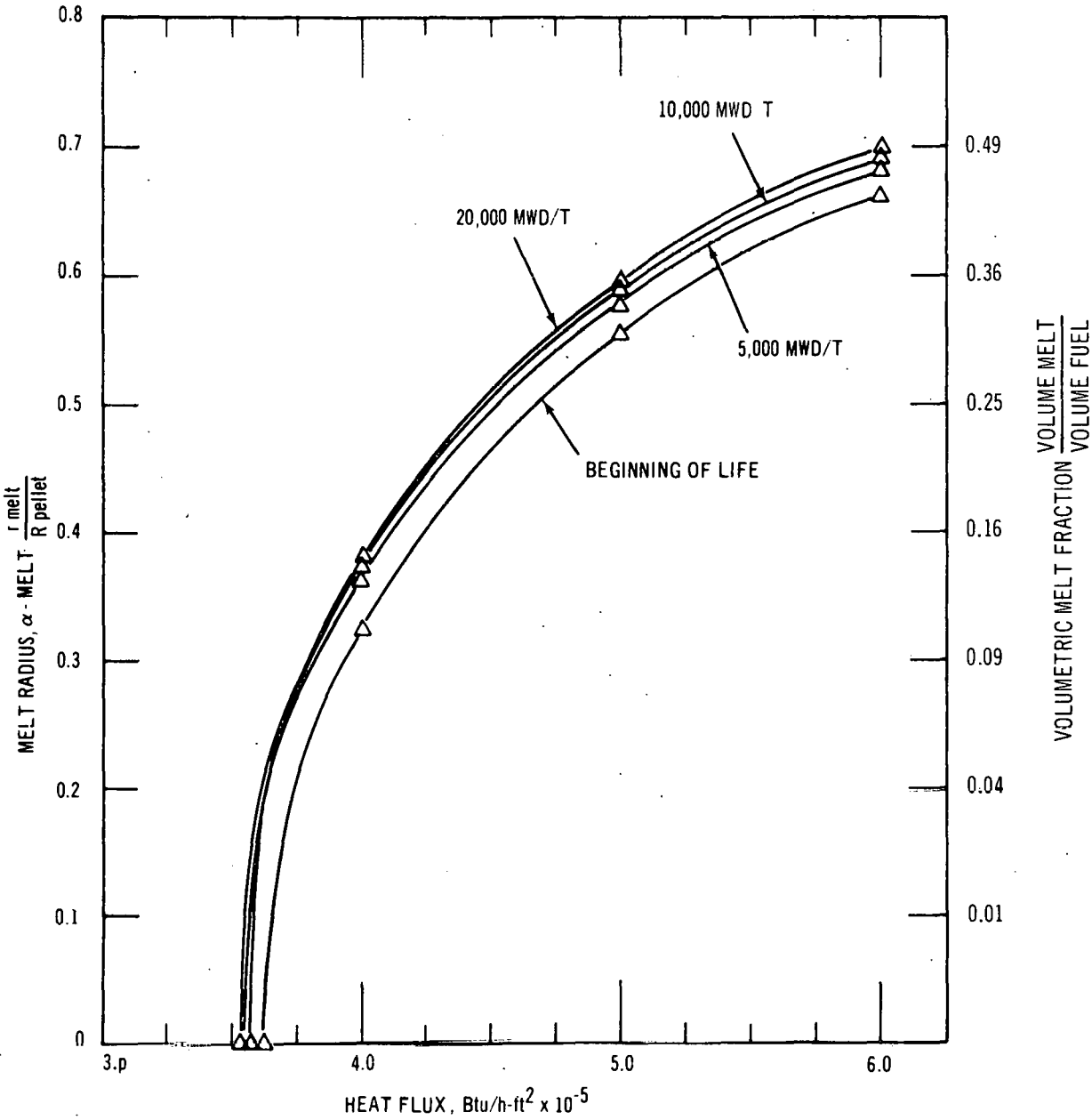

FIGURE 3-16. UO_2 MELT FRACTION VERSUS HEAT FLUX, HIGH PERFORMANCE POWDER FUEL

In reviewing Figures 3-7, 3-10, 3-13, and 3-16, it can be noted that the heat flux required for incipient melting at beginning-of-life varies from approximately 495,000 Btu/h-ft^2 (Figure 3-7) for the intermediate performance pellet fuel to 360,000 Btu/h-ft^2 for the advanced performance powder fuel. To actually achieve incipient melting in the intermediate performance pellet fuel, it is necessary to operate with heat fluxes as high as 500,000 Btu/h-ft^2 rather than 450,000 Btu/h-ft^2. Therefore, with the 1.22 overpower factor applicable in the Consumers Big Rock Point reactor, it is necessary to evaluate the fuel for a beginning-of-life heat flux at overpower of 610,000 Btu/h-ft^2 and an end-of-life heat flux of 575,000 Btu/h-ft^2 (470,000 Btu/h-ft^2 rated power - Figure 3-7), whichever is the most limiting. The higher heat flux values are not of concern from the standpoint of direct damage to the fuel, since the design margins accommodate even higher heat flux values. (See subsection 3.7.5, Fuel Damage Limits). However, the MCHFR for the bundle cannot be maintained greater than 1.5 for all possible axial power shapes encountered in BRP. During the course of the irradiations, the allowable rated power peak heat flux will be calculated before each cycle based on the actual axial power shape predicted for the specific BRP core loading. Occasionally, incipient centralmelting may not be attainable for the intermediate pellet fuel, but the MCHFR criteria always governs.

3.7.3 Linear Heat Generation Required for Melting

Linear Heat generation required to cause melting for three conditions are:

	8 × 8 Bundle		7 × 7 Bundle	
	Pellet	Powder	Pellet*	Powder
Beginning of Life	21.4 kW/ft	19.1 kW/ft	24.2 kW/ft	19.4 kW/ft
10,000 MWd/T	20.1 kW/ft	18.5 kW/ft	22.9 kW/ft	19.0 kW/ft
20,000 MWd/T	20.5 kW/ft	18.7 kW/ft	23.3 kW/ft	19.2 kW/ft

*Value for $\alpha = 0.164$ where $\alpha = \frac{\text{melt radius}}{\text{pellet radius}} \left(\frac{\text{center hole radius}}{\text{pellet radius}} = 0.164 \right)$.

It is evident from the table that for the same linear specific heat generation, a larger percentage of fuel will be molten at intermediate burnup than at beginning-of-life or end-of-life conditions. This is a result of the combined effect of zirconium oxide and crud buildup on the cladding, offset by plutonium buildup in the outer portion of the fuel. In the earlier stages of life, the oxide and crud buildup drives the fuel centerline temperature up, while in later stages of life plutonium contribution to power generation tends to drive the centerline temperature down.

3.7.4 Detailed Temperature Predictions

a. Intermediate Thermal Performance Fuel

Based on the assumptions previously outlined, the predicted cladding temperatures will increase with exposure at the rate shown in Figure 3-17. The increased slope of the curve towards the end-of-life is caused by the inherent exponential effect of higher cladding temperatures on the Zircaloy-2 corrosion rate and oxide thickness increase.

The radial temperature profile across the fuel at the peak heat flux region of the rod is shown in Figure 3-18 for pellet fuel and Figure 3-19 for powder fuel. A general increase in fuel temperatures up to 15,000 MWd/T_e is seen followed by a decrease. The factors

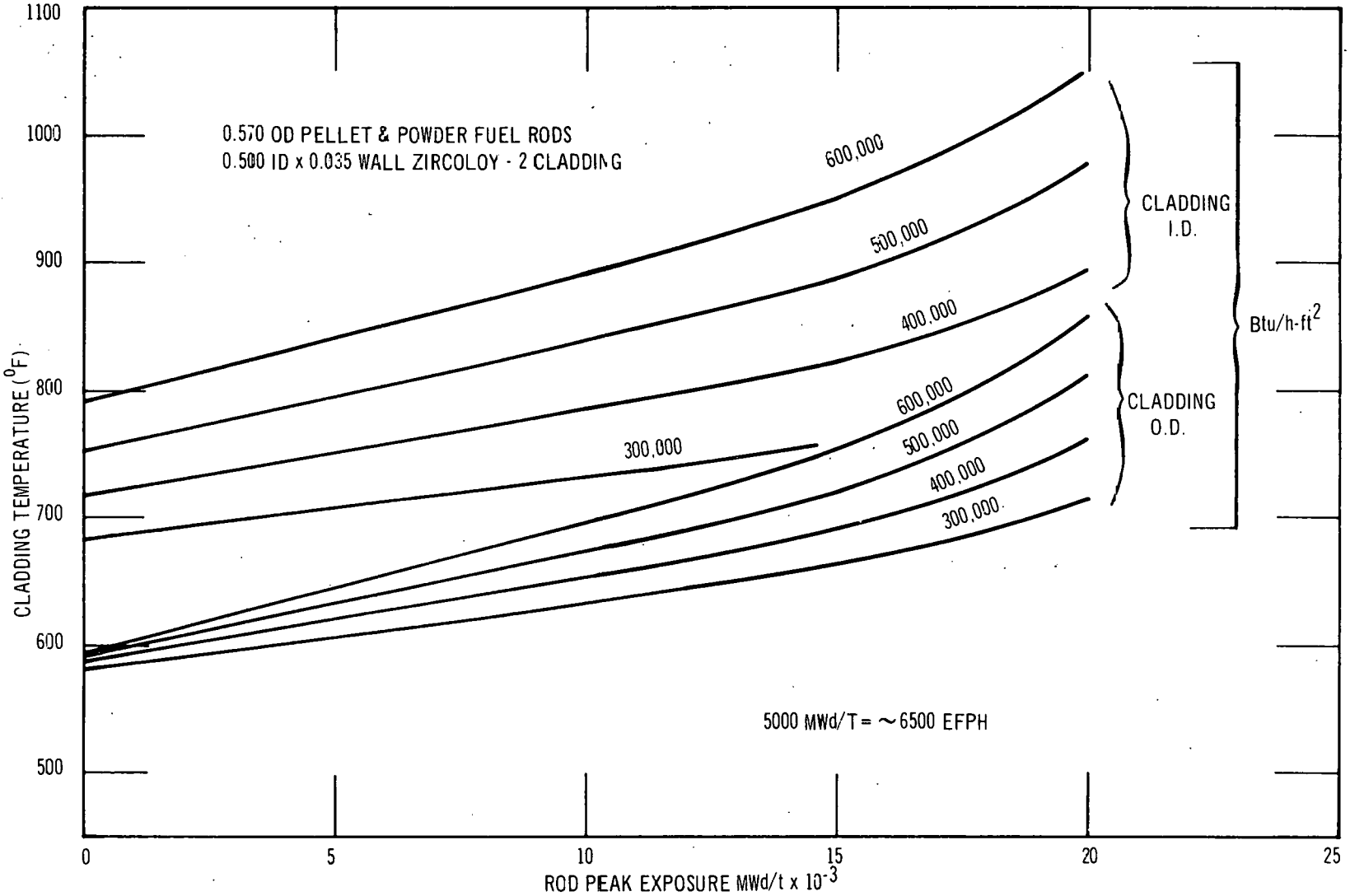

FIGURE 3-17. CLADDING TEMPERATURE VERSUS EXPOSURE AS A FUNCTION OF HEAT FLUX, OXIDE BUILD-UP AND CRUD BUILD-UP (0.4 mil/yr)

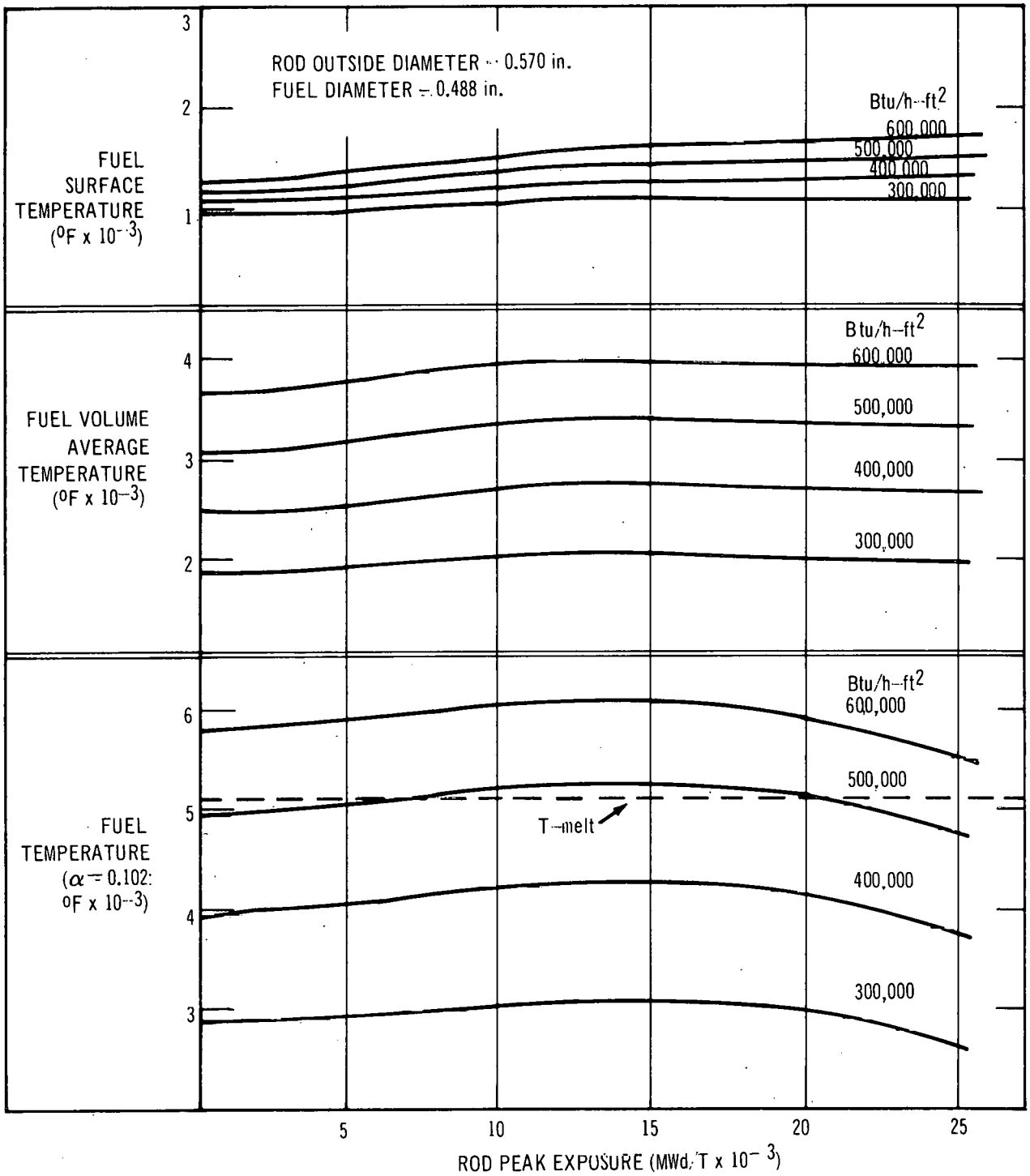

FIGURE 3-18. PELLET FUEL TEMPERATURE VERSUS ROD PEAK EXPOSURE AS A FUNCTION OF HEAT FLUX, OXIDE BUILD-UP AND CRUD BUILD-UP (0.4 mil/yr)

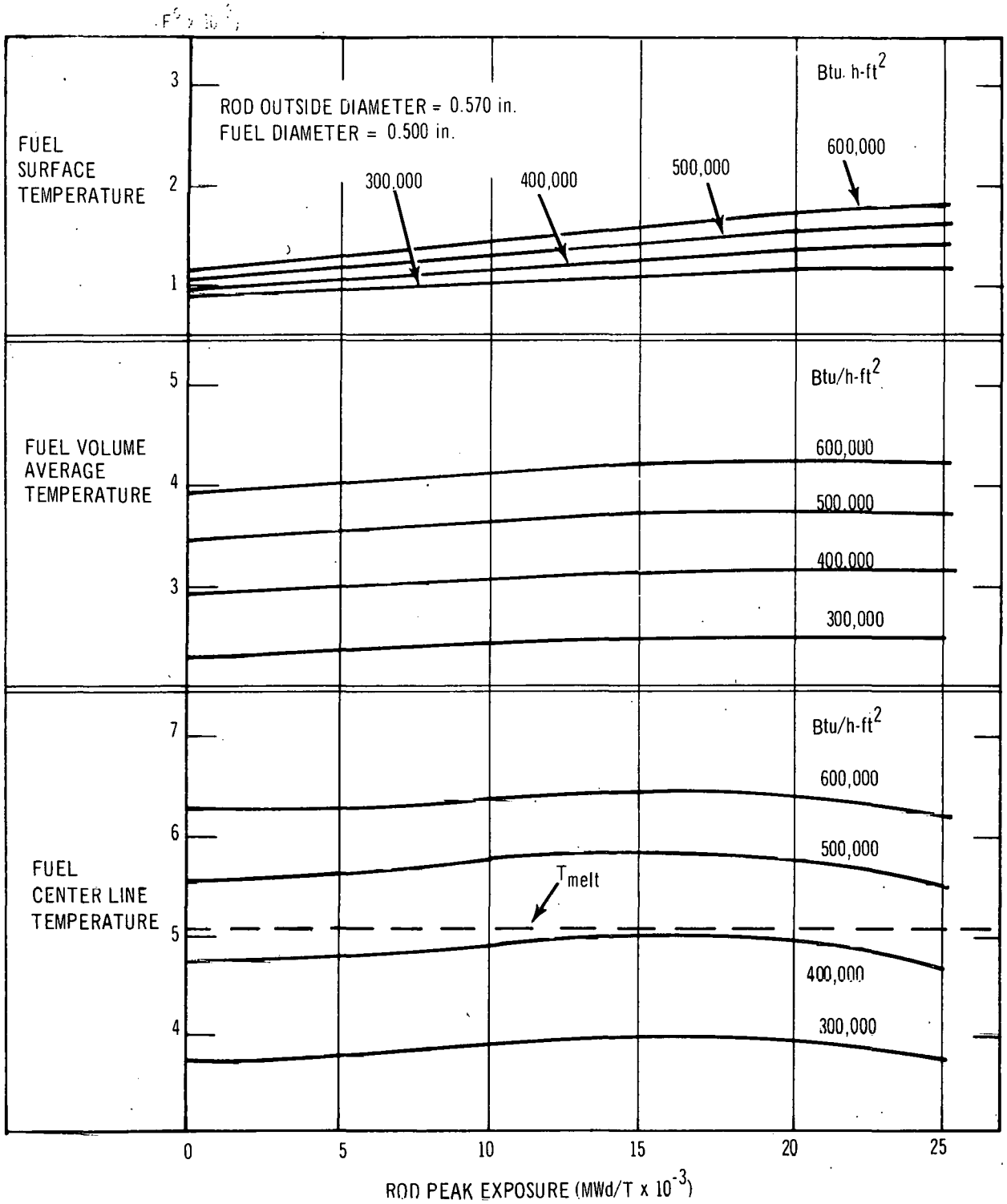

FIGURE 3–19. POWDER FUEL TEMPERATURE VERSUS ROD PEAK EXPOSURE AS A FUNCTION OF HEAT FLUX, OXIDE BUILD-UP AND CRUD BUILD-UP (0.4 mil/yr)

producing this effect have already been noted in the preceding section in connection with the linear heat rating to initiate melting.

As previously noted, incipient melting is expected in the rods at nominal rated power with relatively greater melting in the powder fuel. This prediction is shown in Figure 3-20 and Figure 3-21 for pellet and powder fuel, respectively.

Fuel-to-cladding interaction is the primary potential source of cladding strain. At beginning-of-life and normal rated power, at least 2 mils of diametral clearance will be present in the rods. As burnup proceeds, this clearance will decrease to about 1 mil at 15,000 MWd/TU. This trend, as a function of heat flux is depicted in Figure 3-22.

b. Advanced Thermal Performance Fuel

The 0.700-inch-o.d. fuel rods were sized to operate with a moderate but unequivocal central melting at normal rated power of 450,000 Btu/h-ft^2. The same basic assumptions used in the 0.570-inch-o.d. fuel were used for the heat transfer analysis of the 0.700-inch-o.d. fuel.

Average cladding temperatures are slightly higher than in the 0.570-inch-o.d. fuel because of the increased wall thickness. The trend of cladding temperature versus exposure is depicted in Figure 3-23.

The radial temperature profile in the pellet UO_2 fuel is shown in Figure 3-24. The temperature profile of the powder fuel is shown in Figure 3-25. The central temperature and the volumetric average temperature for powder fuel are higher for a given surface heat flux, reflecting its lower conductivity.

The extent of melting for the pellet and powder fuel is shown in Figure 3-26 and Figure 3-27, respectively.

The hot gap size and fuel-to-cladding interaction as a function of exposure for various levels of heat flux are shown in Figure 3-28. A slight amount of fuel-cladding interaction is possible at the 15,000 MWd/T_e exposure level.

Actually, the fuel-cladding interaction for powder fuel is not well understood and may not equal that predicted by the analysis. Developmental powder fuel rods operating in the Consumers reactor do not show any interaction based on dimensional measurements taken at interim examinations.

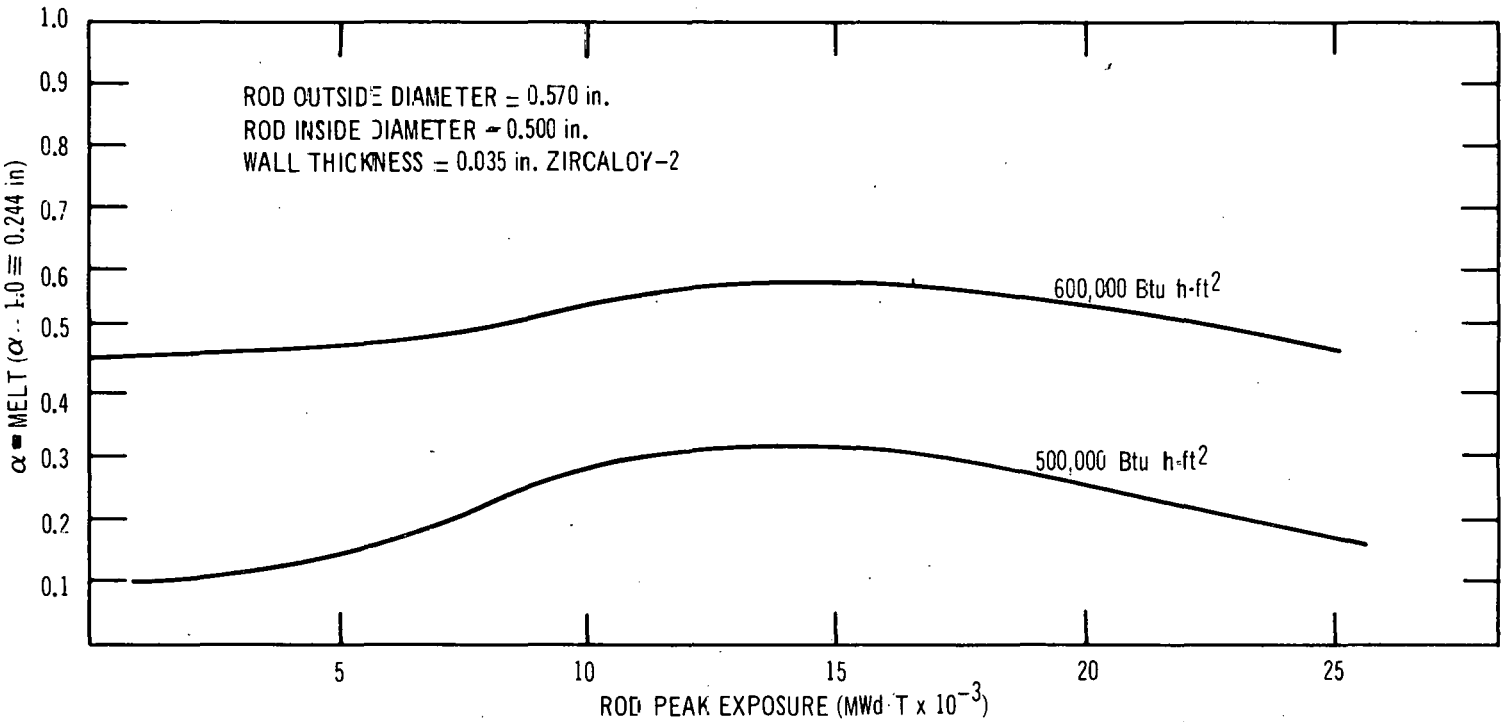

FIGURE 3–20. α – MELT VERSUS ROD PEAK EXPOSURE FOR PELLET FUEL AS A FUNCTION OF HEAT FLUX, OXIDE BUILD-UP AND CRUD BUILD-UP (0.4 mil/yr)

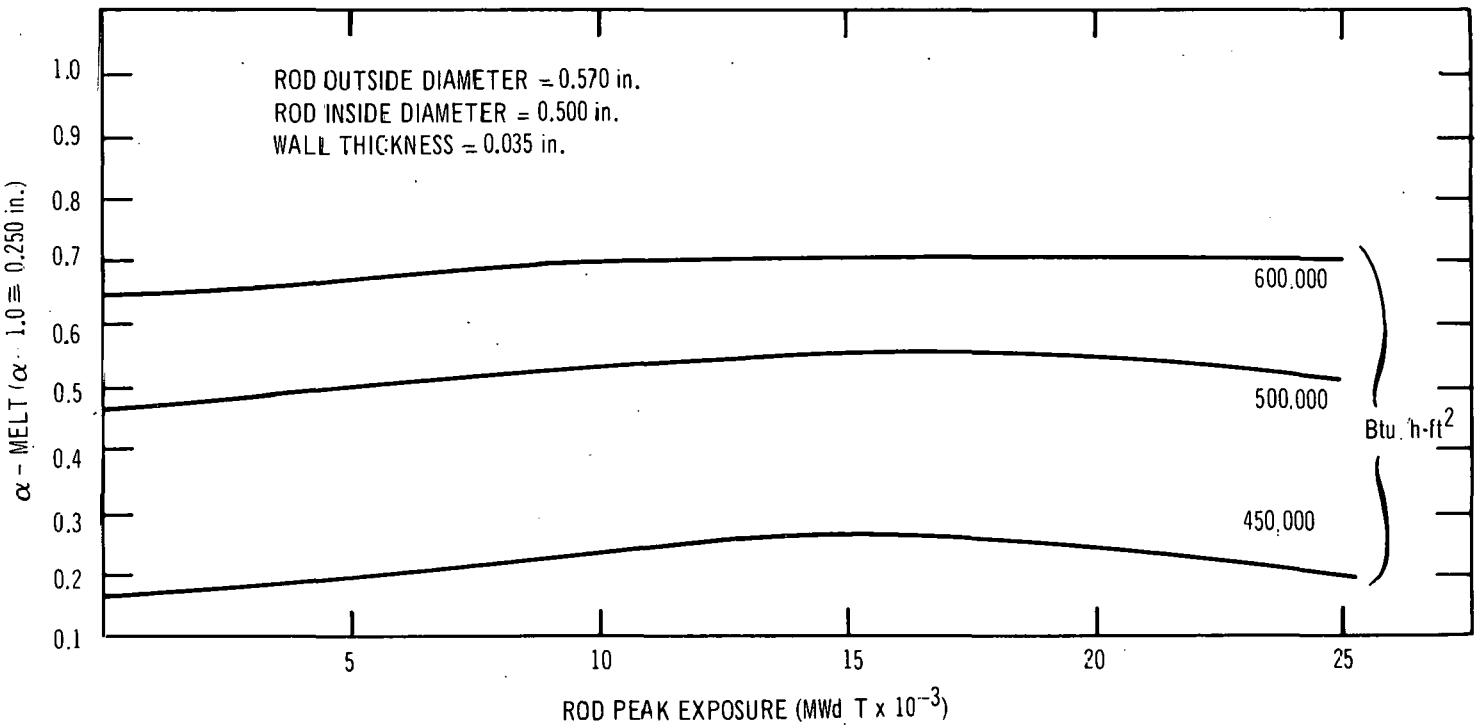

FIGURE 3-21. α- MELT VERSUS ROD PEAK EXPOSURE FOR POWDER FUEL AS A FUNCTION OF HEAT FLUX OXIDE BUILD-UP AND CRUD BUILD-UP (0.4 mil/yr)

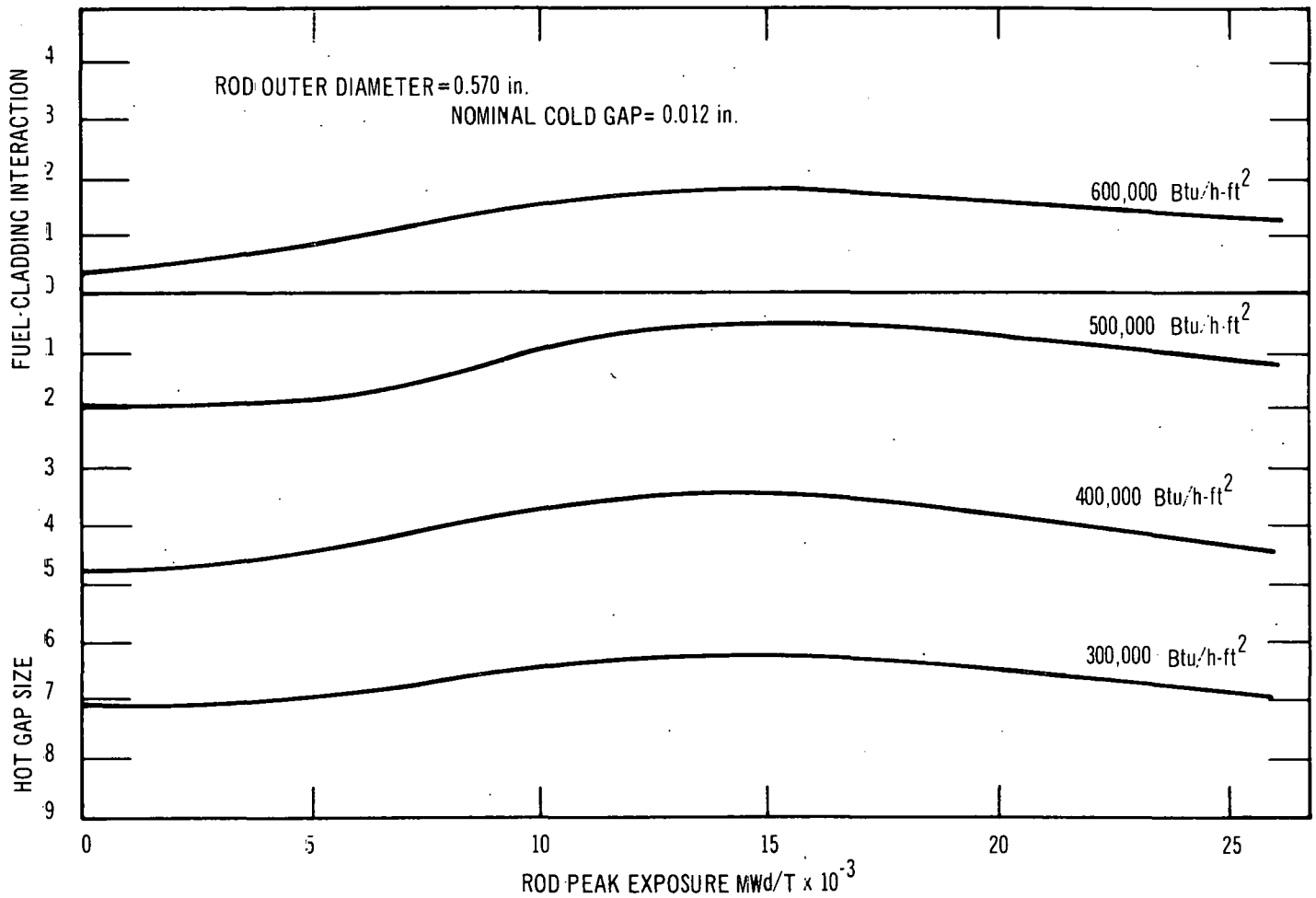

FIGURE 3–22. **HOT GAP SIZE AND FUEL CLADDING INTERACTION VERSUS ROD PEAK EXPOSURE AS A FUNCTION OF HEAT FLUX, OXIDE AND CRUD BUILD-UP (0.4 mil/yr)**

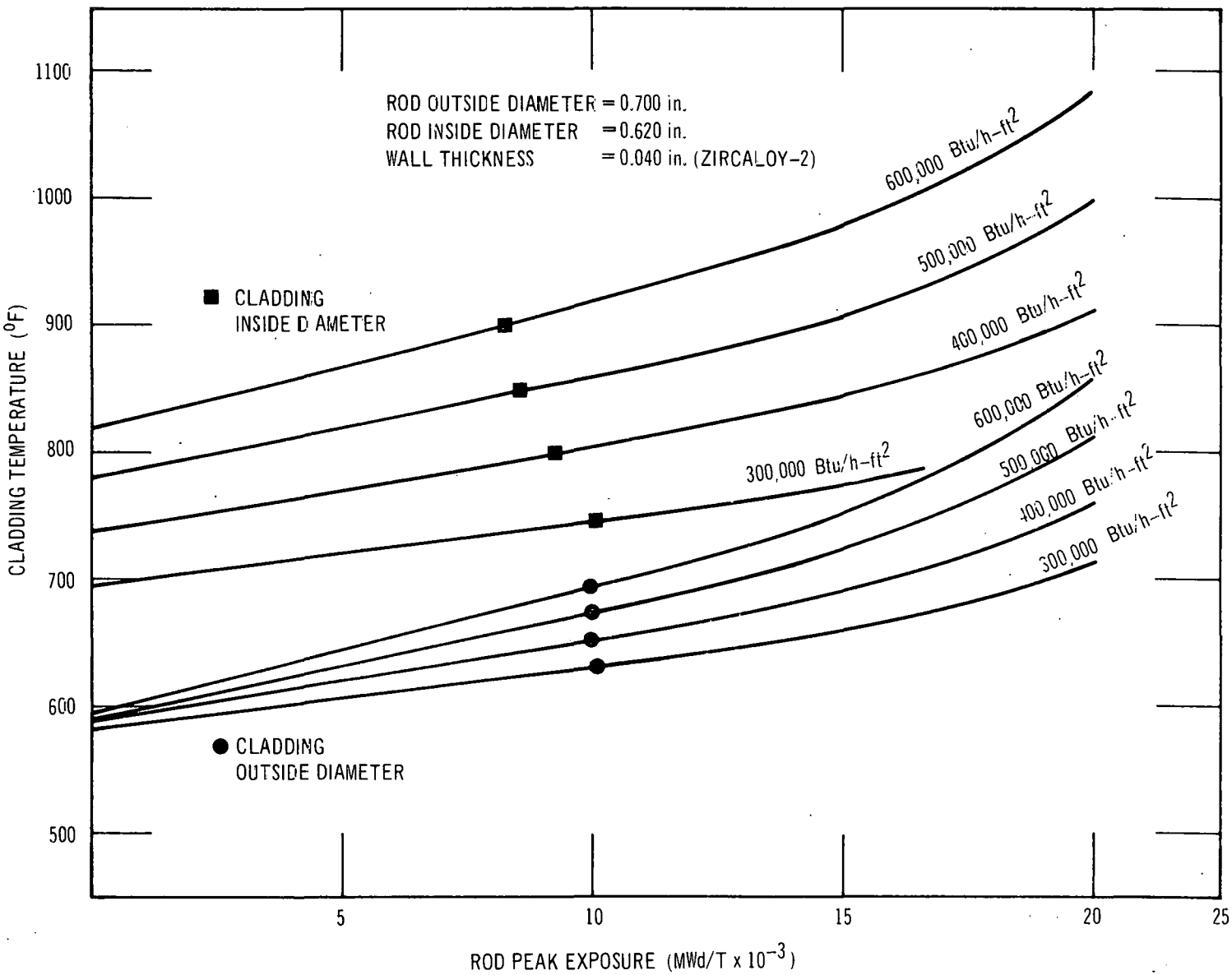

FIGURE 3-23. CLADDING TEMPERATURE VERSUS EXPOSURE AS A FUNCTION OF HEAT FLUX, OXIDE BUILD-UP AND CRUD BUILD-UP (0.4 mil/yr)

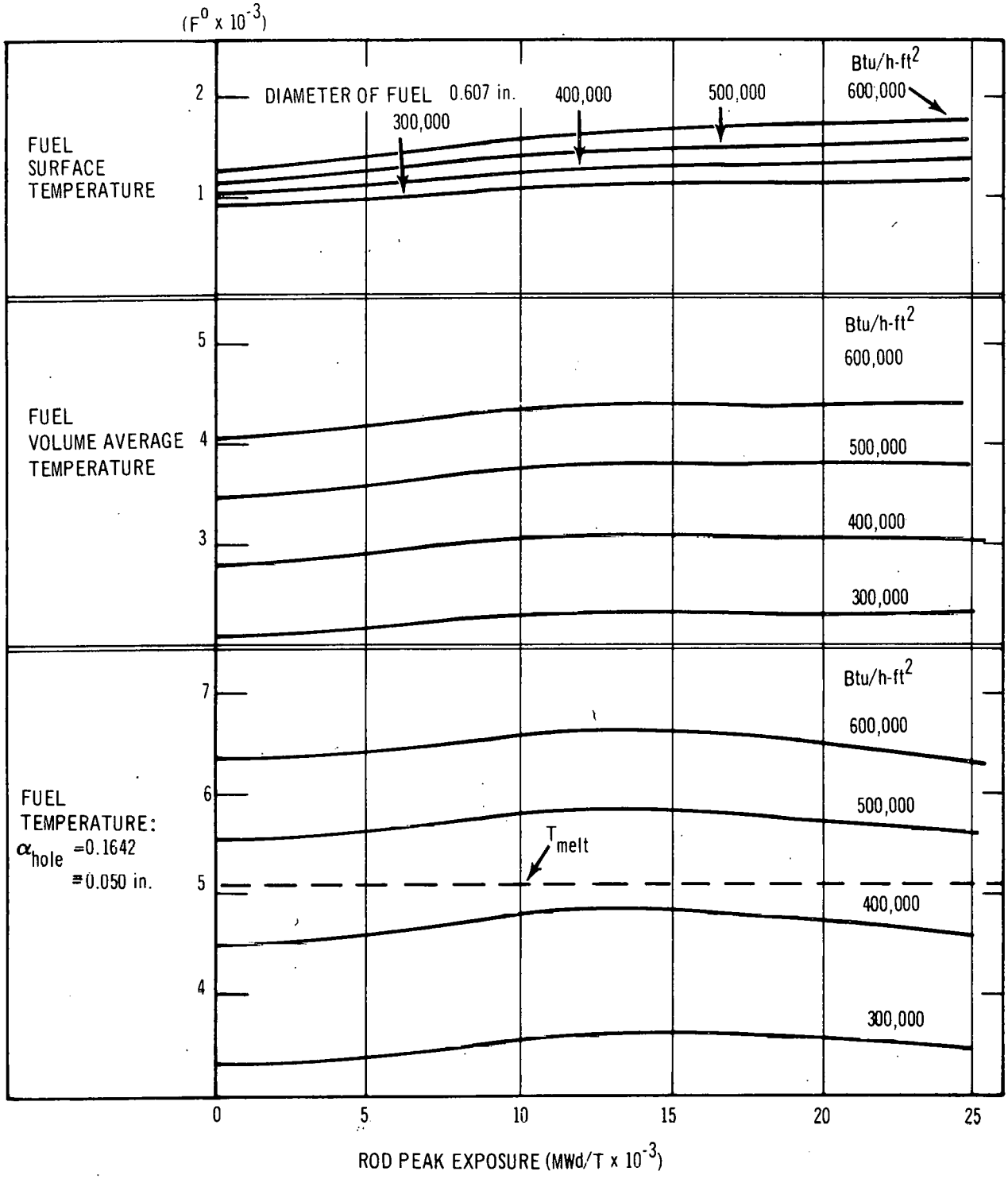

FIGURE 3-24. PELLET FUEL TEMPERATURE VERSUS ROD PEAK EXPOSURE AS FUNCTION OF HEAT FLUX, OXIDE BUILD-UP AND CRUD BUILD-UP (0.4 mil/yr)

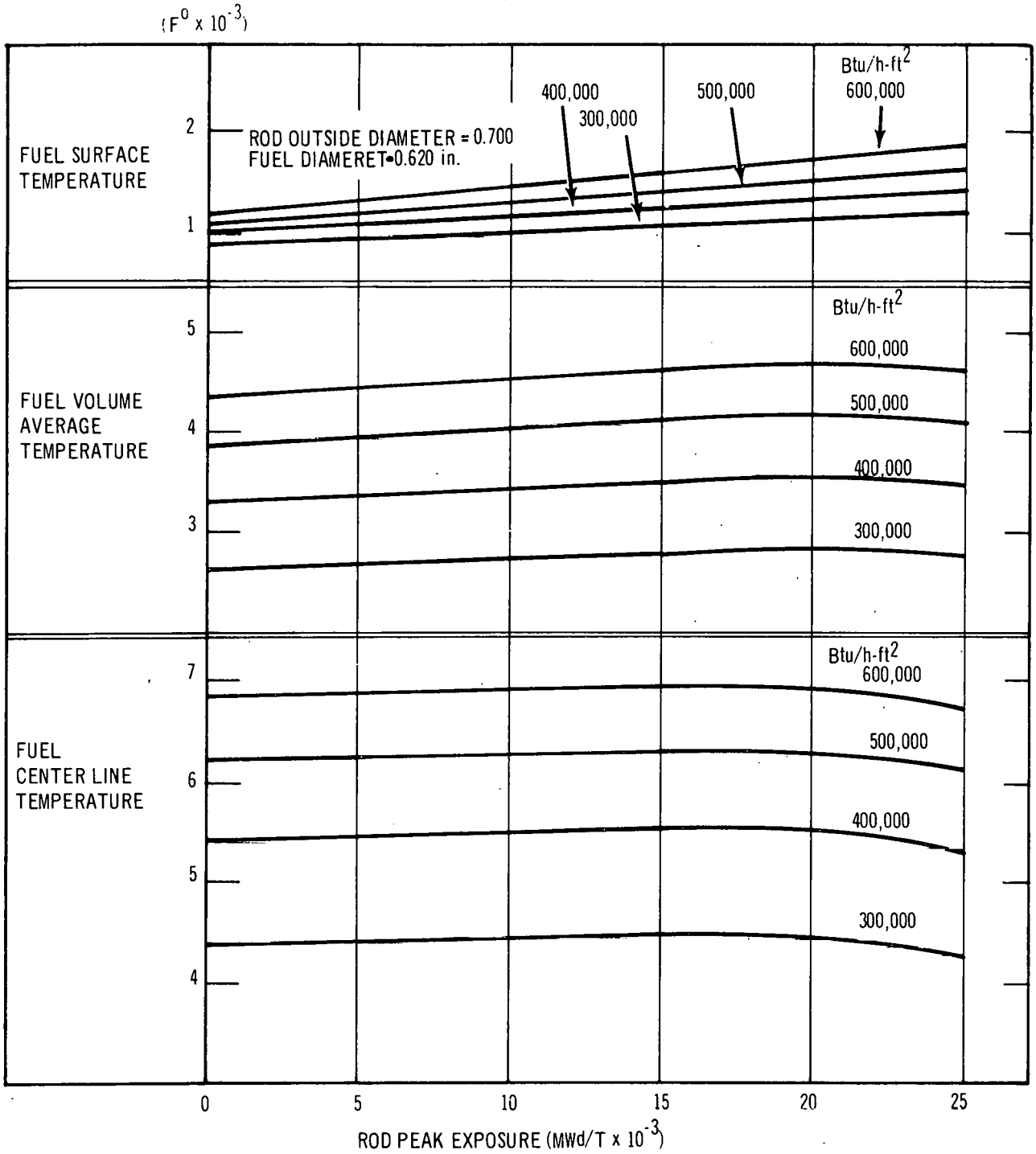

FIGURE 3-25. POWDER FUEL TEMPERATURE VERSUS ROD PEAK EXPOSURE AS A FUNCTION OF HEAT FLUX, OXIDE BUILD-UP AND CRUD BUILD-UP (0.4 mil/yr)

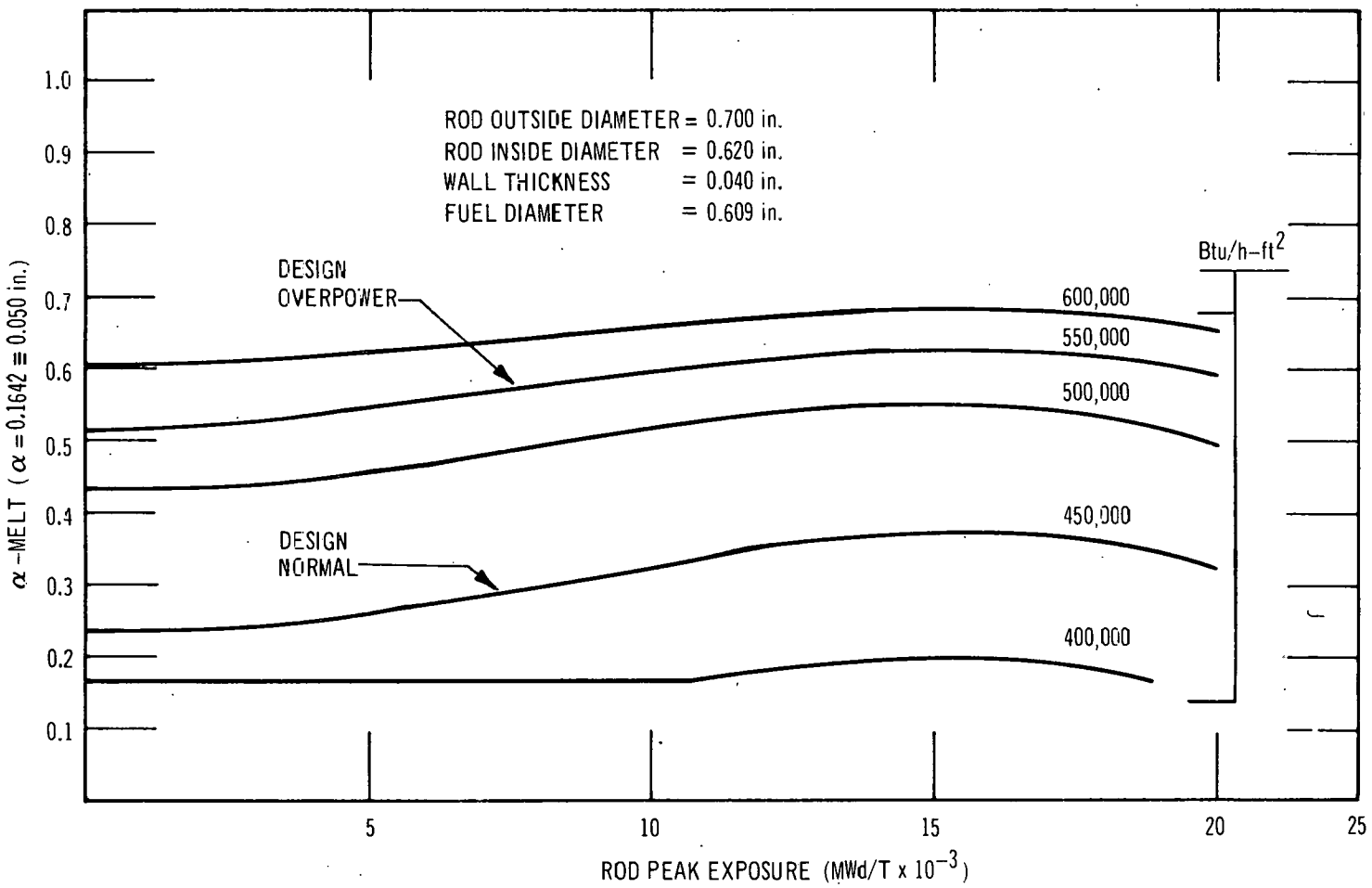

FIGURE 3–26. **α– MELT VERSUS EXPOSURE FOR PELLET FUEL AS A FUNCTION OF HEAT FLUX, OXIDE BUILD-UP AND CRUD BUILD-UP (0.4 mil/yr)**

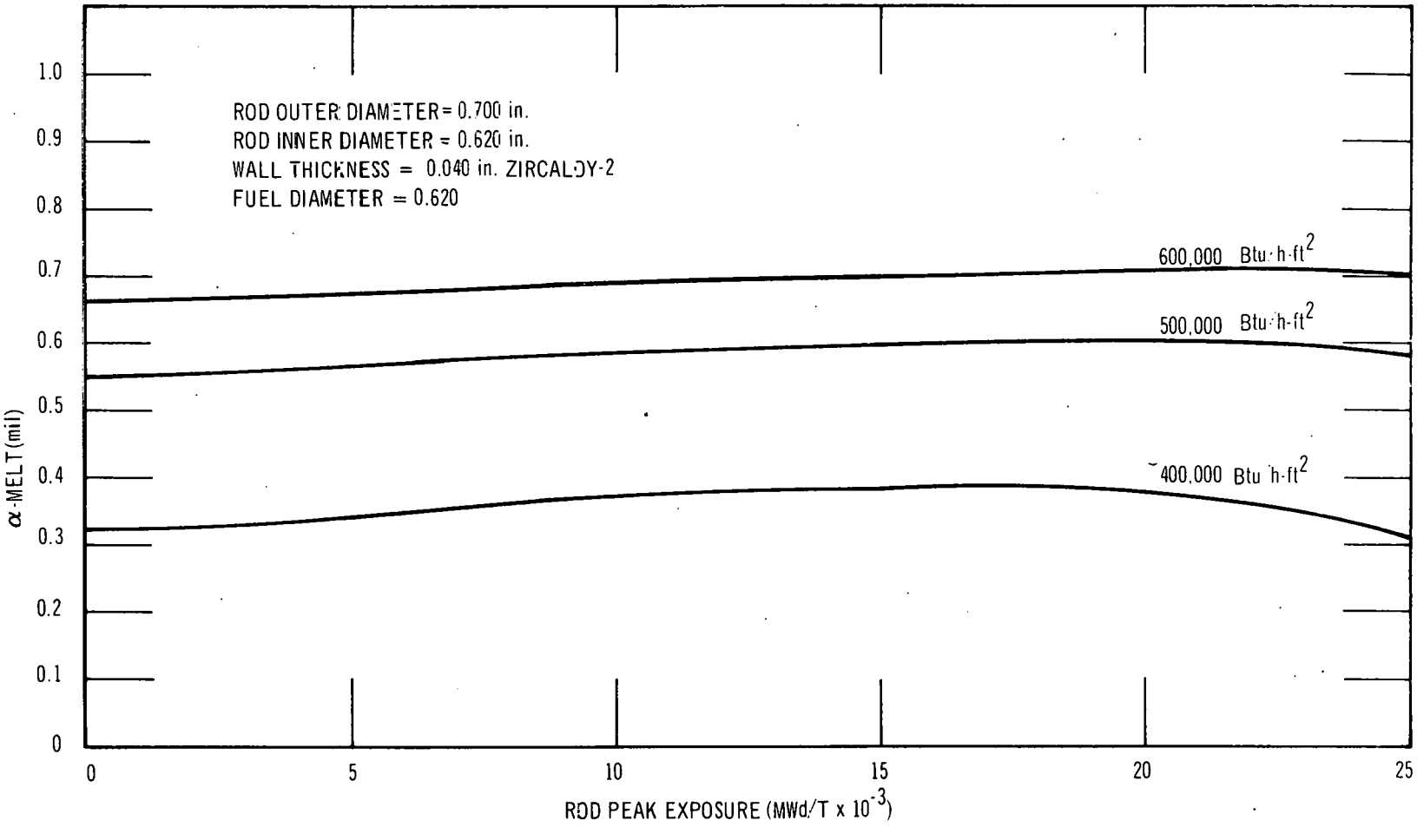

FIGURE 3–27. α– MELT VERSUS EXPOSURE FOR POWDER FUEL AS A FUNCTION OF HEAT FLUX, OXIDE BUILD-UP AND CRUD BUILD-UP (0.4 mil/yr)

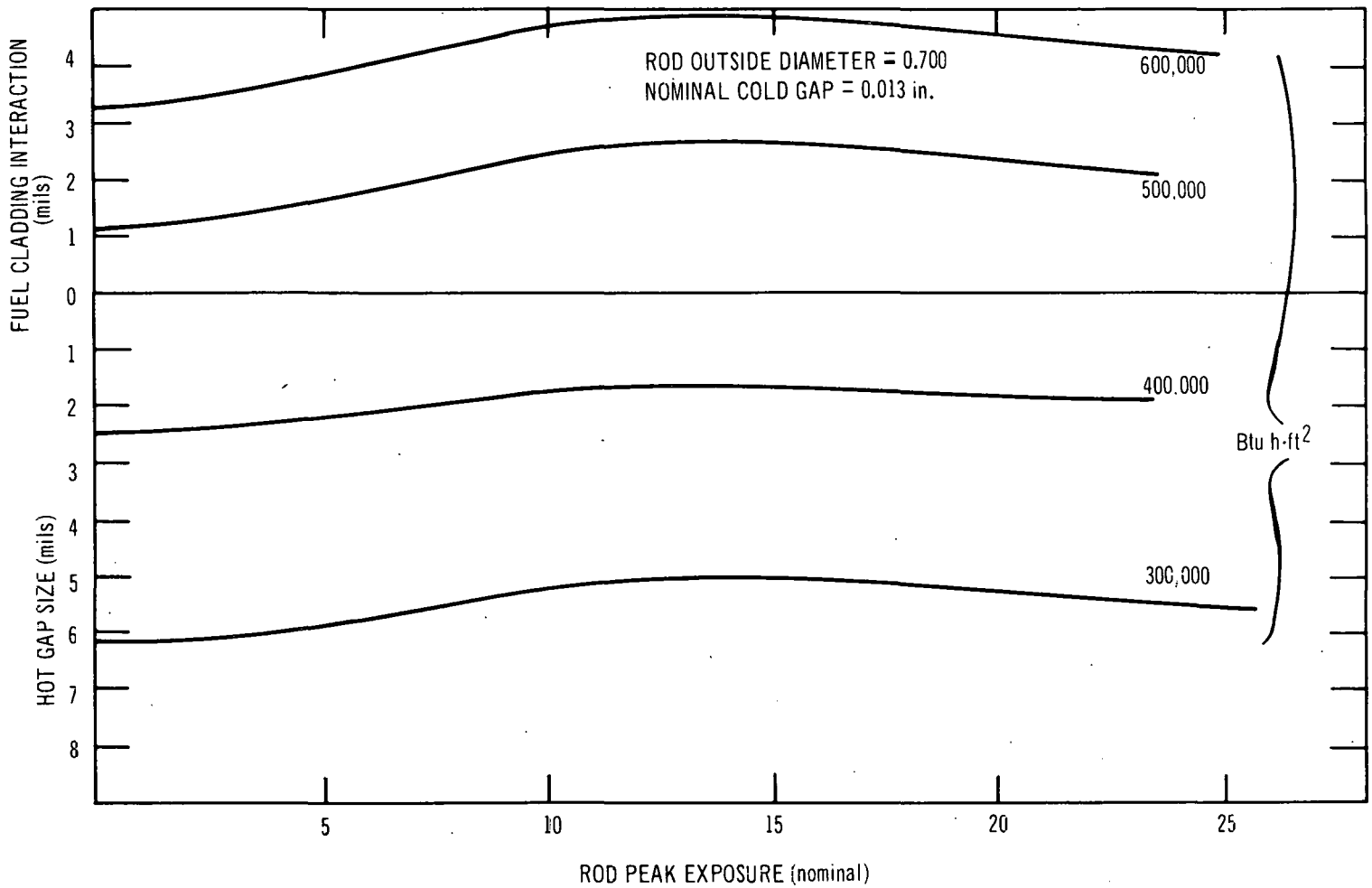

FIGURE 3-28. HOT GAP SIZE AND FUEL CLADDING INTERACTION VERSUS ROD PEAK EXPOSURE AS FUNCTION OF HEAT FLUX, OXIDE AND CRUD BUILD-UP (0.4 mil/yr)

3.7.5 Fuel Damage Limits

One criteria used to evaluate the relative safety of a fuel design with respect to the desired operating conditions is the so-called Fuel Damage Limit. This limit is usually defined as the peak linear heat rating at which fuel interaction with the cladding generates appreciable cladding strain. These limit values have been calculated for each fuel type as follows.

a. Pellet Fuel

1. Intermediate Performance Pellet Fuel

The calculated fuel damage limit is reached at a linear power of 32.5 kW/ft for low exposure and 29.6 kW/ft at an accumulated exposure of 10,000 MWd/T. The damage limit assumed is a total cladding strain of 1.5 percent caused by mechanical interaction between the fuel and the cladding. For comparison the linear power at 1.22 overpower condition is 24.1 kW/ft.

The void space for accommodating the UO_2 phase change volume expansion on melting in the intermediate performance pellet fuel is provided by a dish in one end of each pellet. The dish is shaped like a truncated cone, and is dimensioned to account for 5 percent of the pellet volume. Assuming the UO_2 pellets are 96 percent dense and 2 percent of the void volume is available to accommodate solid fission product swelling, then an additional 2 percent void volume is available to accommodate the molten UO_2. If one assumes the UO_2 volume expansion on melting is 9.6 percent, this results in 7.6 percent which must be accommodated in the pellet dish. The maximum permissible volume percentage molten is defined as that necessary to just fill the void space provided by the dish. No credit is taken for axial expansion of the molten fuel from pellet to pellet. Therefore, the maximum allowable volumetric melt fraction in the peak pellet is 0.71. Expected maximum melt fractions at rated and 1.22 overpower condition are zero and 0.22.

2. Advanced Performance Pellet Fuel

With the same damage limit criterion as above, the calculated fuel damage limit is reached at 67.1 kW/ft for low exposure and 51.8 kW/ft at an accumulated exposure of 10,000 MWd/T. The linear power at 1.22 overpower condition is 29.5 kW/ft.

The void space for accommodating the UO_2 phase change volume expansion on melting in the advanced performance pellet fuel is provided by a 0.100-inch-diameter hole through the center of each pellet. This central hole accounts for 2.8 percent of the pellet volume. Using the same assumptions as in the intermediate performance fuel results in an allowable volume fraction molten of 0.397. Since the 0.100-inch-diameter hole is continuous over the length of the rod, axial expansion of the molten fuel also can take place. Therefore, the 39.7 percent molten volume is the average permissible over the entire rod. The maximum permissible molten fraction at the peak cross section in the rod is 1.4 times the average or 0.556. Expected maximum melt fraction at rated and 1.22 overpower condition are 0.15 and 0.35. The Fuel Damage limits for the intermediate and advanced fuel are summarized in Table 3-3.

TABLE 3-3

FUEL DAMAGE LIMITS—PELLET FUEL

	Linear Power Generation		
	Rated Power (kW/ft)	Overpower (kW/ft)	Damage Limit (kW/ft)
Intermediate Performance Fuel			
1. Beginning-of-Life	19.7	24.1	32.5
2. 10,000 MWd/T	19.7	24.1	29.6
Advanced Performance Fuel			
1. Beginning-of-Life	24.2	29.5	67.1
2. 10,000 MWd/T	24.2	29.5	51.8

b. Powder Fuel

The fuel damage limits for the powder fuels are assumed to be the same as those calculated above for the pellet fuels.

The fuel rods loaded with vibratory-compacted powder have an inherent 15 to 17 percent void volume. The particles are essentially 100 percent dense; therefore, there is no internal porosity available for fission product swelling. However, assuming there is 2 percent void volume required for swelling, there is still 13 to 15 percent void space available for melting. Theoretically, this is sufficient void space for 100 percent melting. The maximum melting permissible in this project is defined as 80 percent in both the intermediate performance and the advanced performance fuel. The basis for this limit can be found in work performed in the AEC-Euratom sponsored "UO_2 High Performance Program" (PA 17), wherein fuel rods of like design were successfully irradiated, with 80 percent of the cross-sectional area molten, to an average burnup of 20,000 MWd/TU.[8] There was no unaccommodated molten volume expansion in these rods as evidenced by the absence of detectable cladding expansion.

Expected maximum fractional cross-sectional areas melted at rated and 1.22 overpower conditions for the intermediate performance powder fuel are 0.07 and 0.27. Corresponding fractional areas melted for the advanced performance powder fuel are 0.25 and 0.41. These values are summarized in Table 3-4.

TABLE 3-4

PREDICTED MELTING AT OVERPOWER (550,000 Btu/h-ft^2)
END-OF-LIFE (20,000 MWd/T)

	Percent Molten Area (Peak Cross Section)	Molten Volume (Percent in Rod)	Molten Length (inches)
7 × 7 Pellet Fuel	36	12.7	38.5
7 × 7 Powder Fuel	41	15.2	49
8 × 8 Pellet Fuel	20	4	21
8 × 8 Powder Fuel	27	5.7	31.5

SECTION IV

FUEL BUNDLE DESIGN

4.1 GENERAL

In most BWR fuel bundle designs the removal from the core of a single failed fuel rod necessitates the removal of the entire fuel bundle. In a research and development program such as planned here, the advantages of being able to remove single rods from the bundle and replace them with other rods are innumerable. For this reason the bundle design concept used earlier in the High Power Density Fuel Development Program was also selected for this program.

Both the 0.700-inch-diameter advanced thermal performance fuel and the 0.570-inch-diameter intermediate thermal performance fuel use this concept. The 0.700-inch-diameter rods are arranged in a full 7 × 7 array. The 7 × 7 fuel assembly is shown in detail in Figure 4-1. The 0.570-inch-diameter rods are arranged in a full 8 × 8 array. The 8 × 8 assembly is shown in detail in Figure 4-2. Key components of the support structure or cage are as follows:

a. Handle - Completely removable to allow rod removal.

b. Pin - Captures the handle to the support structure.

c. Spacer - Double layer wire, constant pressure spring type. Provides maximum protection against fretting wear of the Zircaloy-2 cladding.

d. Angle - Acts as the main axial support member of bundle. Provides a means to position spacers axially. Also minimizes the possibility of damage to rods and spacers during insertion and removal from in-core channel locations.

e. Base - A grid bar arrangement welded to the lower end of each corner angle. The fuel rods rest on the grid.

All parts of the cage assembly are 300 series stainless steel and the structure is fully capable of supporting the rods when resting on the base and when hung from the handle. On the other hand, when resting on a side with a full load of rods, very tight support must be provided for individual rods to prevent damage to the spacers. For this reason, it was decided to ship the rods and cages separately and assemble them at the reactor site.

The fuel bundles in the fully-loaded condition have the following approximate weights (includes weight of cage).

1. 0.700-inch-o.d. Pellet UO_2 Rods: 385 lb
2. 0.700-inch-o.d. Powder UO_2 Rods: 358 lb
3. 0.570-inch-o.d. Pellet UO_2 Rods: 330 lb
4. 0.570-inch-o.d. Powder UO_2 Rods: 309 lb

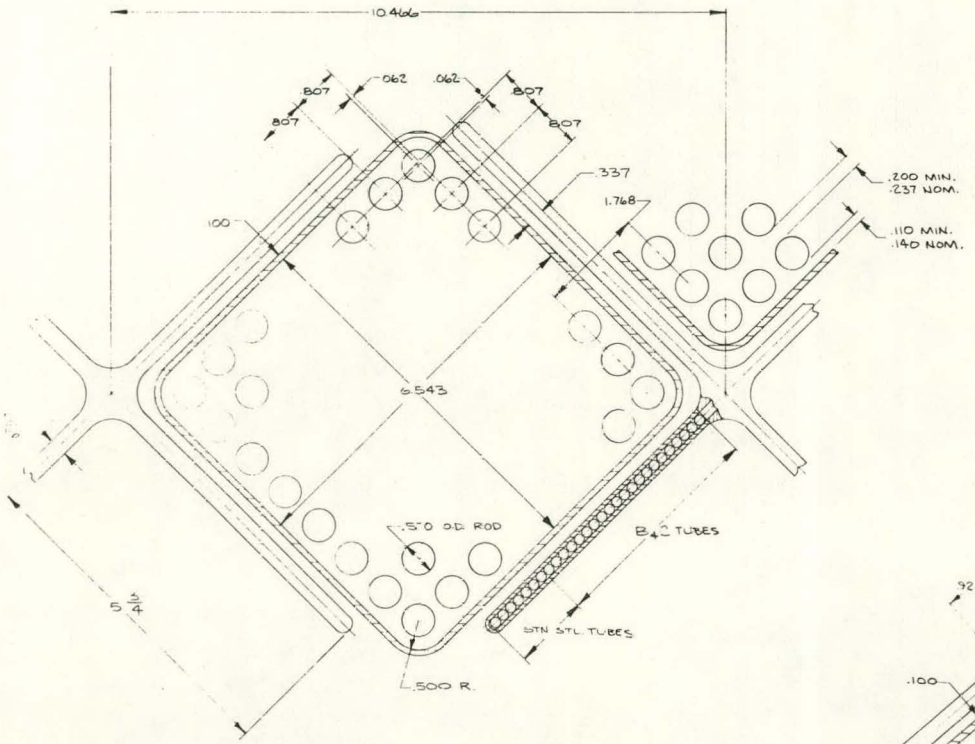

FIGURE 4-1. DRAWING OF 8 x 8 FUEL ASSEMBLY

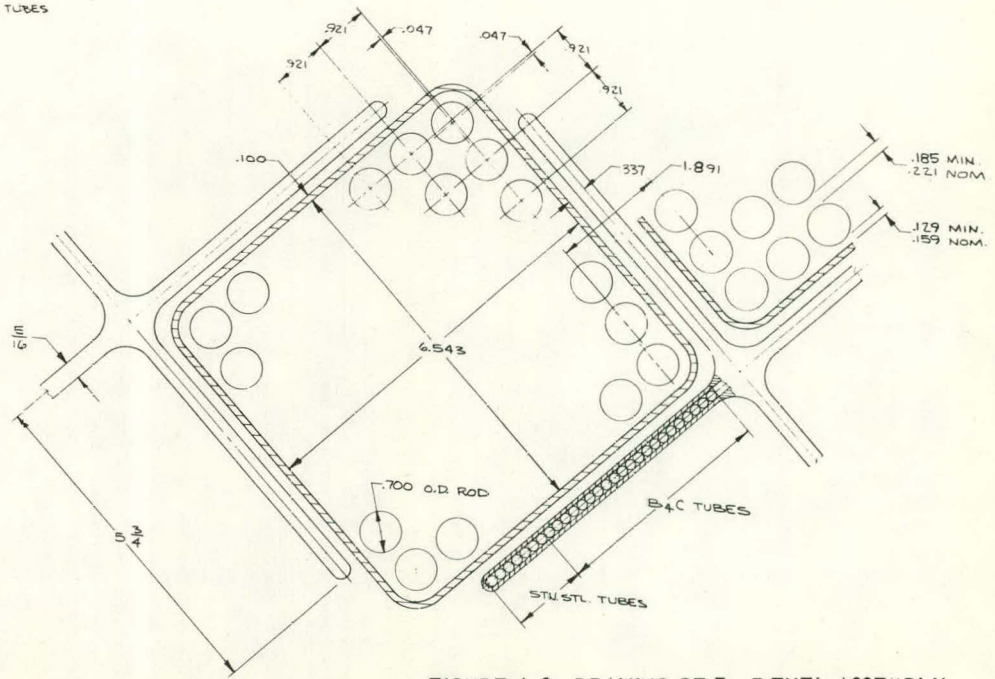

FIGURE 4-2. DRAWING OF 7 x 7 FUEL ASSEMBLY

67-01544

The over-all assembly drawing for the 7 × 7 bundle is shown in Figure 4-3. The comparable drawing for the 8 × 8 bundle is shown in Figure 4-4. The criteria dictating the various rod arrangements are discussed under the physics, critical heat flux, and thermal hydraulic design analyses.

Other considerations factored into the bundle design include:

a. Minimum allowable rod-to-channel clearances.

b. Water-to-fuel ratio.

c. Handling of fuel bundles and rods with existing pool equipment at the Consumers Big Rock Point reactor.

d. Standardization of parts used in both types of bundles; e.g., the corner angle used is identical for both types.

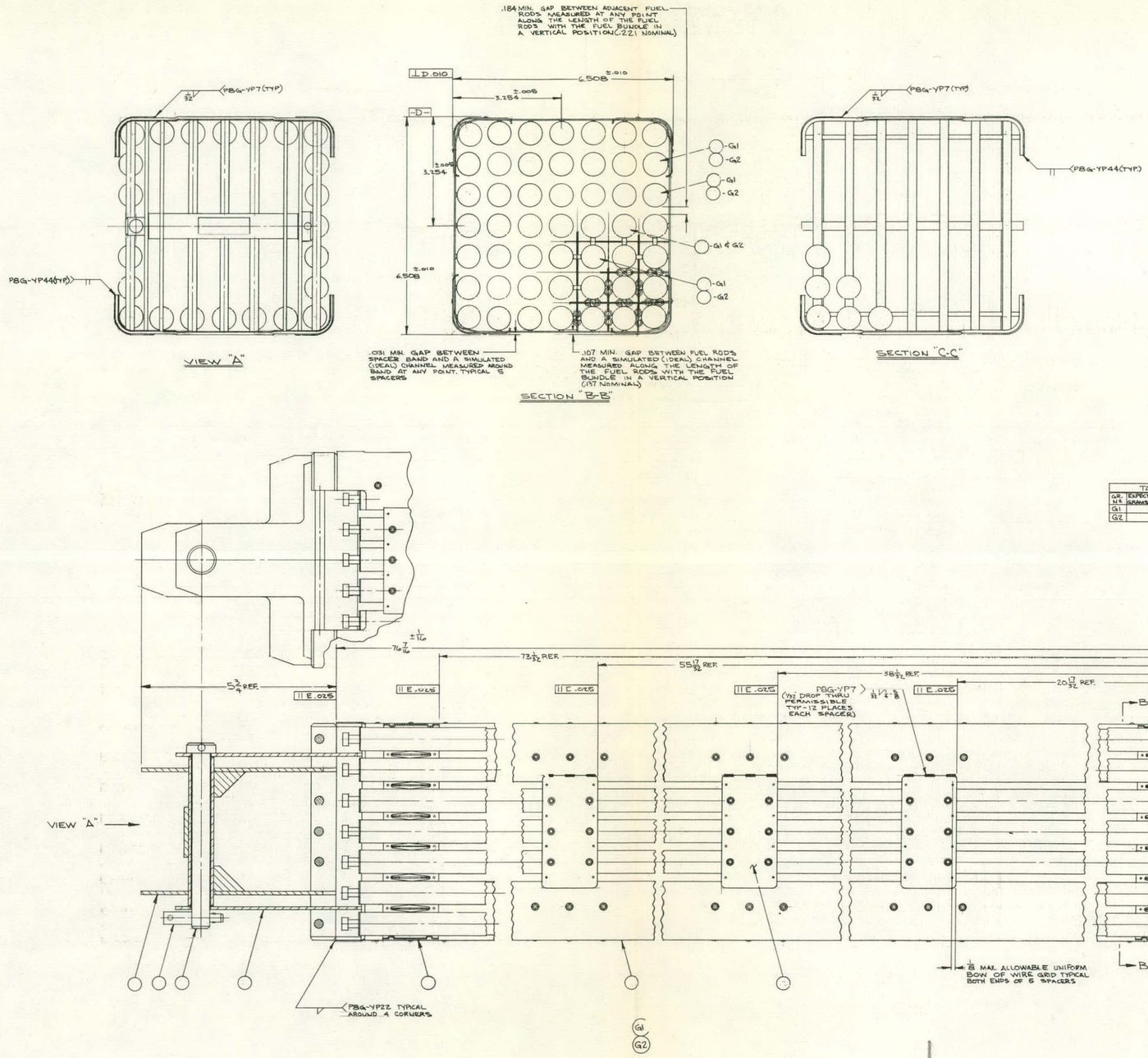

TABLE I	
GR. NO.	EXPECTED UO_2 WT IN GRAMS ±1.0% GRAMS
G1	
G2	

FIGURE 4-3. DRAWING OF 8 x 8 FUEL LATTICE

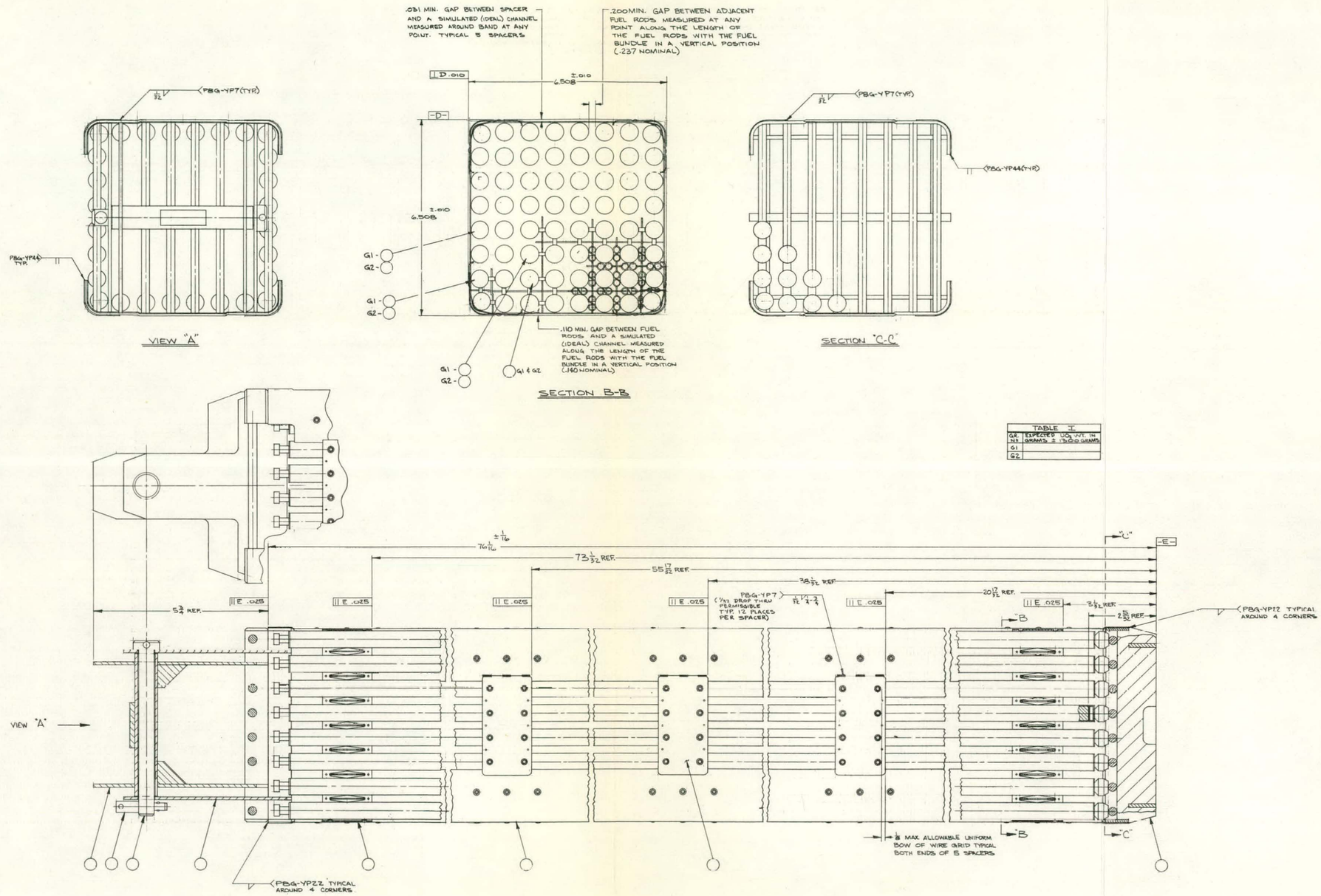

FIGURE 4-4. DRAWING OF 7 x 7 FUEL LATTICE

SECTION V

FABRICATION

5.1 GENERAL

These fuel rods were fabricated following conventional procedures for the sintered UO_2 pellet preparation, dynapak UO_2 powder preparation and compaction, and the "rocked" Zircaloy-2 processing. These detailed procedures and the exact fuel rod assembly sequence will be documented at a later date. Quality control procedures were stringent and 100 percent applied to all rods, following the usual practice at G.E.-NED for research and development fuel. Exceptional or nonroutine steps taken during fabrication are described in the following paragraphs.

5.2 SPECIAL PROVISIONS

Two straight pieces of tantalum wire, 0.094 inch in diameter and approximately 4 inches long, were placed into the gas plenum of all the rods. These wires act as neutron absorbers over a region normally occupied by UO_2 fuel in the regular fuel rods in the other assemblies, and prevent flux peaking.

The tubing was prepared with either both inside and outside surfaces autoclaved or only the outside surface autoclaved. These two inside surface conditions will help in the evaluation of the relative protective nature of the autoclave oxide film. Of the 188 power-producing rods in the six assemblies, 76 rods have tubing without the autoclaved inside surfaces.

Each fuel rod was measured for over-all length and diameter (at 0- and 90-degree orientations) at 12-inch intervals. Outside diameter profiles were also taken on 72 power-producing rods. The profilometer measurements included both the nonrotational type at 0- and 90-degree orientations, and the spiral trace. X rays were taken of the bottom end and upper plenum regions of each rod to verify that the parts were properly assembled.

5.3 ROD IDENTIFICATION

The fuel rods are identified by serial numbers metal-stamped on the bottom end plug. To facilitate separation of the rods by enrichment and to facilitate the loading of the proper fuel rods into the correct locations, the rods are further identified by metal-stamping the end faces of the top plugs with 1/4-inch-high letters referring to the four fuel enrichments as follows: A = 4.3 percent, B = 5.0 percent, C = 5.6 percent, and D = 0.22 percent. As a final verification that the rods are properly assembled, a Polaroid photo of the top of the assembly will be taken and the print checked against another record before the top handle is attached after final inspection at the reactor site.

SECTION VI

THERMAL-HYDRAULIC ANALYSIS

6.1 GENERAL

For this analysis, it was assumed that the centermelt assemblies are loaded in a configuration where the remainder of the reactor core consists of Type B and C reload fuel (Zircaloy-2 cladding in an 11 × 11 array). Evaluation of the minimum critical heat flux ratio was made using the new critical heat flux correlation for beginning-of-life and end-of-life conditions. Over-all results of the analysis are shown in Table 6-1.

TABLE 6-1

THERMAL HYDRAULIC DATA

I. Assumed Reactor Conditions

Reactor Power (Rated) MW	235
Total Core Coolant Flow, lb/h	12.3×10^6
Reactor Inlet Enthalpy, Btu/lb	569.3
Reactor Pressure, psia	1350
Number Fuel Assemblies	84

II. Fuel Bundle Description

	7 × 7	8 × 8
Fuel Rod Diameter, inches	0.700	0.570
Number of Rods per Assembly	49	64
Water to Fuel Ratio	2.4	3.0
Active Fuel Length, inches		
Pellet Fuel	66-1/4	67-9/32
Powder Fuel	64-1/2	66-1/16
Heat Transfer Area per Assembly, ft^2		
Pellet Fuel	49-9/16	53-5/8
Powder Fuel	48-11/16	52-5/8

III. Power Distribution required to produce a heat flux of 450,000 Btu/h-ft^2 at rated reactor power

Axial[1]	1.4	1.4
Water Power Fraction[2]	0.03	0.03
Radial × local		
Pellet	1.720	1.858
Powder	1.690	1.825

(1) Peaked toward top of core at beginning of cycle, peaked toward bottom of core at end of cycle.

(2) Portion of reactor power that does not go through cladding in the form of heat flux (gamma heating, etc.).

TABLE 6-1 (Continued)

IV. Conditions to give a MCHFR of 1.5 at 1.22 percent overpower

	7 × 7	8 × 8
Beginning of Cycle		
Axial	1.4[3]	1.4[3]
Radial	1.14	1.21
Local	1.51	1.54
Water power	0.03	0.03
Overpower	1.22	1.22
End of Cycle[4]		
Axial[5]	1.4	1.4
Radial	1.43	1.55
Local	1.20	1.20
MCHFR	1.62	1.62

(3) Peaked 80 percent of distance from bottom of core.

(4) Peak heat flux does not occur in the quality sensitive region of the CHF correlation.

(5) Peaked 25 percent of distance from bottom of core.

Because of the high heat fluxes and associated bundle powers, the ability to achieve a satisfactory MCHFR must be carefully evaluated. The product of the axial, radial, and local peaking factors* is fixed by the specified peak heat flux. The axial peaking factor is fixed by the particular power shape chosen to represent the beginning and end of cycle conditions. Thus, only the bundle of radial and local peaking factors are free to be varied, yet their product must also be held constant.

It may be desirable to review the effect the various peaking factors have on the MCHFR:

a. Axial Peaking Factor - Location of the axial peak can have a strong effect on the MCHFR, because of the axial variation of quality within the channel. The critical heat flux (CHF) is quality dependent, with the CHF decreasing with increasing quality (for quality values above about 10 percent at the mass flow rate involved here). For beginning-of-life (or cycle) conditions, the axial shape tends to be skewed toward the top of the core, placing the peak heat flux in a relatively high quality region and reducing the CHF. For end-of-cycle conditions, the axial shape is skewed toward the bottom of the core where the peak heat flux is in a nonquality-sensitive region of the CHF correlation, giving higher MCHFR's.

   Other factors being equal, the MCHFR will be lower with the axial power shape peaked toward the top of the core.

*Axial = Peak axial power (heat flux)-to-average power for a given bundle.
Radial = Bundle power-to-average bundle power.
Local = Peak rod power-to-average rod power in bundle.

b. Radial Power Factor - Has a direct effect on both steam quality and heat flux, thus has a strong effect on MCHFR.

c. Local Peaking Factor - Only a heat flux multiplier.

The MCHFR analysis was only specifically performed for the pellet assemblies since for a fixed peak heat flux and designated core radial power position, holding local and axial peaking factors constant, the powder assemblies will always have a lower bundle power output because of their lower density, shorter active fuel length, and smaller heat transfer area. Thus, the actual radial power factor will be smaller and the MCHFR higher than the comparable pellet bundle.

The power distributions required to give a MCHFR of at least 1.5 for the overpower condition are given in Table 6-1. For the end-of-cycle condition, the peak heat flux does not occur in the quality sensitive region of the CHF correlation. Over the range of local peaking factor evaluated, from 1.2 to 1.5, the MCHFR was not affected. Therefore, the local peaking factor can be allowed to go at least as low as 1.2 at the end-of-cycle.

SECTION VII

CRITICAL HEAT FLUX ANALYSIS AND TESTS

7.1 GENERAL

The preceding thermal-hydraulic analysis was developed based on bulk average channel properties, the hot rod heat flux, and the CHF limit curve shown in Figure 7-1. This procedure has been shown to be conservative for normal fuel bundle designs; however, these centermelt bundles are unique because of the inclusion of depleted, nonpower-producing rods within the bundle.

As can be noted from Figures 7-2 and 7-3, the heat flux from adjacent rods may differ by a factor of 17. This condition is atypical of the usual bundle situation and, thus, no specific experimental data are available to verify the CHF characteristics of such a design. For this reason, an analytical and experimental investigation was conducted to determine the validity of calculating the CHFR for the centermelt bundles by established procedures.

7.2 EVALUATION BASIS

Both the 8×8 intermediate and 7×7 advanced performance assembly designs have four enrichments: 4.3, 5.0, 5.6, and 0.22 (depleted) weight percent U-235. The enriched rods are arranged in the assembly in such a manner to maximize the number of rods operating at or very close to the desired peak heat fluxes. The number of depleted UO_2 rods was chosen iteratively, taking as a limit the allowable MCHFR, with the low power production of the depleted UO_2 rods being used to offset and effectively increase the allowable power of the remaining enriched fuel rods at the same over-all bundle power output. The initial rod arrangements and associated local peaking factors, for both the 7×7 and 8×8 assemblies, are shown in Figures 7-2 and 7-3. The local peaking factors indicated are for a new bundle with the average rod power normalized to 1.0 in each case.

To compare the MCHFR based on local conditions with that predicted using bulk conditions and the design limit curve, an analytical model which predicts local flows and qualities in a heated channel was applied to the 8×8 and $\bar{7} \times \bar{7}$ centermelt bundles as designed and to the same bundles with slight changes in the local peaking values. The changes in the peaking values were brought about in one case by interchanging the corner rods (4.3 percent enriched UO_2) with the adjacent rod on the diagonal (0.22 percent enriched UO_2). This interchange is shown by the arrows shown in Figures 7-2 and 7-3. The changes in the peaking values were brought about in a second case by replacing the corner rods (4.3 percent enriched) in each bundle with a rod containing UO_2 enriched to 2.3 percent. In addition, to verify the predictions of the hydraulic model, four critical heat flux data points were obtained in a 3×3 test section with 0.700-inch-diameter, electrically-heated tubes, adjusted to yield local peaking values of the same order as those in the centermelt bundles.

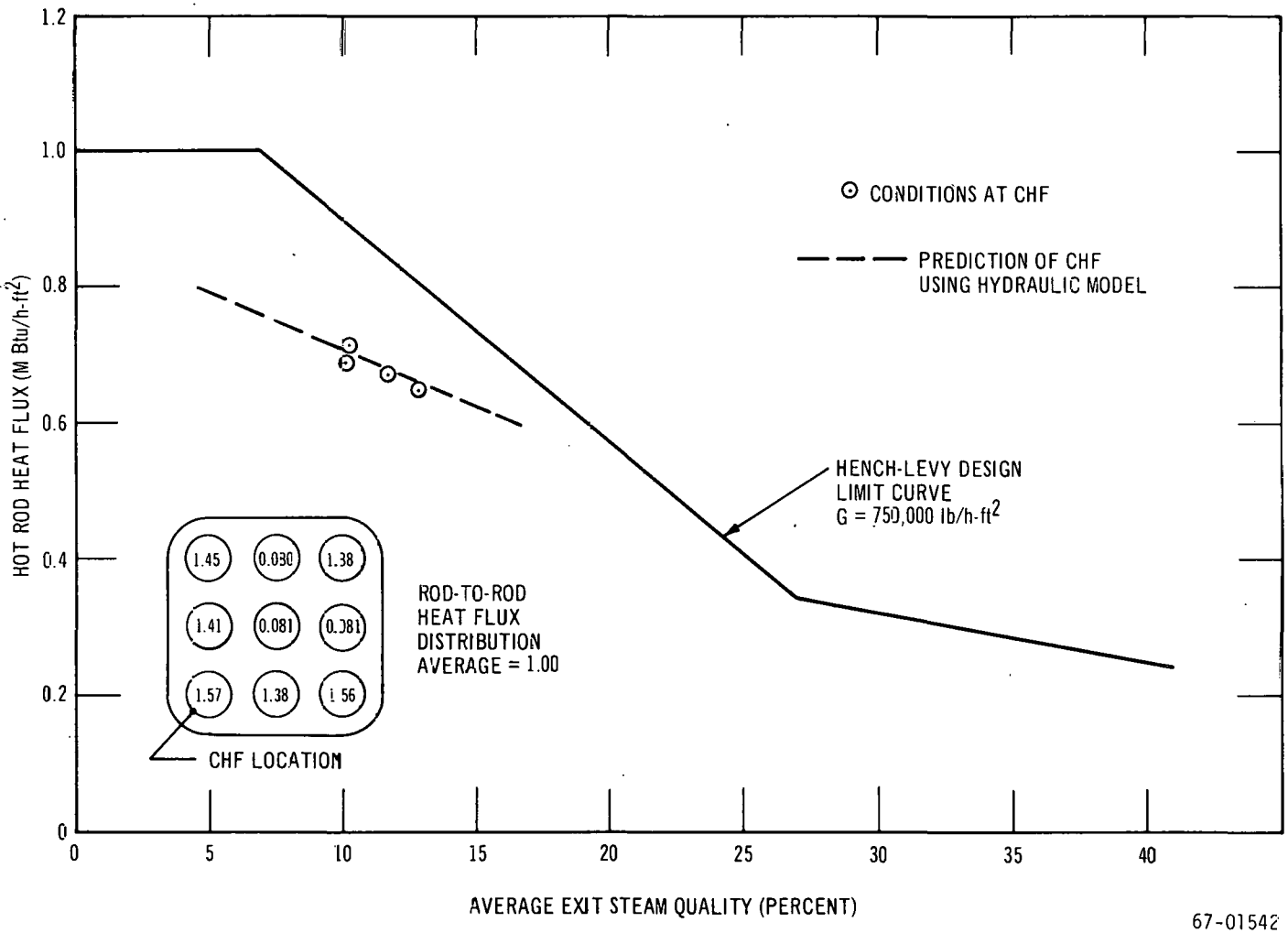

FIGURE 7-1. CRITICAL HEAT FLUX DATA POINTS AND LIMIT CURVES

D 1.61	A 1.50	B 1.67	B 1.66	B 1.67	A 1.50	D 1.61
A 1.50	A 0.10	D 0.10	D 0.10	D 0.10	A 0.10	A 1.50
B 1.67	D 0.10	C 1.75	D 0.10	C 1.75	D 0.10	B 1.67
B 1.66	D 0.10	D 0.09	C 1.67	D 0.09	D 0.10	B 1.66
B 1.67	D 0.10	C 1.75	D 0.10	C 1.75	D 0.10	B 1.67
A 1.50	D 0.10	D 0.10	D 0.10	D 0.10	D 0.10	A 1.50
A 1.61	A 1.50	B 1.67	B 1.66	B 1.67	A 1.50	A 1.61

TYPE A U-235 ENRICHMENT = 0.043
TYPE B U-235 ENRICHMENT = 0.050
TYPE C U-235 ENRICHMENT = 0.056
TYPE D U-235 ENRICHMENT = 0.0022 (depleted)

CASE 1:
PEAKING FACTORS AND ROD PLACEMENT AS SHOWN.

CASE 2:
ROD INTERCHANGE AS SHOWN. PEAKING FACTOR SHOWN IN FIGURE 3-8b

CASE 3:
EACH CORNER ROD REPLACED WITH 2.3% ENRICHED UO_2. PEAKING FACTORS SHOWN IN FIGURE 3-8c

67-01540

FIGURE 7-2. INDIVIDUAL FUEL ROD RELATIVE POWERS IN THE 7 x 7 CENTERMELT BUNDLE. BEGINNING OF LIFE. AVERAGE ROD POWER = 1.0.

A 1.65	A 1.57	B 1.74	B 1.71	B 1.71	B 1.73	A 1.55	D 0.11
A 1.57	D 0.12	D 0.11	D 0.11	D 0.11	D 0.11	A 1.64	A 1.55
B 1.74	D 0.12	D 0.11	C 1.80	D 0.11	C 1.83	D 0.11	B 1.73
B 1.72	D 0.11	C 1.80	D 0.10	C 1.72	D 0.11	D 0.11	B 1.71
B 1.71	D 0.11	D 0.11	C 1.72	D 0.10	C 1.80	D 0.11	B 1.72
B 1.73	D 0.11	C 1.83	D 0.11	C 1.80	D 0.11	D 0.12	B 1.74
A 1.55	D 0.11	D 0.11	D 0.11	D 0.11	D 0.11	D 0.12	A 1.57
A 1.64	A 1.55	B 1.73	B 1.71	B 1.71	B 1.74	A 1.57	A 1.65

TYPE A U-235 ENRICHMENT = 0.043
TYPE B U-235 ENRICHMENT = 0.050
TYPE C U-235 ENRICHMENT = 0.056
TYPE D U-235 ENRICHMENT = 0.0022 (depleted)

CASE 1:
PEAKING FACTORS AND ROD PLACEMENT AS SHOWN

CASE 2:
ROD INTERCHANGE AS SHOWN. PEAKING FACTORS SHOWN IN FIGURE 3-9b

CASE 3:
EACH CORNER ROD REPLACED WITH 2.3% ENRICHED UO_2. PEAKING FACTORS SHOWN IN FIGURE 3-9c

67-01541

FIGURE 7-3. INDIVIDUAL FUEL ROD RELATIVE POWERS IN THE 8 x 8 CENTERMELT BUNDLE. BEGINNING OF LIFE. AVERAGE ROD POWER = 1.0.

7.3 CRITICAL HEAT FLUX TESTS

The test section for experimentally determining the CHF was made up of nine electrically-heated tubes of 0.700-inch o.d. in a 3 × 3 square array. The rod number system and the test section dimensions are shown in Figure 7-4. It should be noted that this test array represents the nine rods in the corner of the 7 × 7 assembly, as shown in Figure 4-2, except for the exact corner position. The corner rod in the real assembly is set back 0.047 inch to allow increased coolant flow in the corner. Because of this difference in the corner, the test section will be conservative, i.e., will yield lower MCHFR values.

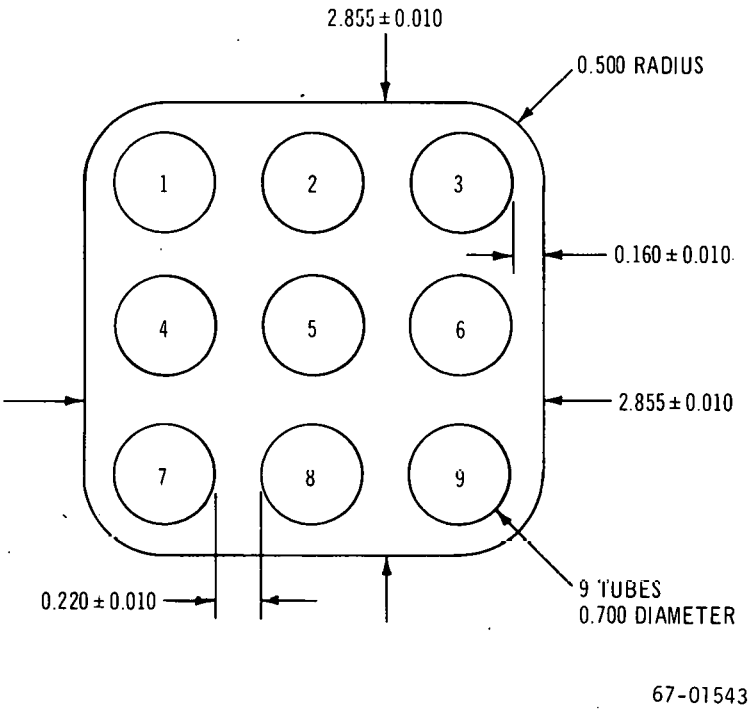

FIGURE 7-4. TEST SECTION DIMENSIONS AND NUMBERING SYSTEM (3x3)

The heat flux for a particular rod was uniform axially but varied from rod to rod. Variations in rod heat flux were obtained by adjusting the heated lengths of the rods and by adding resistance in series with the colder rods to force higher current flow into the hot rods. The heated lengths are given in Table 7-1 with the local peaking values. Also, the ratio of the heat flux of each rod to the heat flux of the coldest rod is shown for comparative purposes.

The test section was instrumented at the exit end only, since the axial heat flux was uniform. Eight thermocouples were used on each of the corner rods, on the side facing the channel wall.

TABLE 7-1

TEST SECTION DESCRIPTION (3 × 3)

Rod	(P/A) local	Heated Length (inches)	o_i/o_2
1	1.45	39.5	18.10
2	0.080	72.0	1.00
3	1.38	39.5	17.30
4	1.41	47.2	17.70
5	0.081	72.0	1.01
6	0.081	72.0	1.01
7	1.57	44.4	19.70
8	1.38	47.2	17.30
9	1.56	44.4	19.50

All runs were made at 1000 psia and a mass velocity of 750,000 lb/h-ft^2. When the temperature recorded by one of the thermocouples rose rapidly to 800°F, the CHF condition was assumed to exist at that thermocouple.

The conditions at which the CHF was encountered are shown in Table 7-2, and the data points are shown plotted in Figure 7-1 along with the local peaking and the location of the CHF in the test section.

TABLE 7-2

RESULTS OF 3 × 3 CHF TESTS AT 1000 psia

Run	G (M lb/h-ft^2)	X_{exit}	ΔHs (Btu/lb)	CHF (M Btu/h-ft^2)
1	0.769	0.129	22.0	0.645
2	0.759	0.118	35.0	0.672
3	0.734	0.101	51.0	0.681
4	0.746	0.102	53.0	0.709

7.4 MULTICHANNEL HYDRAULIC MODEL ANALYSIS OF 3 × 3 BUNDLE RESULTS

The test section was represented in the Multichannel Hydraulic Model (MHM) by dividing it into subchannels, as shown in Figure 7-5. Because the assembly was nearly symmetric, only half was modeled. The dimensions in Figure 7-4 were used to determine the flow area, heated perimeter, and friction perimeter for each subchannel and the interface perimeter between the connecting subchannels. The effect of the differing heated lengths was included by the model.

Three cases were run with the hot rod heat flux equal to 0.600, 0.700, and 0.800×10^6 Btu/h-ft^2. The CHFR was calculated along each subchannel using an annular CHF correlation based on a best fit to APED annular CHF data for the corner subchannels and those

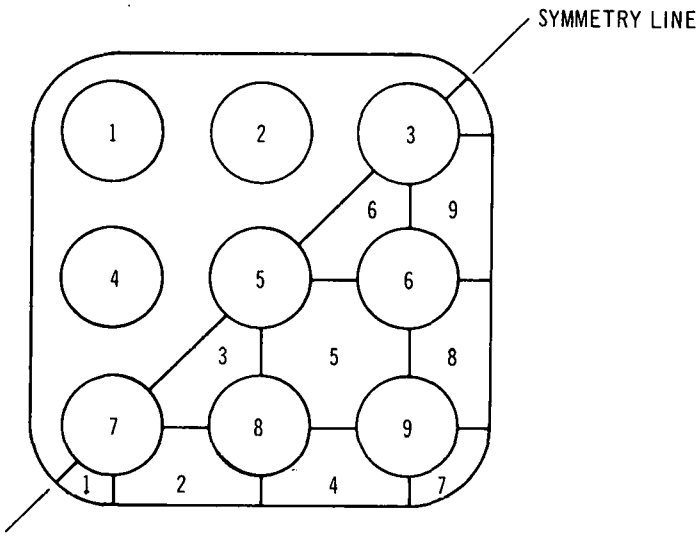

67-01545

FIGURE 7-5. MULTICHANNEL HYDRAULIC MODEL SUBCHANNELS (3x3)

along the channel wall and a CHF correlation based on a best fit to APED four- and nine-rod bundle data for the interior subchannels. The inlet subcooling was adjusted so that the local MCHFR was equal to 1.00 at the end of the heated length of subchannel 1. The remaining subchannels all had a MCHFR greater than 1.0. The CHF prediction line is shown in Figure 7-1, and was obtained by plotting the hot rod heat flux versus the bulk quality at the test section exit.

From Figure 7-1, it can be seen that the experimental CHF results for this particular test arrangement fall below the design limit curve. This situation can be better understood by more detailed examination of the MHM predictions. By dividing the test section into subchannels as shown in Figure 7-5, the model yielded the conditions at the exit given in Table 7-3 and depicted in Figure 7-6. From this, it can be seen that the flow migrates to the cold rods and to the side of the channel away from the hot rods 7, 8, and 9. This results in a quality in a subchannel 1, by rod 7, which is much higher than the average exit quality. This, in turn, results in a lower CHF in the corner. With uniform heat flux, a typical run on a similar 3 × 3 geometry yielded 19 percent quality in the corner with an average exit quality of 15 percent.

From Figure 7-1, it can be seen that the model was very effective in predicting the test results. These predictions by the model were also compared to CHF measurements made in other four- and nine-rod test sections. In these earlier comparisons, the corner rod peaking was not as extreme as tested here. Predictions by the model in these earlier cases fell slightly below the test results.

Thus, the results verify that the MHM can be used to predict whether the local peaking in the centermelt bundles will affect the validity of using the design limit curve and bulk average properties to predict the MCHFR.

TABLE 7-3

EXIT CONDITIONS FOR MHM APPLICATION TO 3 × 3 TEST SECTION WITH φ H = 700,000

Subchannel	X (%)	G (M lb/h-ft^2)	φ ave (M Btu/h-ft^2)	CHFR
1				
1	26.22	0.461	0.700	1.003
2	19.71	0.636	0.657	1.159
3	13.64	0.794	0.490	1.338
4	15.16	0.683	0.654	1.301
5	8.232	0.852	0.345	1.531
6	3.216	0.906	0.181	1.922
7	16.92	0.524	0.693	1.250
8	8.925	0.731	0.364	1.495
9	5.429	0.792	0.326	1.810
10	10.23	0.603	0.615	1.734
Total Channel	10.51	0.750	0.446	1.272

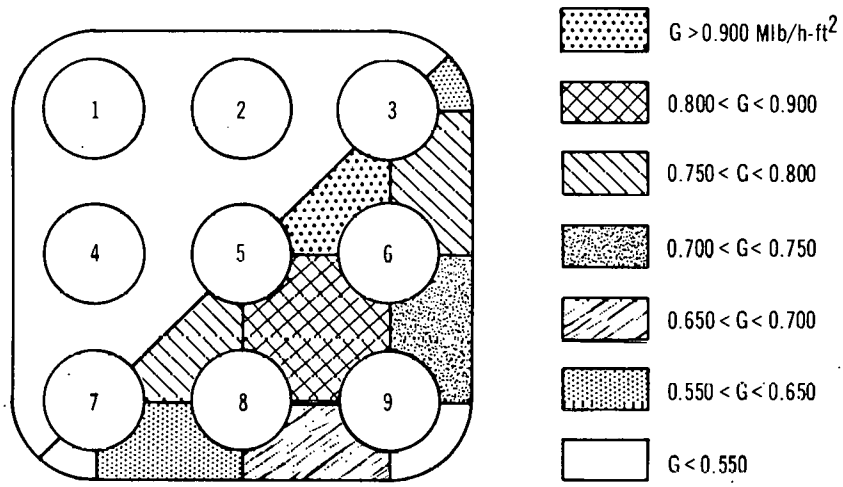

67-01546

FIGURE 7-6. FLOW DISTRIBUTION IN TEST SECTION WITH ϕ_7 = 700,000 Btu/h-ft^2

7.5 MULTICHANNEL HYDRAULIC MODEL APPLICATION TO CENTERMELT BUNDLES

The MHM was then applied to the centermelt bundles at rated flow and 22 percent overpower to compare the MCHFR using local and bulk properties. The dimensions of the 7 × 7 and 8 × 8 bundles for all cases and the local peaking values for the first case for each are those shown in Figures 7-2 and 7-3. Because the 7 × 7 bundle is one-eighth symmetric, it was divided into subchannels as shown in Figure 7-7. The 8 × 8 bundle is one-fourth symmetric, but one-eighth symmetry was assumed, and two runs were made for each case, as shown in Figure 7-8.

The axial power distribution, shown in Figure 7-9, was used for all cases. The axial peaking factor was 1.4. The CHFR calculations were based on local subchannel conditions and the annular correlation for the corner and wall subchannels and the multirod correlation for the interior subchannels.

Three cases were run for each bundle array at 1350 psia with the flows given in Table 7-4. The first case was the original rod arrangement shown in Figure 7-2 and 7-3. The second set of local peaking values was obtained by swapping each of the corner rods with the rod adjacent to it on the diagonal. The third set was obtained by reducing the enrichment in the corner from 4.3 to 2.3 percent. These local peaking values are also given in Figures 7-8 and 7-9. In addition, the location of MCHFR based on local conditions is shown for each case.

TABLE 7-4

RESULTS OF MHM APPLICATION TO CENTERMELT BUNDLES AT 1.22 OVERPOWER

Bundle	Case	Description	Local MCHFR	Bulk MCHFR
7 × 7	I	Original design	1.537	1.601
G = 790,000	II	Corner rod exchange	1.539	1.581
	III	Corner rod enrichment reduced to 2.3 percent	1.637	1.605
8 × 8	I	Original rod exchange	1.52	1.54
G = 740,000	II	Corner rod exchange	1.56	1.53
	III	Corner rod enrichment reduced to 2.3 percent	1.60	1.59

The results of the MHM analysis summarized in Table 7-4 show a MCHFR greater than 1.5 for all cases using either the local conditions or bulk conditions at 22 percent overpower. Although all cases provide a MCHFR greater than 1.5, it was decided to change the rod pattern to case II for extra margin. The rod pattern and peaking factor calculated for this arrangement are shown in Figures 7-10 and 7-11.

This revision moves the lowest CHFR location away from the corner to the third rod from the corner along the channel wall (see Figures 7-7b and 7-8b). This is desirable because of the angle present at each corner of the bundles which reduces the flow area in the corner section. Thus, the best over-all local peaking arrangement from a CHF standpoint is obtained with the corner rod exchanged with the cold rod next to it on the diagonal.

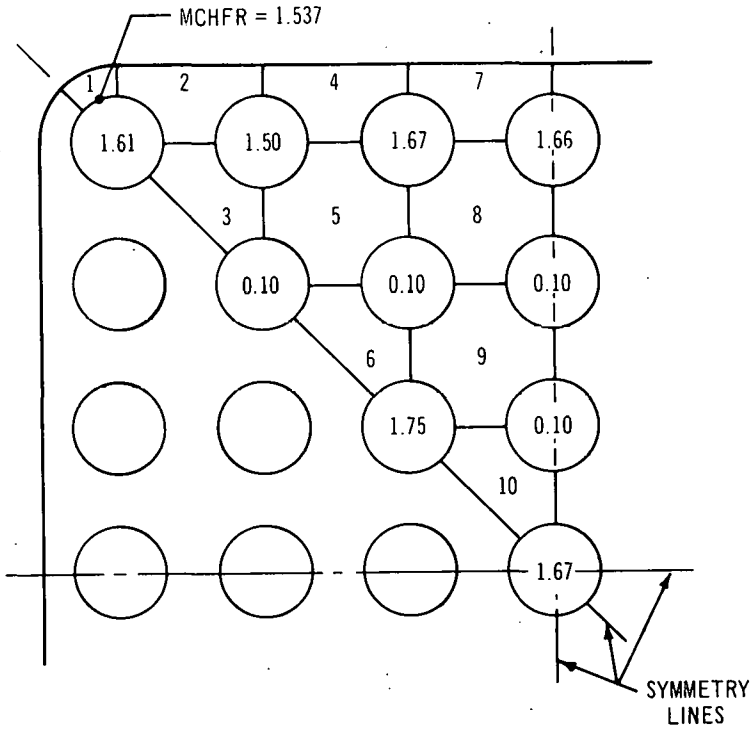

67-01547

FIGURE 7-7a. CASE I (7x7) LOCAL PEAKING (ORIGINAL DESIGN) AND LOCAL MCHFR LOCATION

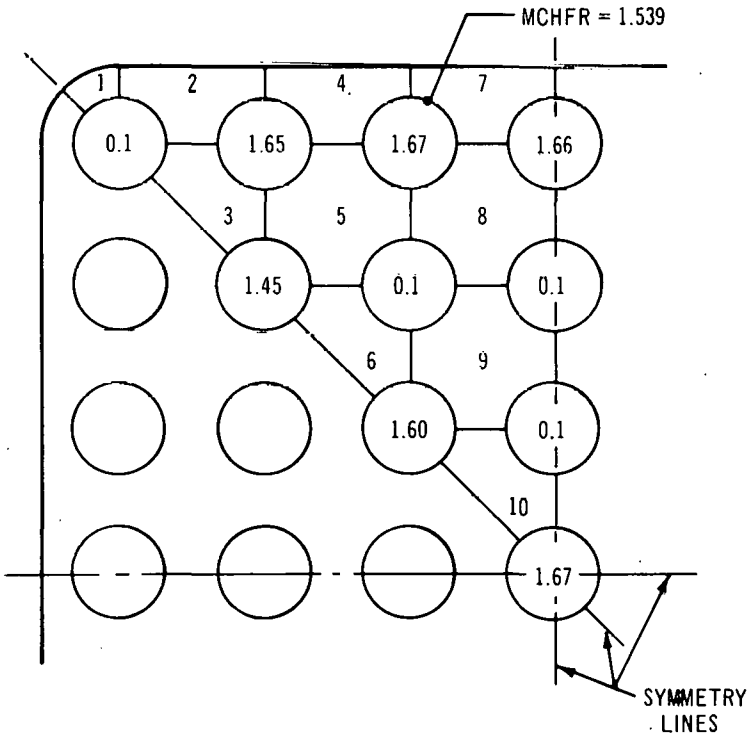

67-01548

FIGURE 7-7b. CASE II (7x7) LOCAL PEAKING (CORNER ROD EXCHANGED WITH NEXT-TO-CORNER ROD ON DIAGONAL) AND LOCAL MCHFR LOCATION

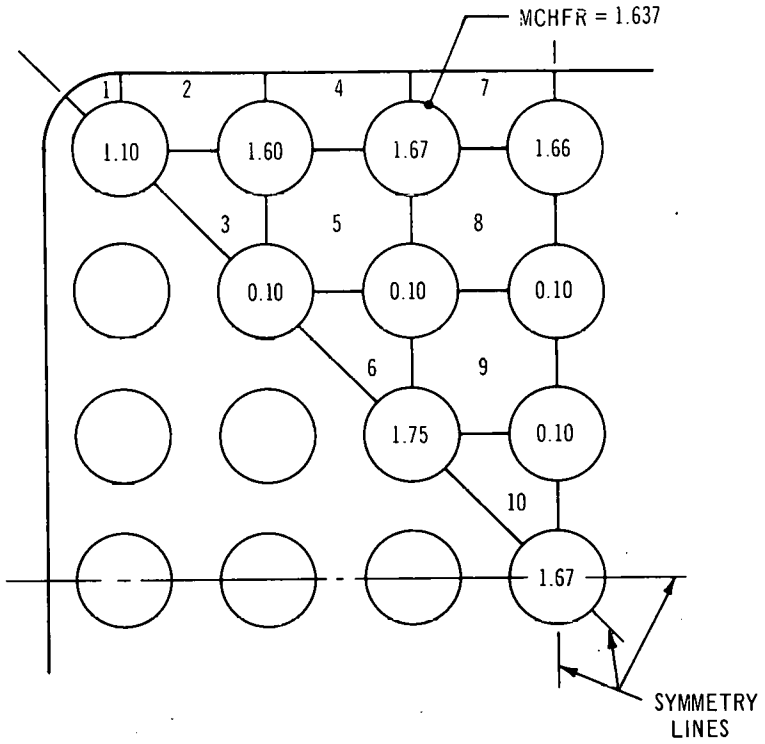

67-01549

FIGURE 7-7c. CASE III (7x7) LOCAL PEAKING (CORNER ROD ENRICHMENT REDUCED FROM 4.3 TO 2.3 PERCENT) AND LOCAL MCHFR LOCATION

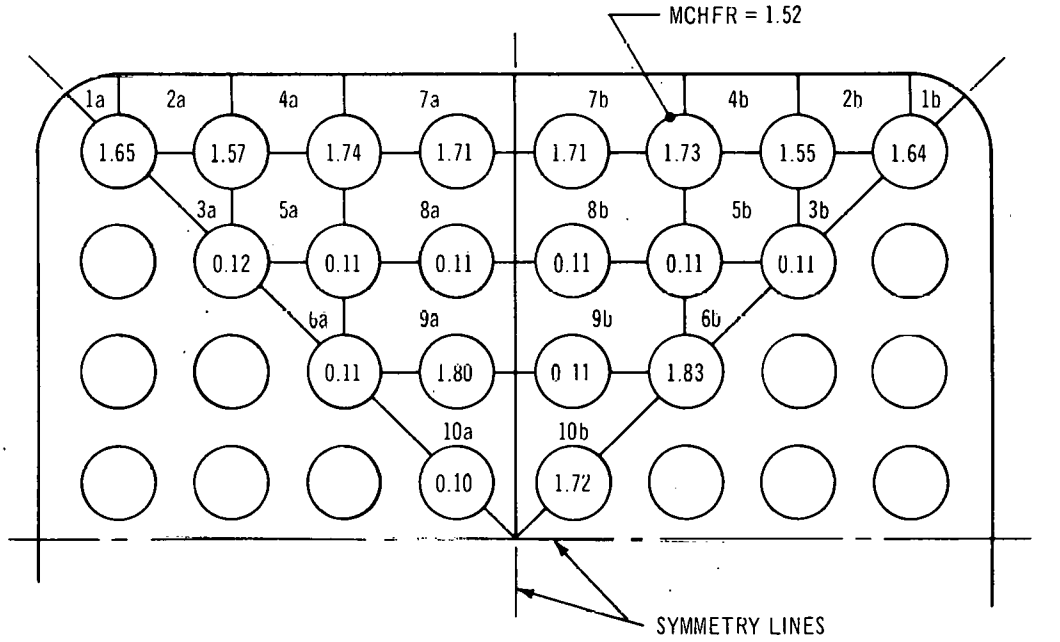

67-01550

FIGURE 7-8a. CASE I (8x8) LOCAL PEAKING (ORIGINAL DESIGN) AND LOCAL MCHFR LOCATION

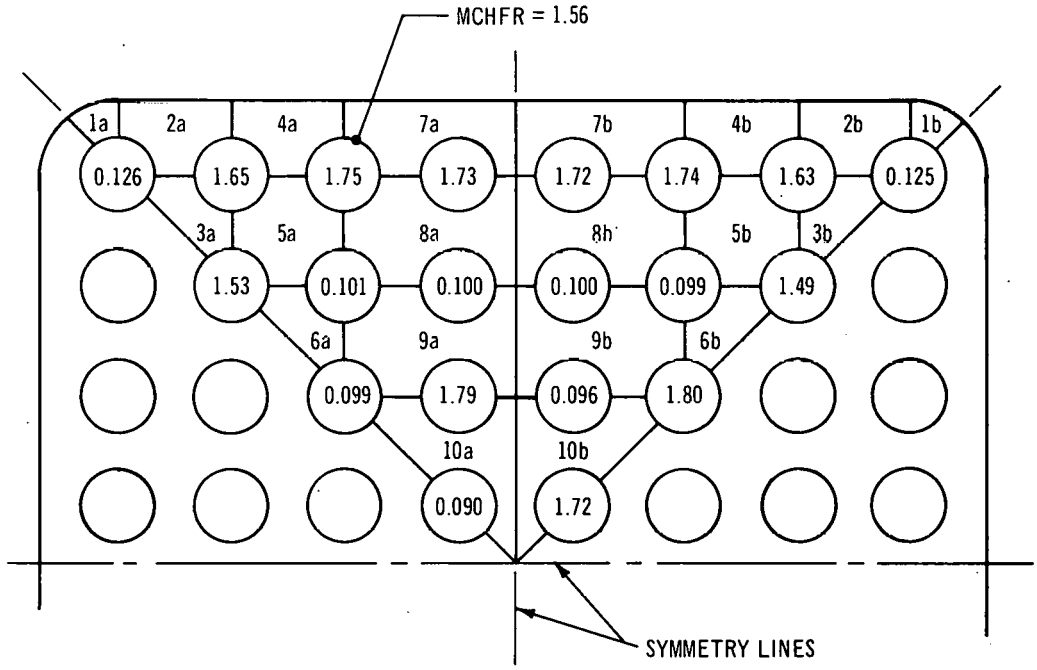

67-01551

FIGURE 7-8b. CASE II (8x8) LOCAL PEAKING (CORNER RODS EXCHANGED WITH NEXT-TO-CORNER ROD ON DIAGONAL) AND LOCAL MCHFR LOCATION

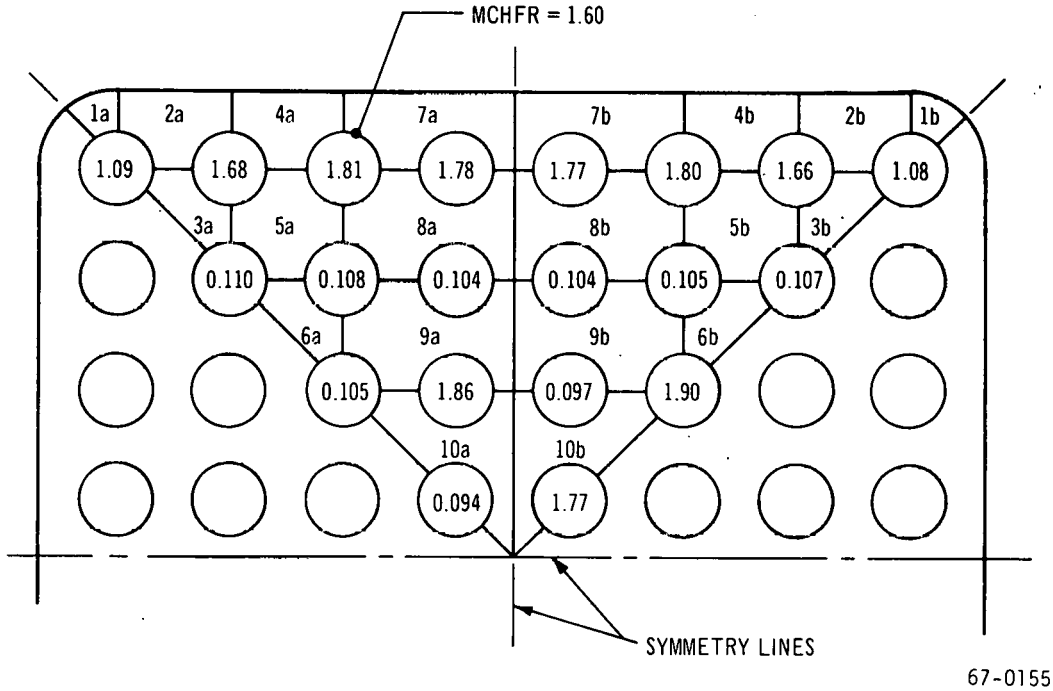

67-01552

FIGURE 7-8c. CASE III (8x8) LOCAL PEAKING (CORNER ROD ENRICHMENT REDUCED FROM 4.3 TO 2.3 PERCENT) AND LOCAL MCHFR LOCATION

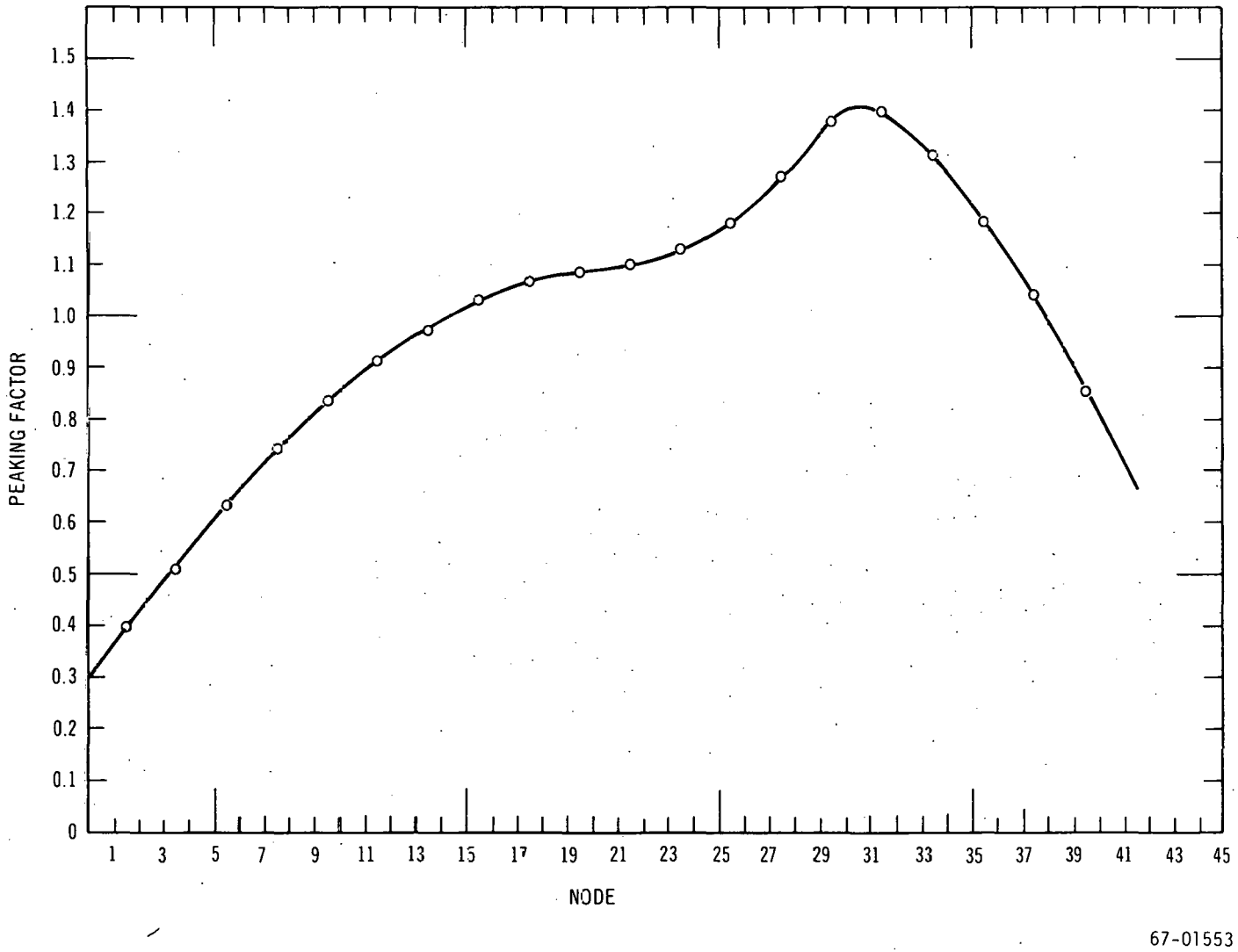

FIGURE 7-9. AXIAL POWER DISTRIBUTION FOR 7 x 7 AND 8 x 8 CASES

D 0.13	A 1.60	B 1.68	B 1.67	B 1.68	A 1.60	D 0.13
A 1.60	A 1.42	D 0.10	D 0.10	D 0.10	A 1.42	A 1.60
B 1.68	D 0.10	C 1.71	D 0.09	C 1.71	D 0.10	B 1.68
B 1.67	D 0.10	D 0.09	C 1.65	D 0.09	D 0.10	B 1.67
B 1.68	D 0.10	C 1.71	D 0.09	C 1.71	D 0.10	B 1.68
A 1.60	A 1.42	D 0.10	D 0.10	D 0.10	A 1.42	A 1.60
D 0.13	A 1.60	B 1.68	B 1.67	B 1.68	A 1.60	D 0.13

TYPE A U-235 ENRICHMENT = 0.043
TYPE B U-235 ENRICHMENT = 0.050
TYPE C U-235 ENRICHMENT = 0.056
TYPE D U-235 ENRICHMENT = 0.0022 (depleted)

67-01554

FIGURE 7–10. INDIVIDUAL FUEL ROD RELATIVE POWERS IN THE 7 x 7 CENTERMELT BUNDLE. BEGINNING OF LIFE. AVERAGE ROD POWER = 1.0.

D 0.13	A 1.65	B 1.75	B 1.73	B 1.73	B 1.74	A 1.63	D 0.13
A 1.65	A 1.53	D 0.10	D 0.10	D 0.10	D 0.10	A 1.49	A 1.63
B 1.75	D 0.10	D 0.10	C 1.79	D 0.10	C 1.81	D 0.10	B 1.74
B 1.73	D 0.10	C 1.79	D 0.09	C 1.72	D 0.10	D 0.10	B 1.73
B 1.73	D 0.10	D 0.10	C 1.72	D 0.09	C 1.79	D 0.10	B 1.73
B 1.74	D 0.10	C 1.81	D 0.10	C 1.79	D 0.10	D 0.10	B 1.75
A 1.63	A 1.49	D 0.10	D 0.10	D 0.10	D 0.10	A 1.53	A 1.65
D 0.13	A 1.63	B 1.74	B 1.73	B 1.73	B 1.75	A 1.65	D 0.13

TYPE A U-235 ENRICHMENT = 0.043
TYPE B U-235 ENRICHMENT = 0.050
TYPE C U-235 ENRICHMENT = 0.056
TYPE D U-235 ENRICHMENT = 0.0022 (depleted)

67-01555

FIGURE 7–11. INDIVIDUAL FUEL ROD RELATIVE POWERS IN THE 8 x 8 CENTERMELT BUNDLE. BEGINNING OF LIFE. AVERAGE ROD POWER = 1.0.

SECTION VIII

PHYSICS ANALYSIS

8.1 GENERAL

The centermelt bundle designs employ four different U-235 enrichments to maximize the number of fuel rods operating at or very near 450,000 ±50,000 Btu/h-ft^2, without exceeding the Big Rock Point reactor thermal limits. The nuclear design ground rules were as follows:

a. Adherence to the present license limits of 1.5 MCHFR at 1.22 steady-state overpower,

b. Reactivity coefficients which are as negative as possible,

c. Bundle average exposure capability of 15,000 MWd/T without bundle modifications, i.e., without burnable poison.

8.2 GENERAL FEATURES COMMON TO BOTH DESIGNS

Both the 7 × 7 and 8 × 8 designs have four enrichments: 4.3, 5.0, 5.6, and 0.22 (depleted) weight percent. The combination of enrichments and rod positions was specified such as to provide the maximum number of fuel pins operating at or very close to the desired peak heat flux.

The following general arrangement plan was used: The lowest enrichment (4.3 percent) was placed in the fuel pins nearest the corners of the bundle where the highest thermal neutron flux occurs. The remaining rods adjacent to the water gaps experience somewhat lower thermal flux, and consequently must be enriched higher to produce approximately the same power.

The number of depleted UO_2 rods was decided from a thermal limit MCHFR evaluation, wherein their low power production effectively increases the allowable power of the remaining enriched fuel rods at the same over-all bundle power output. The depleted rods were arrayed in a roughly annular zone inside the corner and side rods above. Then the highest enrichment rods were placed in a symmetrical arrangement near the center of the bundle. Their enrichment is sufficient to produce rod powers similar to the other outer power producing rods.

The bundles have adequate thermal margins throughout their lifetime based on assumed "beginning" and "end-of-cycle" power shapes. These power shapes are very important to the design, and were determined from typical recent operating shapes experienced at Big Rock Point and are not the "worst conceivable" that may be encountered during operation.

The occurrence of a "worst" power shape is not a safety problem, however, because the reactor must be operated within its existing license limits at all times. The core power and the operating heat flux of the centermelt bundles are the dependent variables. To observe license limits, the peak heat flux may occasionally not be exactly at the target centermelting limits. This is unavoidable and must be expected; either fuel rod power or optimum centermelt bundle

performance cannot always be met during a cycle. The presence of these bundles in the core places additional burden on the operating physicist and on the thermal engineer, but it is not a safety problem in any sense.

Both bundle designs have been enriched to attain approximately 15,000 MWd/T average (22,000 MWd/T_e average for the power producing rods) in a core of the same type. This is the standard method of specifying fuel bundle exposure capability, and it is possible to "push" any desired bundle, or bundles, past the specified exposure capability at some expense in core reactivity.

8.3 DOPPLER COEFFICIENT

The Doppler coefficient for the 8 × 8 bundle design has been calculated to be -0.86×10^{-5} $\Delta k/k/°F$ at ~ 1000°K. This compares to the standard fuel designs (A, B, C, and E) for Big Rock which have values in the range of -1.0 to -1.1×10^{-5} $\Delta k/k°F$. The 7 × 7 design is about 0.96×10^{-5} $\Delta k/k°F$. These calculations are simple hand calculations of the effect according to the department standard method, and do not include spatial weighting of the individual rods.

8.4 TEMPERATURE AND VOID COEFFICIENT

The temperature and void coefficients for the cold centermelt bundles have been calculated. The coefficients are noticeably more positive than standard BRP fuel, as can be seen in the following comparison with BRP "B reload" fuel presently loaded into the reactor.

	Temperature Coefficient at 25°C ($\Delta k/k/°C$)		Void Coefficient at 20°C ($\Delta k/k/\%$ Void)	
Fuel Type	Beginning of Life Approximation	End-of-Life Approximation	Beginning-of-Life Approximation	End-of-Life Approximation
B-Reload	$+3.2 \times 10^{-6}$	$+5.5 \times 10^{-5}$	-2.8×10^{-3}	-3.8×10^{-4}
Centermelt 8 × 8	$+1.04 \times 10^{-4}$	$+1.8 \times 10^{-4}$	-2.4×10^{-3}	$+5.3 \times 10^{-5}$
Centermelt 7 × 7	$+5.6 \times 10^{-5}$	$+1.7 \times 10^{-4}$	-2.7×10^{-3}	-1.3×10^{-4}

The coefficients have been approximated according to the following equation:

$$\frac{\Delta k}{k} \Big/ °C \sim \frac{1}{T_1 - T_2} \; \frac{k_\infty T_1 - k_\infty T_2}{k_\infty T_1} \; \frac{\left(M_1^2 - M_2^2\right) B^2 + M_1^2 \left(B_1^2 - B_2^2\right)}{k_\infty T_1} ,$$

where k_∞ and U^2 have the usual meaning, B^2 is B_g^2 for the end-of-life approximation, and B^2 is B_m^2 for beginning-of-life approximation. The term $\left(B_1^2 - B_2^2\right)$ reflects the change of geometric buckling due to reflector savings changes, and can be ignored. This calculation is useful for comparison purposes, but coefficients measured in the reactor itself are substantially more negative than the end-of-life approximation due to the presence of control rods and are usually slightly more positive than the beginning-of-life coefficients due to the presence of positive reflector effects.

The small number of centermelt bundles in the reactor core (six of an 84 total) will produce a very small, if even detectable, effect on over-all reactor behavior with temperature and void.

The total addition of reactivity due to any possible cold voiding of the two 8 × 8 bundles has been estimated at much less than 0.001 ΔK/K.

8.5 BURNUP BEHAVIOR

Although the bundles do not resemble other designs in the core to a great extent, the behavior with lifetime is very similar. The burnup slope for the 7 × 7 bundle is 0.0113 ΔK/1000 MWd/T and 0.0116 ΔK/1000 MWd/T for the 8 × 8 bundle. This compares to the new reload (E bundle with cobalt) value of 0.0115 ΔK/K/1000 MWd/T. The beginning reactivities are comparable for all the designs, and no special power shape or lifetime behavior problems are expected.

8.6 CALCULATED LOCAL PEAKING FACTORS

The initial calculated local peaking factors for both the 7 × 7 and the 8 × 8 bundles are shown in Figures 7-2 and 7-3. These peaking factors were later modified by the rod rearrangement described in the previous section on CHF analysis. The local peaking factors shown are for the new bundle, and are normalized to 1.0 average power. Because of plutonium production in each of the fuel rods, the peaking factors of the depleted rods will increase with time, and because of normalization, the peaking factors for the enriched, higher power producing rods will decrease. The behavior of each enrichment group is shown in Figure 8-1 for the 7 × 7 bundle. The relative power of the three high enrichment groups decreases with exposure and the depleted group increases. The thermal performance capability has been evaluated using the expected decreased locals at the start of the last cycle. This combination provides the most severe of the expected operating conditions, i.e., the axial power shape is skewed to the top of the bundle and the local peaking factors are decreased (due to depleted rod power increase) at this late point in the life of the bundle. The bundles are still capable of target heat fluxes at 15,000 MWd/T with a typical start of cycle power shape.

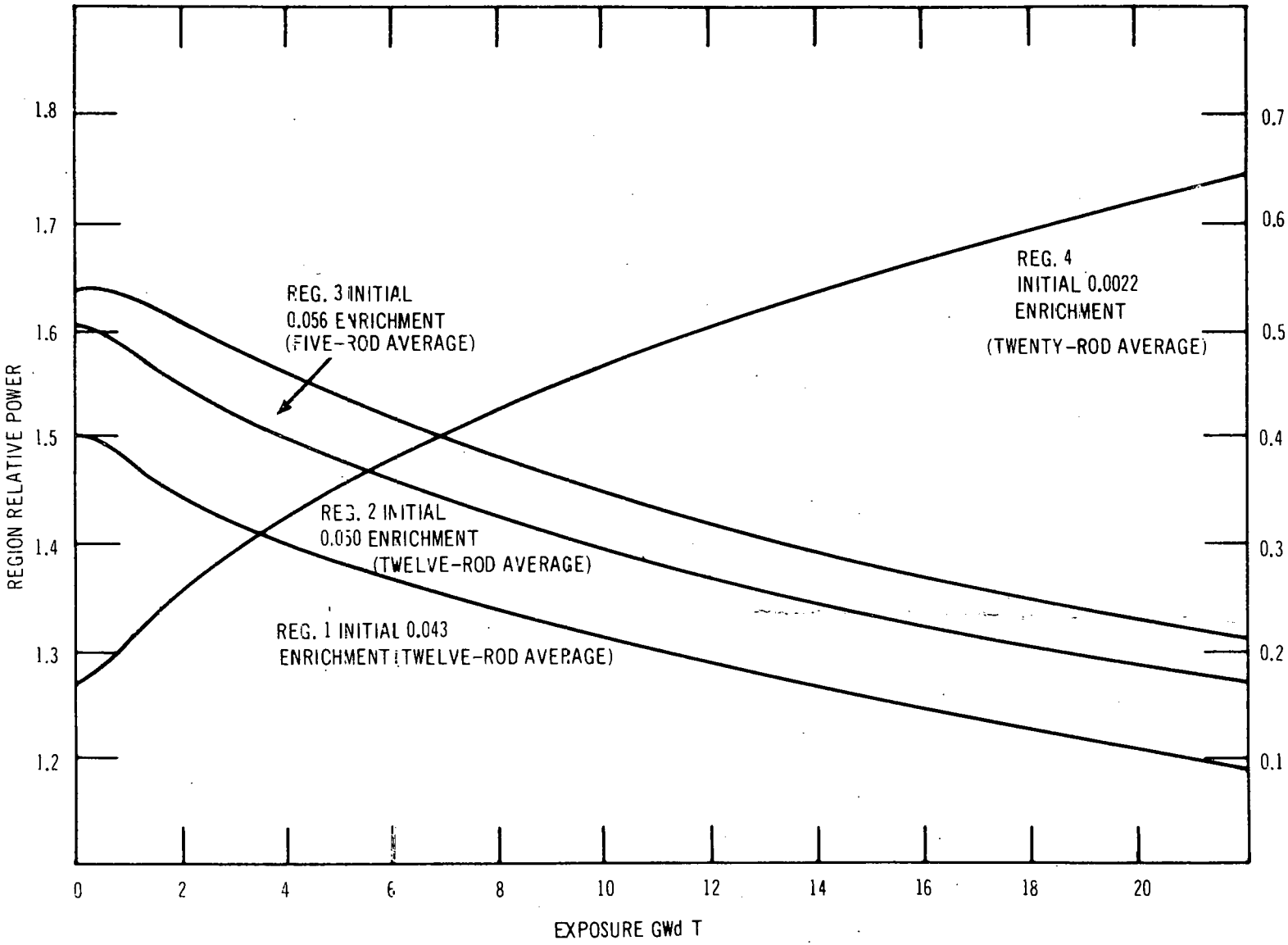

FIGURE 8-1. RELATIVE POWER OF THE FOUR ENRICHMENT REGIONS IN THE 7 x 7 BUNDLE DESIGN AS A FUNCTION OF EXPOSURE

SECTION IX

SAFEGUARDS, LICENSING, AND PROGRAM STATUS

9.1 GENERAL

An amendment to the existing Consumers Big Rock Point reactor license was required in order to proceed with these irradiations. Because the basic objective of these irradiations—the demonstration of centermelt operation in a commercial power reactor—is the first test of its kind, with potential for greater fission product release if a rod fails, licensing was expected to be substantially more difficult than for previous fuel assemblies. For this reason, considerably more effort than heretofore expended was applied to prepare the initial draft license amendment, Amendment No. 13. The extensive CHF analysis described in Section VIII was one reflection of this concern and was an attempt to anticipate one likely area of concern by the licensing body. Despite this and other anticipatory work, licensing proved quite difficult, and implies a generally cautious, conservative attitude by AEC-DRL and AEC-ACRS toward advanced performance fuel testing in a commercial power reactor. This experience is briefly recapped in the following subsections to indicate the major technical obstacles.

9.2 AMENDMENT NO. 13, BRP REACTOR

The initial submittal of this amendment was made to AEC-DRL on May 26, 1967, by Consmers Power Company. This 61-page document presented the objectives of the irradiations, a synopsis of previous irradiation experience at centermelt conditions, the detailed design and supporting analysis for the fuel rods and assemblies, analysis of the effect of the centermelt bundles on the usual loss of coolant and reactivity insertion accidents. The first review of this document with DRL representatives was held on June 27, 1967. Major topics of discussion at the meeting were on: a.) techniques and accuracy of operational calculations (bundle power prediction, effect of burnup on UO_2 thermal conductivity, effect of plutonium buildup on bundle performance, etc.), b.) reactivity insertion accidents, c.) critical heat flux correlation, d.) loss-of-coolant accidents, and e.) loss of recirculation pump accidents. As a result of this meeting, a list of specific questions was received from AEC-DRL and answered in detail by letter. The questions focused concern in these areas: a.) magnitude and consequences of reactivity-induced transients, b.) potential situations for high rod worth, and c.) consequences of loss-of-coolant accidents.

9.3 INITIAL ACRS REVIEW

Consideration of BRP Amendment No. 13 and supplementary documents was placed on the ACRS agenda for September 6 through 8, 1967. Consumers Power Company and G.E.-NED personnel presented the program scope and hazard analysis, first to the ACRS subcommittee and then to the full committee, at the two separate sessions. Subjects discussed in addition to those already noted were: a.) previous centermelt fuel operating experience, b.) procedural controls during control rod movement, and c.) the planned inspection program for the centermelt fuel.

At the conclusion of the meeting, the ACRS indicated that approval to proceed could not be granted and that further questions would be transmitted. On September 27, 1967, thirteen

questions, each extensive and detailed in scope, were received. Most of the questions concerned various phases of the reactivity insertion accident, e.g., possible rod worths involved and consequent sudden deposition of energy in the fuel, transient fuel damage threshold, rate of energy transfer to the coolant, etc. Other areas where additional information was requested were as follows:

a. Loss-of-coolant accidents: Maximum fuel pin temperature as a function of pipe break size. The initial submittal included an evaluation for the maximum credible accident only.

b. Administration and procedural controls: Proposed technical specification which will be in effect while the centermelt fuel is in the core. These specifications are to include: 1.) action to be taken in the event of detected or suspected primary system leak; 2.) notification and approach that will be required for reactor startups; and 3.) requirements for the presence of technical specialists during startups, power increases, or other significant operating events.

c. A detailed fuel inspection program: The main question here is to show how this inspection program will enhance the safe operation of the fuel rods.

d. Loss of generator accident: Discussion of such an accident in which the generator loses its load, with and without automatic opening of the turbine bypass valve.

9.4 FINAL ACRS REVIEW

The written answers to the preceding thirteen questions raised by ACRS were completed and submitted on November 6, 1967. The required document included 109 pages of text and figures. BRP license Amendment No. 13 was again placed on the ACRS agenda for December 1967. Both the subcommittee and full committee reviewed the submittal on December 5 and 8.

In this review, Consumers Power Company personnel provided, in response to a direct request, a review of their progress in modifying the BRP plant to comply with the general AEC directive on updating safety systems, issued early in 1967 to all the first generation nuclear plants. General Electric Company personnel then presented more concrete plans for monitoring the centermelt fuel condition, including the expected timing for nondestructive fuel examinations at the site and destructive examinations of selected rods brought back to the Vallecitos Nuclear Center hot cells. This schedule was based on the projected BRP operating schedule commencing in January 1968, after a refueling shutdown. This was followed by a presentation on additional results from analyses regarding potential reactivity insertion accidents and probable consequences.

The formal session concluded with an extensive question-and-answer period where, inevitably, several new questions regarding the BRP plant and systems were raised and explored. Not all of these questions could be satisfactorily answered because the specific facts and data were not readily available during the discussion.

At the conclusion of this second ACRS review, the committee indicated that they believed a generally favorable action on the license Amendment was justified, but that one or more of

approximately eight reservations might be attached to the approval. Subsequently, a formal letter authorizing the irradiation of the centermelt bundles was issued on December 20, 1967, with the following specific stipulations.

a. Caution is to be exercised in the operation of the reactor during the test program. Extra caution is to be used if signs of fuel failure appear.

b. Improved methods are to be developed for prompt detection of gross failure of the experimental fuel.

c. After the accumulation of about 3000 MWd/T burnup, the advanced performance fuel (0.700-inch-o.d. rods, all four assemblies) are to be removed from the core, and four selected rods from these assemblies destructively examined to ascertain and confirm that the fuel conditions and performance during irradiation were essentially as predicted, and that the irradiation of the bundles can be continued safely.

d. An emergency cooling water line connecting the site fire protection system to the reactor pressure vessel is to be completed as additional protection against core meltdown in the unlikely event of rupture of the core spray line.

e. A detailed in-service inspection of the primary system piping and components is to be completed. In addition, a hydrostatic test at a pressure only slightly lower than the pressure relief valve settings of the primary system is to be conducted prior to the insertion of the centermelt assemblies.

9.5 CURRENT PROGRAM STATUS

General Electric, Consumers Power Company, and AEC-DRD have accepted these stipulations and the necessary work to comply is underway. The fuel bundles have been shipped to BRP and are expected to be installed about mid-February with start of irradiation approximately March 1. After approximately 3 months of irradiation ($\sim$3000 MWd/T_e average burnup), the four advanced performance assemblies will be removed from the core and stored in the reactor pool for approximately 6 months while destructive examination proceeds on four rods at the Vallecitos Nuclear Center to verify the predicted degree of melting. Once satisfactory verification is obtained, the bundles will be reconstituted with spare rods and they will be reinstalled and their irradiation continued to the target burnup, with additional interim nondestructive examinations coinciding with scheduled reactor refueling shutdown. The operation of the two intermediate performance fuel bundles will not be intentionally interrupted, except for interim rod examinations and removals, once the irradiations commence.

REFERENCES

1. Lyons, M. F., et al., "Molten UO_2 Fuel Rod Operation to High Burnup," GEAP-5100-2.

2. Fowler, W. D., "Mechanical Design and Testing of Developmental Fuel for Consumers Power Big Rock Point Reactor," GEAP-3851, April 1962.

3. Timoshenko, S., "Strength of Materials, Part 2, Third Edition," D. Van Nostrand, New York, 1956, pp 186 - 190.

4. Klepfer, H. H., et al., "Specific Zirconium Alloy Design Program, Fifth Quarterly Progress Report, April - June 1963," GEAP-4284.

5. WAPD-MRP-107.

6. Lyons, M. F., et al., "UO_2 Thermal Conductivity from Irradiation with Central Melting," GEAP-4624, July 1964.

7. Lyons, M. F., et al., "UO_2 Powder and Pellet Thermal Conductivity during Irradiation," GEAP-4100-1, March 1966.

8. Lyons, M. F., "High Performance UO_2 Program Quarterly Reports," GEAP-3771.

DISTRIBUTION

	Copies
U.S. Atomic Energy Commission San Francisco Operations Office 2111 Bancroft Way Berkeley 4, California	24
U.S Atomic Energy Commission Division of Reactor Development Washington 25, D.C. Attn: Fuels and Materials Development Branch - Nuclear Technology	2
U.S. Atomic Energy Commission Chicago Operations Office 9700 South Cass Avenue Argonne, Illinois. Attn: Director, Reactor Engineering Div.	1
Babcock and Wilcox Company Atomic Energy Division P.O. Box 1260 Lynchburg, Virginia	1
Oak Ridge National Laboratory P.O. Box X Oak Ridge, Tennessee Attn: D. B. Trauger	1
Westinghouse Electric Corporation Bettis Atomic Power Laboratory P.O. Box 79 West Mifflin, Pennsylvania 15122 Attn: Dr. R. J. Creagan	2
Commissariat a l'Energie Atomique Joint U.S.-Euratom Program "Sintered Uranium Oxide" Direction des Relations Exterieurs et des Programmes Boite Postale 307 Paris 7, France	1
Atomics International P.O. Box 309 Canoga Park, California Attn: C. Weber	1
United Nuclear Corporation Development Division Grasslands Road Elmsford, New York 10523 Attn: S. Strasser	1
Westinghouse Electric Corporation Bettis Atomic Power Laboratory P.O. Box 79 West Mifflin, Pennsylvania 15122 Attn: Mrs. V. Sternberg	2
Division of Technical Information Extension U.S. Atomic Energy Commission P.O. Box 62 Oak Ridge, Tennessee 37831	50
U.S. Atomic Energy Commission Division of Reactor Development Washington 25, D.C. Attn: Office of Foreign Activities	1
U.S. Atomic Energy Commission Division of Reactor Development Washington 25, D.C. Attn: Water Reactors Branch Civilian Reactors	1
Argonne National Laboratory 9700 South Cass Avenue Argonne, Illinois Attn: Robert Macherey	1
USAEC Liaison Office Scientific Representative Chalk River, Ontario	1
Combustion Engineering, Inc. Nuclear Division Prospect Hill Road Windsor, Connecticut Attn: W. P. Chernock	1
Fiat Joint U.S.-Euratom Program "Swaging of Uranium Dioxide: and "Uranium Dioxide Fuel Development" Corso g-Marconi, 10/20 Torino, Italy	1
Battelle Memorial Institute 505 King Avenue Columbus 1, Ohio Attn: S. Paprocki	1
E.I. DuPont de Nemours and Co. Atomic Energy Division 2430 Nemours Bldg. Wilmington, Delaware Attn: E. E. Hayes	1
U.S. Atomic Energy Commission Naval Reactors Branch Division of Reactor Development Washington, D.C. 20545 Attn: R. Steele	1
U.S. Atomic Energy Commission New York Operations Office 376 Hudson Street New York 14, New York Attn: J. Dissler	1
Battelle Memorial Institute Pacific Northwest Laboratory Richland, Washington Attn: D. R. DeHalas	